ABSTRACT

Title of Document: FUNCTIONAL STUDIES OF THE LC PROTEIN IN VESIVIRUSES OF THE *CALICIVIRIDAE*

Eugenio Abente, Doctor of Philosophy, 2012

Directed by: Dr. Kim Y. Green, Adjunct Professor Department of Cell Biology and Molecular Genetics

Viruses of the family *Caliciviridae* are non-enveloped, single-stranded, positive sense RNA viruses. Feline calicivirus (FCV), a virus in the genus *Vesivirus*, is used as a model to study basic mechanisms of replication of caliciviruses because it grows well in cell culture and it has a reverse genetics system. A feature unique to vesiviruses is the presence of a ~14-18 kDa protein of unknown function designated as leader of the capsid (LC) that is expressed as part of a capsid precursor encoded in open reading frame 2 (ORF2). The ORF2 precursor contains the LC fused to the major capsid protein, VP1, which is proteolytically cleaved by the viral protease to release the LC and the mature VP1. The LC is not found in purified virions, and therefore does not appear to have a structural role, but it has previously been associated with promoting the human norovirus RNA replicon when provided in *trans*. In order to study the role of the LC in virus replication I employed the reverse genetics system to generate recombinant full-length FCV genomes, and performed transient expression experiments with the LC alone. By applying deletional mutagenesis and scanning alanine mutagenesis to the LC coding sequence I identified regions and conserved residues critical for viral replication and

virus spread. Transient expression of the LC caused cells to round and die, and the same residues important for virus spread were important for the cell-rounding phenotype. Immunoprecipitation of recombinant LC in FCV infected cells identified the cellular protein annexin A2 as a binding partner, providing a potential mechanism for the cell-rounding phenotype observed in transient expression experiments. Understanding the role of the LC in FCV replication is important because there are currently no antiviral drugs available for FCV and there are numerous reports of vaccine failure. Additionally, elucidating the mechanism responsible for the enhancement of the Norwalk virus replicon may provide new insight into the establishment of a cell culture system for the human noroviruses, which is the leading cause of viral gastroenteritis outbreaks.

FUNCTIONAL STUDIES OF THE LC PROTEIN IN VESIVIRUSES OF THE *CALICIVIRIDAE*

by

Eugenio J. Abente

Dissertation submitted to the Faculty of the Graduate School of the
University of Maryland, College Park in partial fulfillment
of the requirements for the degree of
Doctor of Philosophy
2012

Advisory Committee:
Professor Jeffrey DeStefano, Chair
Professor Jim Culver
Professor Brenda Fredericksen
Professor Siba Samal
Adjunct Professor Kim Green

DEDICATION

This work is dedicated to the memory of my aunt, Carolina Rojas Bahr (1952-2007).

ACKNOWLEDGEMENTS

I would like to thank Dr. Kim Y. Green for her constant support and encouragement throughout my graduate studies. I would like to thank the members of my committee, Dr. Jeff DeStefano, Dr. Jim Culver, Dr. Brenda Fredericksen, and Dr. Siba Samal for their professional guidance. To Dr. Albert Z. Kapikian, Dr. Karin Bok, Dr. Stanislav Sosnovtsev, Dr. Carlos Sandoval-Jaime and Dr. Gabriel I. Parra I extend gratitude for their patience, leadership and assistance throughout my training experience at the NIH. To my family and friends, I will always be indebted to you for your support and inspiration.

TABLE OF CONTENTS

LIST OF TABLES

LIST OF FIGURES

LIST OF ABBREVIATIONS

ANXA2	annexin A2
bp	base pair
CaCV	Canine calicivirus
CPE	cytopathic effect
CRFK	Crandell-Rees feline kidney cells
ER	endoplasmic reticulum
EBHSV	European brown hare syndrome virus
eIF4E	eukaryotic initiation factor 4E
FCV	Feline calicivirus
ICTV	International Committee on Taxonomy of Viruses
IEM	immune electron microscopy
IRES	internal ribosomal entry site
JAM-1	junction adhesion molecule 1
kDa	kilodalton
MNV	Murine norovirus
MOI	multiplicity of infection
NS	non-structural
nt	nucleotide
ORF	open reading frame
P	protruding domain corresponding to the VP1 protein
P.F.U.	plaque forming units
PTB	polypyrimidine tract binding protein
RC	replication complex
RdRp	RNA-dependent RNA polymerase
RHDV	Rabbit hemorrhagic disease virus
RT-PCR	reverse transcriptase-polymerase chain reaction
S	shell domain corresponding to the VP1 protein
S.O.C.	Super Optimal broth with Catabolite repression
SMSV	San Miguel Sea Lion virus
TNT	coupled transcription/translation
TURBS	termination upstream ribosomal binding site
VESV	Vesicular Exanthema of Swine Virus
VLP	virus-like particle
VPg	virion protein, genome-linked
VS-FCV	virulent-systemic FCV
wt	wild-type

CHAPTER 1: LITERATURE REVIEW

1.1. *Caliciviridae*

Caliciviruses are non-enveloped positive-sense single stranded RNA viruses found in a wide range of animal hosts. The genome length ranges from approximately 7.3 to 8.5 kb, and the relatively small icosahedral virions range in diameter from 27-40 nm. The name of the family has its origins from the first images captured by electron microscopy, in which virions were observed to have cup-like surface indentations. They were called “calici-” viruses, based on the Latin word for cup (“calyx”). Initially, because of their similarity to picornaviruses in size and RNA content, caliciviruses were considered members of the family *Picornaviridae.* However, with the establishment of major differences in their replication strategies, the caliciviruses were eventually classified into a new family, the *Caliciviridae* (236). The International Committee on Taxonomy of Viruses (ICTV) recognizes at this time five genera within the family *Caliciviridae*: *Vesivirus*, *Lagovirus*, *Norovirus*, *Sapovirus* and *Nebovirus* (Fig. 1.1).

The first known occurrence of the prototype virus for the genus *Vesivirus*, Vesicular Exanthema of Swine Virus (VESV), was determined retrospectively from an atypical foot-and-mouth disease outbreak that occurred on a farm in Southern California in 1932. For the next 20 years, little attention was paid to VESV because it was thought to be limited to California and VES illness was referred to as "California Disease" and the "California Problem". In 1952, an epizootic outbreak of VESV was determined to have originated in a swine herd in Cheyenne, Wyoming fed raw garbage unloaded from transcontinental trains that had departed from California (164). The outbreak spread throughout 42 states and the District of Columbia over a period of 15 months, prompting

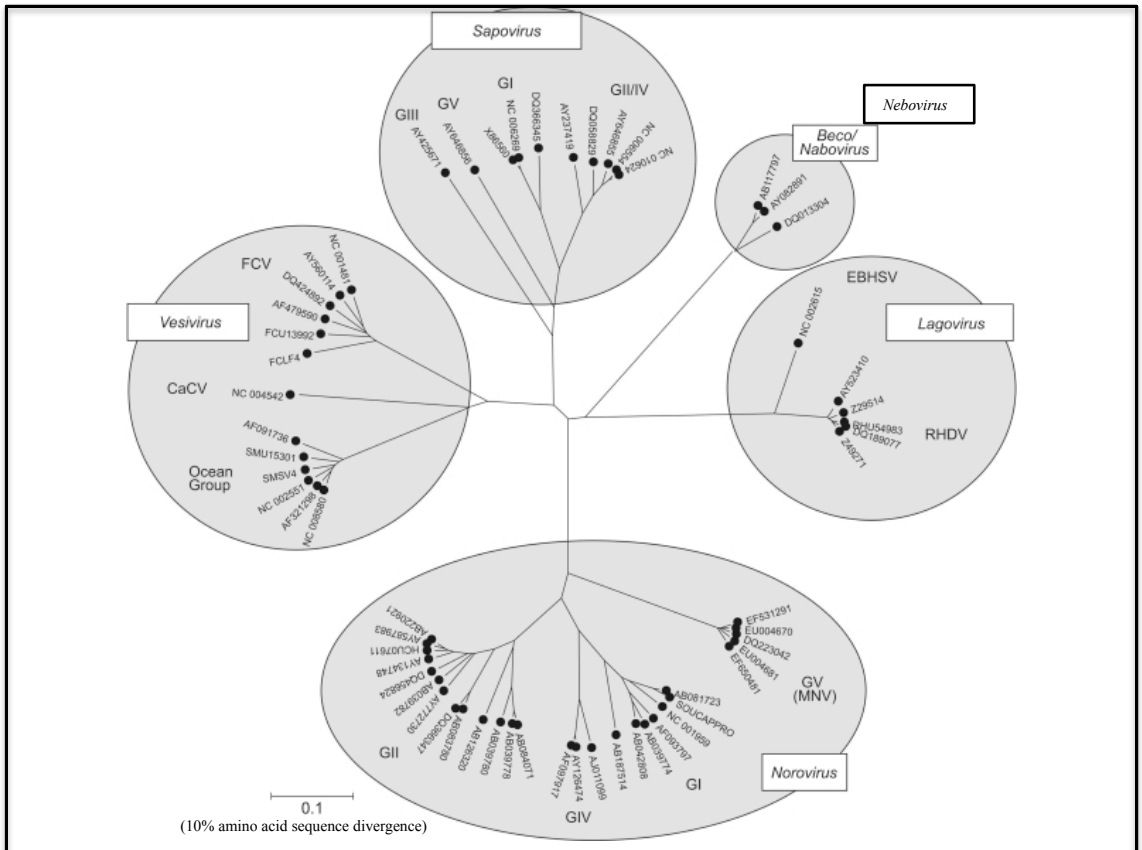

Fig. 1.1. Phylogenetic analysis of caliciviruses. Neighbor-joining phylogenetic tree constructed from pair wise distances based on the amino acid sequence alignment of a region corresponding to the RNA-dependent RNA polymerase (245).

a national program to eradicate the virus. The Secretary of Agriculture declared VESV eradicated in 1959, although the etiological agent of the 1952 outbreak was never determined. Subsequently, a virus was isolated from an aborting sea lion on San Miguel Island, California in 1972 and adapted to growth in Vero cells (248). This virus, designated as San Miguel Sea Lion virus (SMSV), was indistinguishable from VESV serologically and caused vesicular disease when administered to swine; it was proposed as the agent that caused the VES outbreak of 1952 (247, 248). A second important member of the genus *Vesivirus* is feline calicivirus (FCV), which will be described in detail below.

The genus *Lagovirus* has two type species that have been well characterized: Rabbit hemorrhagic disease virus (RHDV) and European brown hare syndrome virus (EBHSV) (130). The genus takes its name from the taxonomic order *Lagomorpha*, which includes the family *Leporidae* (rabbits and hares). Rabbit hemorrhagic disease virus (RHDV) was first described in 1984 with the deaths of Angora rabbits in the Jiangzu province in the People's Republic of China (150). Subsequent studies found that serum samples from 1978 were positive for RHDV (227), and that viral RNA could be detected in tissue samples dating back to the 1950s (176). Similarly, EBHSV was first reported in 1980, and a serum sample collection from 1971 samples that were positive by ELISA for EBHSV (47), and paraffin-embedded tissue samples dating to the 1970s were retrospectively identified as positive by RT-PCR (232). Pathogenic strains from both RHDV and EBHSV have high lethality rates (81, 87, 196), and disease in both cases is characterized by hepatocyte degeneration and liver necrosis (81). In 1989, the governments of Australia and New Zealand initiated studies to determine whether RHDV

could be used as a biological agent to control the population of wild rabbits, an approach that had previously been attempted in the 1940s with the poxvirus, myxoma virus (75). Having first established the species specificity of RHDV in quarantined facilities (142), field studies were established off the coast of the Australian mainland on Wardang Island (the same island used for field studies with myxoma virus) to test for virus spread and persistence among European rabbits native to Australia. Spread of the virus outside the designated quarantined pens, albeit still on the island, was first detected on September 25,1995, and by October 12, 1995 the virus had reached the mainland (131). The virus rapidly spread throughout the mainland, and one outbreak in a national park was associated with a 95% fatality rate (178). However, since the unintentional release of RHDV in Australia, rabbit populations have steadily increased and they continue as environmental and economic pests.

The genera *Norovirus* and *Sapovirus* contain viruses that predominantly infect humans, although their host ranges have been expanding as more sensitive methods of detection are employed. In 1968, a gastroenteritis outbreak occurred at an Elementary school in *Nor*walk, Ohio affecting half the students and teachers (116/232) (2). It had been determined that the cause of gastroenteritis was not of bacterial origin because bacteria-free stool filtrates from sick patients caused gastroenteritis when administered orally to adult volunteers (64). The etiological agent that caused the gastroenteritis was discovered with a "particle virology" approach of using immune electron microscopy (IEM) that was implemented at the NIH by Dr. Albert Kapikian (123). Using the relatively new technique of IEM along with paired sera from volunteers in a challenge study, Kapikian et al. were able to show that there was a specific antibody response to

what was then called the Norwalk agent (124). Since its discovery, it is now clear that human norovirus is the most common cause of gastroenteritis outbreaks (44) and it is estimated to cause ~200,000 deaths/year in children of developing countries (203). There is presently no cell culture that can support the replication of human noroviruses, although the "molecular age" of human noroviruses can arguably be said to have begun in 1990 with the cloning of the Norwalk virus genome (291). Another major advance in the study of human norovirus was the development of virus-like particles (117), which is currently being tested as a potential vaccine candidate (12, 28).

A few years after the Norwalk agent had been established as the cause of the gastroenteritis outbreak at the elementary school in Norwalk, Ohio Chiba et al. described a virus that caused gastroenteritis disease in infants and children at an infant home in Sapporo, Japan (52). Virus particles were purified from stool samples collected from the same infant home and used to raise hyperimmune sera in guinea pigs in order to antigenically characterize the virus, which was found to be antigenically distinct from the Norwalk virus by IEM (181). After the genetic characterization of this virus strain, and other strains, it was clear that it was a member of the family *Caliciviridae* and it was chosen as the prototype strain of the genus *Sapovirus*. While not as widespread as human norovirus, sapoviruses have primarily been detected in young children (51).

The genus *Nebovirus* is the most recent one to be established (40). The type species is Newbury-1 virus, which was experimentally shown to cause diarrhea when given to gnotobiotic calves (98, 289). Antigenically distinct strains have been described (33), but the epidemiology and prevalence of neboviruses has not yet been determined. Other *Nebovirus* strains isolated from calves with diarrhea have been described (62, 246),

and while the virus has been used for pathogenesis studies in challenge studies with gnotobiotic calves, there is no cell culture system available or a reverse genetics system.

1.2. Disease and epidemiology

1.2.1. Feline Calicivirus

FCV is an important veterinary pathogen that causes upper respiratory tract disease in cats. Despite its link to conjunctivitis, oral ulceration and respiratory disease (86, 207, 220), it was first isolated from the gastrointestinal tract of a sick cat (74). The clinical outcome of an FCV infection can be varied and the role of host and viral factors in determining virulence is not understood. A thorough longitudinal study that involved more than 6800 cats over a 9-year time-span found that FCV was detected in ~20% of the cats (101), and similar prevalence levels have been reported in a more recent publication (25). In one longitudinal study, FCV was detected in ~30% of cats with upper respiratory disease, and in 44% of cats that presented with chronic gingivitis/stomatitis alone (101). Asymptomatic shedding has been documented in the literature. For example, a recent longitudinal study in a group of catteries identified long-term shedders that had no overt clinical signs (54), consistent with previous findings in asymptomatic cats (25, 54, 55, 205, 221).

While FCV has generally been considered self-limiting in most cases, a particularly virulent FCV strain was described in 1998 that caused febrile hemorrhagic disease with a high mortality rate ranging from 33-50% (204). The strain was subsequently designated as virulent-systemic FCV (VS-FCV), and additional outbreaks have been reported (56, 208, 238). An epidemiologic study carried out by Pederson et al.

reported that at least 26 of the 54 affected cats in one VS-FCV outbreak had a history of vaccination, suggesting that current vaccines may not fully protect (114). Furthermore, in a small challenge study, it was observed that immunization with the vaccine strain resulted in a less severe outcome when challenged with FCV-ari (204), although the same was not true in vaccinated cats that were naturally exposed to a different virulent strain, FCV-kaos (114).

1.2.2. Murine Norovirus

In 2003, murine norovirus (MNV) was discovered as an agent causing disease in severely immunocompromised transgenic mice (*Rag2*$^{-/-}$/*Stat1*$^{-/-}$) at a U.S. university research facility (127). Subsequently, it was shown that MNV has a tropism for dendritic cells and macrophages (287), and a cell culture system for MNV was established in a macrophage-like cell line (RAW264.7) that has led to advances in the understanding of norovirus biology. Murine norovirus is characteristically asymptomatic in immunocompetent mice, and several studies have shown a high prevalence of MNV in laboratory mice (16, 206, 282). Given its prevalence, one concern was that MNV might act as a confounding factor in studies involving immunocompromised transgenic mice. The presence of MNV did not negatively affect the recovery of the Friend retrovirus (7, 104), or the adaptive immune response to vaccinia virus and influenza virus (104), and it did not affect a bacterially-driven mouse model of inflammation-associated colon cancer (140). However, MNV was associated with an acceleration of bacteria-induced inflammatory bowel disease (141), and subtle changes in the lymphoid tissue of a mouse model for obesity and insulin resistance (201).

A recent study determined that MNV is prevalent also in wild mouse populations (249), but there have been no reports of MNV causing disease in wild mice. Several different strains of MNV have been characterized (111, 269), and while they have distinct biological characteristics, it appears that there is only one MNV serotype (112, 269). Some of the diseases displayed by immunocompromised mice include hepatitis, peritonitis, and pneumonia (282), and MNV continues to be a concern for biomedical studies that involve immunocompromised transgenic mice. Due to its genetic relatedness to human norovirus, the availability of a small animal model and a reverse genetics system, MNV is currently the most widely adopted model to study the basic biology of noroviruses.

1.2.3. Human Noroviruses

Since its discovery as the etiological agent of an acute gastroenteritis outbreak that occurred in 1968 (124), human norovirus has become established as the leading cause of acute gastroenteritis outbreaks (44). Norovirus outbreaks are common in enclosed areas such as cruise ships, schools, hospitals and nursing homes and the majority of outbreaks occur in the winter (228, 278). Norovirus disease is characterized by a short incubation period (~24-48 hr), followed by symptoms that can include diarrhea, vomiting, nausea and abdominal pain that characteristically resolve within approximately 72 hr. This clinical description of the course of a norovirus infection is consistent with that reported in the 1968 outbreak (124), and has been further corroborated in volunteer studies (12, 63, 64, 94, 290) and outbreak investigations (10, 125, 151, 226, 240).

An interesting aspect of human noroviruses is that despite the wide genetic diversity (298), one genotype in particular, GII.4, is the cause of the majority of the reported outbreaks worldwide (27, 85, 120, 135, 242, 243, 273, 274). Furthermore, specific strains within GII.4 tend to predominate until replaced by another GII.4 strain (27, 35, 71, 134, 193, 213, 241, 277, 281, 285). An "epochal evolution" hypothesis has been used to explain successive strain replacements (39, 145, 146, 244), which proposes the emergence of new lineages followed by large-scale epidemics. Virus-like particle (VLP) vaccine candidates have been tested for protection against homologous challenge (12, 28), but it remains to be determined how successful they will be in providing cross-protection against heterologous viruses.

1.3. Morphology and Genome Organization

The RNA genome of caliciviruses ranges in size from approximately 7.3-8.3 kb, and typically encode 8-9 viral proteins from two (*Sapovirus, Nebovirus, Lagovirus*) or three ORFs (*Norovirus, Vesivirus*) (Fig. 1.3 A). A unique ORF 4 was recently identified and characterized in murine norovirus (166). The 5'-end of the calicivirus RNA genome is covalently linked to a viral protein, VPg, which serves as a cap substitute for viral protein translation, and the 3'-end is polyadenylated (106, 172, 188, 237). The genomic RNA serves as a template for translation of the ORF1 nonstructural proteins, which are released from a large polyprotein via proteolytic cleavage by the viral protease (254, 259). An approximately 2.2-2.6 kb subgenomic bicistronic RNA is used for translation of VP1 and VP2 (106, 189).

Calicivirus virions, which are non-enveloped, are characterized as having a T=3 icosahedral symmetry, and are formed by 90 dimers of the major capsid protein, VP1 (Fig. 1.3 B). The first three-dimensional description of a calicivirus virion structure was reported in 1994, and was achieved by applying electron cryomicroscopy and computer image reconstruction to the analysis of a purified primate vesivirus (217) and a human norovirus VLP (218). These seminal studies were the first to confirm the T=3 icosahedral symmetry that had been proposed previously (6, 37, 210), and they were the first to determine subdomains of the VP1: shell (S), and protruding (P) domains 1 and 2 (Fig. 1.3 C). It is interesting to note that the T=3 icosahedral symmetry is rarely found in animal viruses, although it is commonly observed in plant viruses, and is only found in one other animal virus family, *Nodaviridae* (110). The virion contains 180 copies of VP1, and an estimated 1-10 copies of the minor structural protein VP2 in the virion (89, 90, 255, 286). The VP2 is essential in the production of infectious virions, but the mechanisms involved in this function are not known (252).

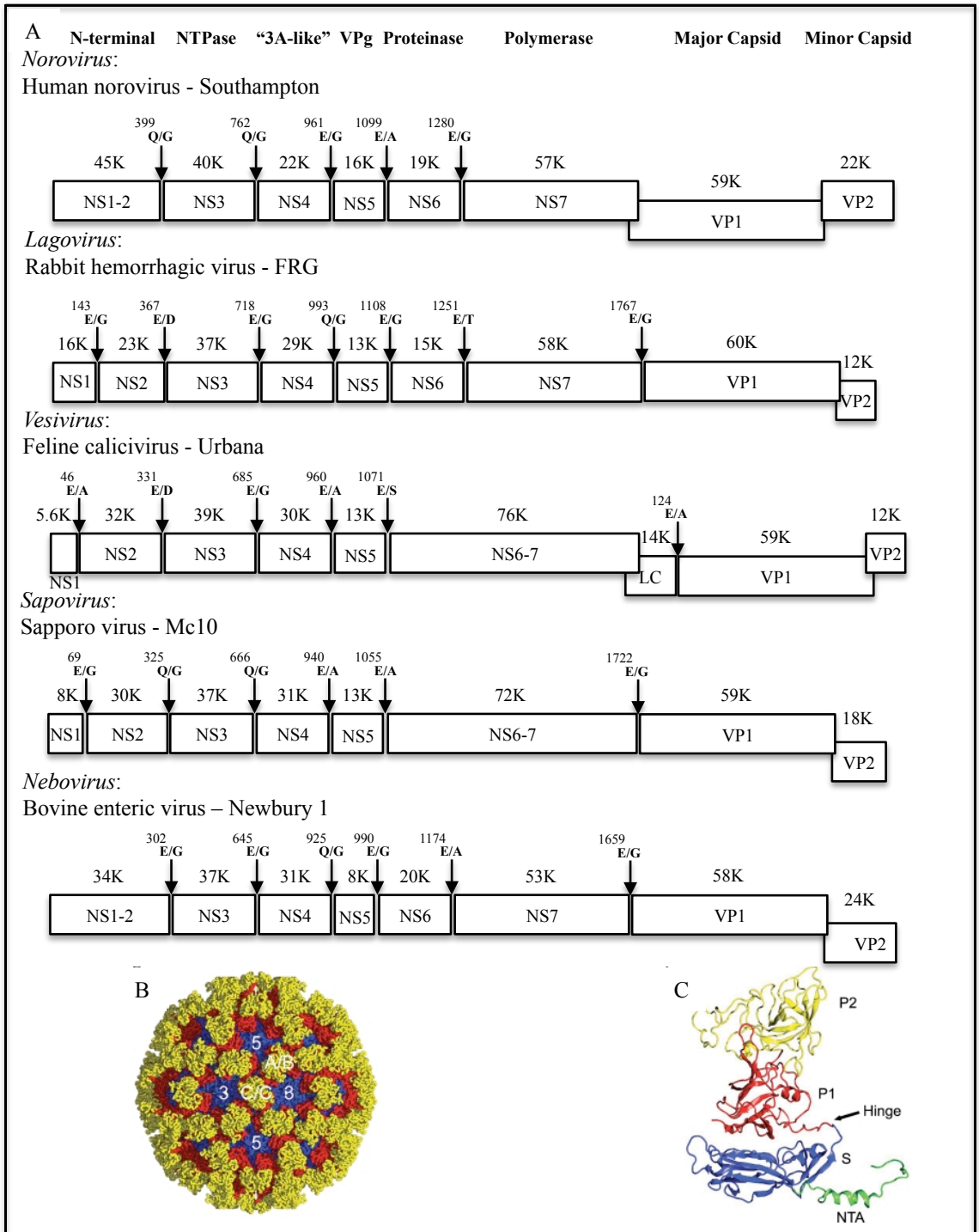

Fig. 1.3. Schematic diagram of genome organization of caliciviruses and virion morphology of FCV. (A) Genome organization of representative strains from the five genera. (B) X-ray structure of FCV-5. (C) Ribbon representation of the virion subunit structure. B and C adapted from Ossiboff et al. 2010.

1.4. Viral Proteins

Caliciviruses encode two (lagoviruses and sapoviruses), three (vesiviruses and noroviruses) or four ORFs (only MNV). ORF1 encodes a polyprotein that is post-translationally processed by the viral protease to release the mature nonstructural proteins (and VP1 as well, depending on the genus). Due to similarities that exist between picornaviruses and caliciviruses, it was proposed that the cleavage of ORF1 might yield functional precursor intermediates, similar to the picornaviruses (202). Intermediate precursors have been detected in the caliciviruses. For example, FCV produces a fully processed NS1 and NS2 as well as a functional and stable NS6-7 (254), while noroviruses produce a stable NS1-2 precursor and a fully processed NS6 and NS7 (20, 253). Additionally, calicivirus nonstructural proteins share functional motifs with the picornaviruses (185). Sapoviruses, lagoviruses, and neboviruses encode the major structural protein (VP1) in ORF1, contiguous with the nonstructural proteins, and vesiviruses and noroviruses encode VP1 in ORF2. A feature common to all caliciviruses is the presence of the VP2 gene, encoded in a separate ORF, near the 3'-end.

1.4.1. NS1-NS2

The first protein encoded in the calicivirus ORF1 is the "N-terminal" protein (NS1-2). During FCV replication, NS1-2 is efficiently processed to release the mature NS1 (5.6 kDa) and NS2 (32 kDa), but in the noroviruses it is expressed as a stable NS1-2 precursor. NS1-2 proteins vary in sequence and predicted molecular mass, although three domains have been defined in the noroviruses: a highly variable N-terminus, a central domain that contains an H-box and NC motifs, and a hydrophobic C-terminal domain

predicted to interact with membranes (68, 76). The H-box/NC motif, which is found in the class II tumor suppressor protein H-rev-107, is shared with its picornavirus counterpart, 2B, and is predicted to play a role in the control of cell proliferation (113). Transient expression studies of human norovirus NS1-2 showed that it interacts with membranes and with the cellular protein VAP-A, which is involved in ER/Golgi transport (68). In addition, the NS1-2 disrupts the Golgi apparatus, and the disassembly of the Golgi was mapped to the N-terminal region of the protein (76).

1.4.2. NS3 (NTPase)

Sequence analysis of the NS3 protein suggests it encodes a viral helicase (92, 185). Biochemical studies have determined that it binds NTPs and possesses NTPase activity (160, 211), although there is no experimental evidence that it can unwind an RNA duplex. Transient expression of NS3 in the MNV-permissive cell line, RAW264.7, induces membrane rearrangements similar to those observed during an MNV infection (100). The ability of NS3 to interact with membranes and cause membranous vesicles similar to what is observed during MNV infection suggests it may play a central role in the formation of replication complexes. Furthermore, mutagenesis studies mapped the membrane interacting domain to the N-terminus (100). A yeast two-hybrid assay performed using viral proteins found that NS3 interacts with NS2 (122), suggesting that NS3 may act as a scaffolding protein as replication complexes are being established during infection.

1.4.3 NS4

NS4 is the proposed counterpart of the 3A poliovirus protein, and recent studies show that it may have a similar function. The poliovirus 3A blocks cellular protein secretion by blocking ER-to-Golgi traffic (53), and the human norovirus NS4 also acts as an antagonist of ER/Golgi trafficking (239). Despite this finding, a di-acidic motif critical for blocking the ER/Golgi trafficking is present only in human norovirus NS4 sequences and not other calicivirus NS4 proteins, including the closely related murine norovirus. Additionally, NS4 is found as an NS4-NS5 (VPg) precursor (253, 254), similar to what is observed for picornaviruses (3AB) (293). It is possible that the NS4-NS5 mimics 3AB in which it acts as a membrane anchor for the VPg protein to assist virus RNA synthesis within the replication complexes.

1.4.4. NS5 (VPg)

NS5 is a small protein (13-15 kDa) known also as *v*irus *p*rotein, *g*enome linked (VPg). VPg is linked to the viral genome at the 5'-end and VPg proteins are found in several virus families, including the animal virus family *Picornaviridae* (139) , the plant virus families *Secoviridae*, *Potyviridae*, and *Luteoviridae*, and the unassigned plant virus genus *Sobemovirus* (115). The VPg proteins from caliciviruses are thought to be involved in three important steps of the virus life-cycle: replication, translation and packaging. *In vitro* studies have demonstrated that the VPg becomes nucleotidylated by the viral polymerase (19, 158, 230). This modification is thought to be essential for viral replication, with the nucleotidylated VPg serving as a primer for template-dependent synthesis of the viral genome similar to the picornaviruses (175). The tyrosine involved

in the linkage of VPg to the viral genome has been determined for both FCV (172) and MNV (99). In contrast to poliovirus, caliciviruses do not have an *i*nternal *r*ibosomal *e*ntry *s*ite (IRES), and the VPg has been proposed to play a key role in driving translation of the viral genome. RNA extracted from purified virions becomes significantly less infectious if treated with proteinase K (37, 67, 106), and studies have shown that VPg interacts with several eukaryotic translation initiation factors (48, 60, 61, 91). The exact role of VPg in packaging has not yet been determined, but the VPg-linked genome is essential for the production of infectious virus (106).

1.4.5. NS6 and NS7 (protease and polymerase)

NS6 (chymotrypsin-like protease) and NS7 (RNA-dependent RNA polymerase) are the viral proteins that have been most extensively characterized. At the primary sequence level, NS6 shares some homology with the 3C proteases of picornaviruses (32, 73, 118, 148, 186, 246). Mutagenesis (26, 32, 147, 197, 254, 259) and protease-inhibitor (26, 250, 257) studies confirmed that calicivirus proteases contain a cysteine in the active site, similar to the picornaviral proteases. Studies suggest that the viral protease alone is sufficient for mediating the cleavage of ORF1 and the cleavage sites have been mapped for representative lagoviruses, noroviruses and vesiviruses (20, 121, 149, 169, 198, 253, 254). Two solved structures for the viral protease have been published (180, 296), confirming the predicted similarities to the picornaviral proteases and the presence of a cysteine-histidine dyad in the active site.

NS7 encodes the RNA-dependent RNA polymerase (RdRp), which shares significant homology with the picornavirus RdRp (185, 276). NS7 plays an essential role

in replication of the viral genome and in the production of the subgenomic RNA that serves as a template for translation of the structural proteins. Several recombinant forms of the polymerase have been successfully expressed and *in vitro* studies have determined that they are active for RNA synthesis and exhibit template-dependent activity (18, 83, 275, 276, 284). As mentioned above, the polymerase nucleotidylates VPg and this enzymatic process is likely important in virus replication. Several structures of the calicivirus RdRp have been solved (84, 191, 192, 295) and all demonstrate a 'right hand' conformation with canonical ringer, palm, and thumb domains.

1.4.6. LC (leader of the capsid)

The leader of the capsid, LC, is a protein unique to the genus *Vesivirus*, and little is known about its structure and function. The precursor cleavage event that releases the LC from the mature VP1 occurs shortly after the capsid precursor is translated (41, 43, 257) and is essential for a productive virus infection. Recent data suggests that the LC enhances the replication of the Norwalk norovirus RNA replicon (46), in association with an increase in low density lipoprotein receptor mRNA levels (45); however, the mechanism of enhancement is not clear. It has been proposed that the LC may function as a nonstructural protein because it was not detected in purified FCV virions (272). The LC is diverse in sequence and in length among vesiviruses, and is discussed in further detail below.

1.4.7. VP1 (major capsid protein)

VP1 is the major capsid protein. The role of VP1 in virus assembly is described above along with several virion structures that have been solved. The protein itself is divided into two domains: a conserved *s*hell domain (S), and a *p*rotruding domain (P) that is subdivided further into P1 and the hypervariable region P2 (216). VP1 forms stable dimers, and 90 dimers interact to form the virus particle. The S domain forms the internal T=3 icosahedral sphere-like structure in which the RNA genome is packaged. The P domain interacts among dimers, forming protrusions that bind functional receptors and attachment factors. The only functional receptor that has been described for a calicivirus is the *j*unction *a*dhesion *m*olecule 1 (JAM-1) for FCV (22, 23, 159, 199), while carbohydrates have been described as attachment factors for RHDV (233), human noroviruses (161, 264), and MNV (128, 265).

1.4.8. VP2 (minor capsid protein)

VP2 is a minor structural protein that is expressed from a separate ORF by all caliciviruses. Only a few copies, 1-10, of VP2 are present in an infectious virion (89, 90, 255, 286). VP2 proteins vary greatly in length, ranging from 106 (FCV) to 225 (nebovirus) amino acids (Fig. 1.3 A), and its function has not yet been determined. One possible role for VP2 may be to confer stability to the major capsid protein VP1 (21), although VP1 alone is sufficient to self-assemble into virus-like particles. Due to the basic nature of VP2, it has been proposed to stabilize the acidic viral RNA during assembly of infectious particles (189, 216, 286).

Although encoded in the same subgenomic RNA, studies suggest that the level of VP2 expression corresponds to approximately 10% of that of VP1 (105). One possible explanation for the lower levels of VP2 expression is the mechanism by which VP2 is expressed. It was initially postulated that VP2 expression was regulated at the translational level (105, 189). The mechanism that has been proposed to explain expression of VP2 involves termination/reinitiation of the ribosome (156, 157, 167, 168). An important finding that supports this mechanism was the identification of a sequence upstream of the VP2 coding sequence that has been termed "termination upstream binding site" (TURBS). The mechanism proposes that upon termination of the translation of VP1, the 60S large subunit of the ribosome becomes detached, the 40S small subunit is repositioned to the initiation codon of VP2. At this point, the 60S subunit forms a complex with the 40S subunit and translation "reinitiates" to express VP2.

1.5. FCV virus life cycle

Several steps involved in the life cycle of FCV have been determined and are summarized in Figure 1.5. Junction adhesion molecule 1 (JAM-1) has been identified as the functional receptor for attachment of FCV and entry into the host cell (159). Transient expression of JAM-1 in non-permissive cell lines (hamster lung cells, 293T cells) conferred susceptibility to several FCV strains. JAM-1 residues important for the interaction with the FCV virion have been mapped to the D1 domain, although all of the JAM-1 domains are required to confer susceptibility when provided transiently in non-permissive cell lines (199).

Upon engagement of FCV with JAM-1, penetration into the host cell occurs by clathrin-mediated endocytosis (132, 133, 262). Furthermore, endosome acidification is required for successful viral entry, suggesting that it may be an early step involved in the uncoating of the virion (262). Interaction of the FCV virion with JAM-1 induces structural changes of the virion providing an additional mechanism for the uncoating of the virion (22, 23, 200).

Once the virion has uncoated, the VPg-linked positive-strand viral RNA serves as a template for translation of the ORF1 viral proteins. FCV VPg interacts with the initiation factor eIF4E and this interaction has been proposed as a key step in recruiting the ribosome for viral protein translation (91). This is consistent with studies that have shown that other calicivirus VPg proteins interact with translation initiation factors and that these interactions are essential for expression of the viral proteins (48, 60, 61).

The processed ORF1 polypeptide releases intermediate and mature forms of the viral proteins (254, 257, 259), which in turn establish membrane bound replication complexes (RC) in the cytoplasm, a common theme of positive strand RNA virus replication (170). Establishment of replication complexes is characterized by gross rearrangement of host cellular organelles (152, 263), and enzymatically active RCs can be isolated from infected cells (95). Transient expression of NS2, NS3, and NS4 results in co-localization of the viral proteins with endoplasmic reticulum (ER) markers and expression of NS3 and NS4 alone can disrupt the ER (15), suggesting that the ER may be a source of membranes for the formation of RCs.

Viral RNA replication occurs within the RCs and is a multi-step process. Similar to other positive-strand RNA viruses, FCV has to switch from translation to replication,

and produce excess amounts of positive-strand RNA genomes via a negative-strand intermediate in order to assemble new infectious virions (4, 143). A common mechanism by which all caliciviruses switch from translation to replication has not been determined, but for FCV it has been proposed that the host cellular protein, polypyrimidine tract binding protein (PTB), is recruited from the nucleus to the RC early on during the viral infection (126). Once recruited to the RC, PTB interacts with the 5'-end of the FCV genome and acts as a negative regulator of translation, driving the switch from translation to replication either directly, or by recruiting other proteins.

The viral RNA-dependent RNA-polymerase (expressed as a fusion protein with the viral protease in the case of FCV) drives transcription of the negative-strand RNA. The negative-strand RNA serves as a template for synthesis of the positive-strand viral genome and subgenomic RNA (106, 174, 189). The mechanism by which caliciviruses generate their abundant positive-strand subgenomic RNA is not clear (171). Studies of RHDV suggest that the subgenomic RNA is generated by an internal initiation mechanism on the genome-length negative strand (174). It should be noted that negative-sense subgenomic RNA is detected during FCV infection (42, 95), and it remains to be determined whether this represents a functional template for new RNA synthesis, or is simply a by-product of transcription.

Many details of virion assembly have yet to be determined, but the virion itself is well characterized (described above). Virions are formed by 180 copies of the major capsid protein (VP1) and 1-10 copies of the minor capsid protein (VP2). Packaged within the virion is the full-length genome that is linked to the viral protein VPg at the 5'-end. It is not clear how efficiently packaging occurs, because a significant proportion of virions

are packaged with subgenomic RNA which is not infectious (187). A packaging signal has not been identified, but because subgenomic RNAs can be packaged into virions, assembly may require an interaction between the 3'-end of the genome, or VPg, with VP1 or VP2. Deletion mutants that lacked a VP2 could replicate, but they were not able to produce infectious virus, indicating a crucial role for VP2 in virion maturation (252).

The final step in the virus life cycle is release of the assembled virions in order to further propagate infectious virus. As a non-enveloped, cytopathic virus, FCV is released as cell lysis occurs. For FCV in particular, several studies have determined that apoptosis is induced during viral replication (182, 225, 256), providing at least one mechanism by which the plasma membrane of the cell is permeabilized to allow release of newly formed particles.

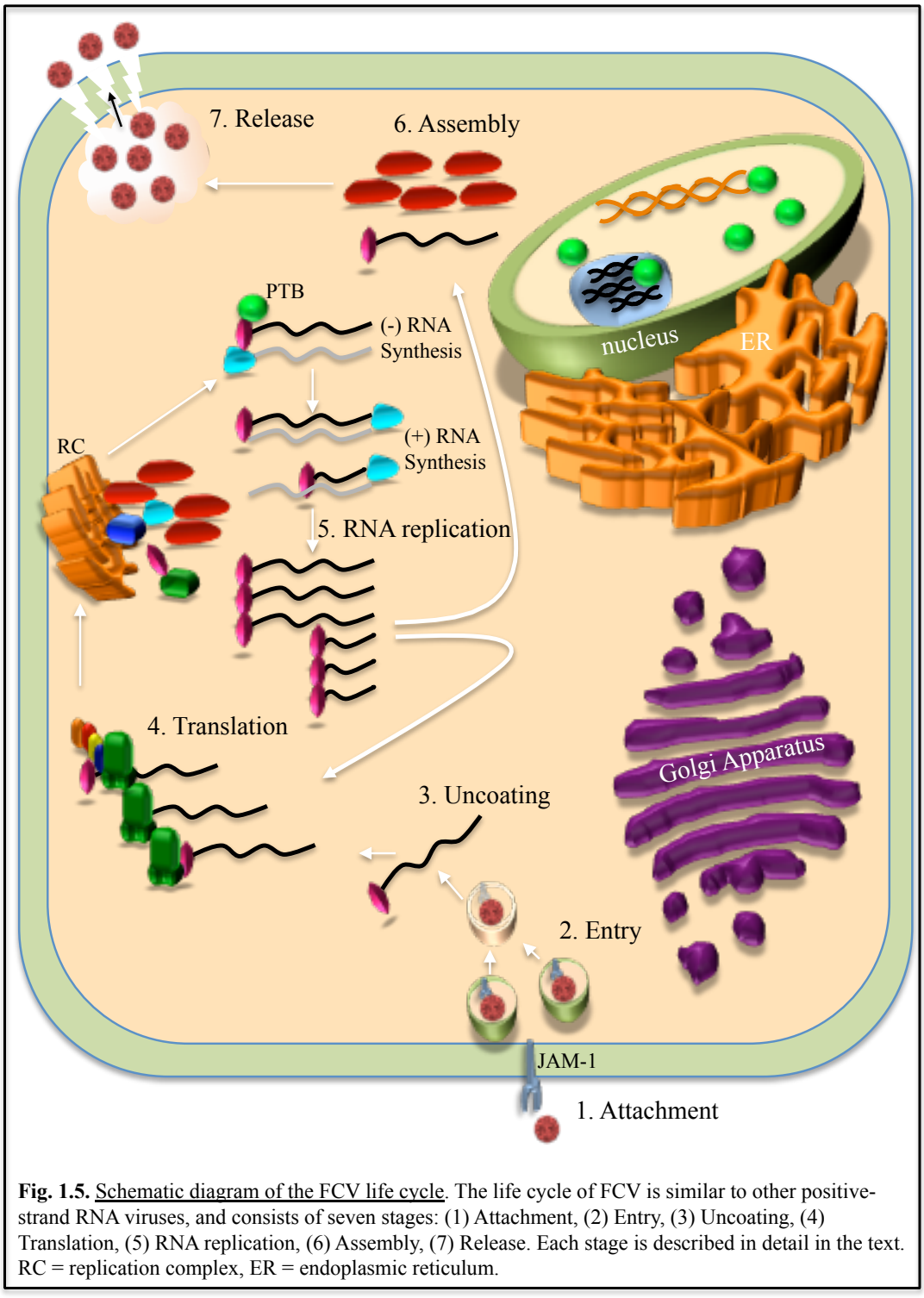

Fig. 1.5. Schematic diagram of the FCV life cycle. The life cycle of FCV is similar to other positive-strand RNA viruses, and consists of seven stages: (1) Attachment, (2) Entry, (3) Uncoating, (4) Translation, (5) RNA replication, (6) Assembly, (7) Release. Each stage is described in detail in the text. RC = replication complex, ER = endoplasmic reticulum.

1.6. Reverse genetics of FCV

The first reverse genetics system for the family *Caliciviridae* was for FCV, and it was based on the transfection of full-length RNA into a susceptible cell line, (251). A plasmid-based recovery system was subsequently reported in which a modified vaccinia virus (MVA-T7) was used to provide the T7 bacteriophage RNA polymerase in *trans* (258). These two systems for recovery of infectious FCV were based on the Urbana strain (Figure 1.6), which was isolated from a sick cat at the University of Illinois Veterinary School, Urbana, Illinois. A plasmid-based reverse genetics system has been developed for the FCV vaccine strain 2024 (271).

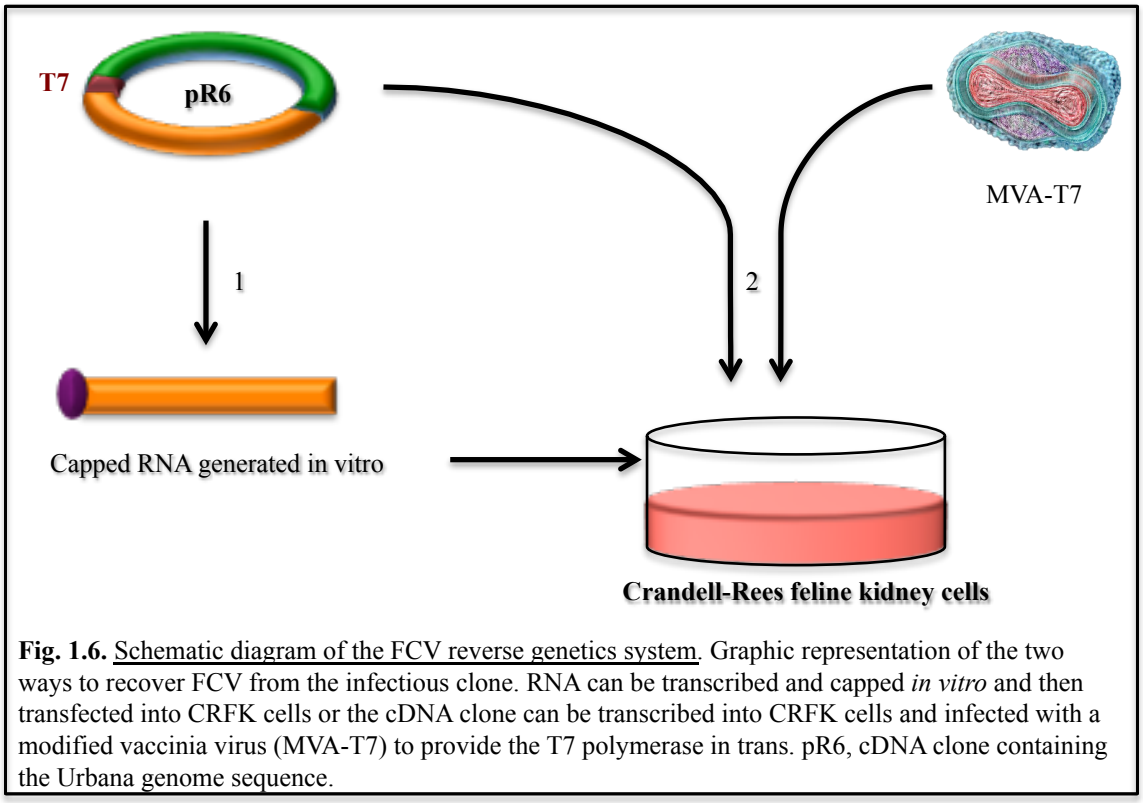

Fig. 1.6. Schematic diagram of the FCV reverse genetics system. Graphic representation of the two ways to recover FCV from the infectious clone. RNA can be transcribed and capped *in vitro* and then transfected into CRFK cells or the cDNA clone can be transcribed into CRFK cells and infected with a modified vaccinia virus (MVA-T7) to provide the T7 polymerase in trans. pR6, cDNA clone containing the Urbana genome sequence.

The availability of a reverse genetics system facilitated several important findings regarding the basic biology of caliciviruses. The fact that *in vitro* transcribed full-length RNA with a cap analogue was infectious provided further support that one important role for VPg was to drive viral protein translation (see section 1.4.4). Another important finding was that chimeric viruses could be produced using an infectious FCV clone, in which capsid sequences of antigenically distinct FCV strains were swapped (190). The ability to generate recombinant viruses had important vaccine implications, in particular for an RNA virus with a high mutation rate and for which vaccine failure had already been reported (219). An FCV virus expressing green fluorescent protein (GFP) was generated by replacing part of the capsid sequence with GFP, but an intact VP1 was required in *trans* and the assembled virus was infectious for only a single-round of replication (271).

1.7. Transposon mutagenesis

One strategy to engineer recombinant viruses using a reverse genetics system is to apply transposon mutagenesis to the infectious cDNA clone. Transposon mutagenesis employs modified Tn7 transposon proteins and inserts a 15-base pair sequence into infectious cDNA molecules at random sites (24, 58, 209, 260, 261). The mutagenized cDNA clones are then used to recover virus, and those that can tolerate insertions can be characterized. Some of the advantages of using this modified transposon system is that the insertion is small, each cDNA molecule is limited to only one transprimer insertion, the insertion is completely random, and samples can be pooled in order to improve coverage of the region of interest.

1.7.1. Applications in other positive sense RNA viruses

The Tn7 transposon system has been successfully applied to several single-stranded RNA viruses to identify sites within the viral genome that can tolerate and stably express heterologous sequences (11, 173, 266, 267). Generation of recombinant viruses has been used for tracking Hepatitis C virus replication complexes *in vivo* (288), characterization of Sindbis virus replication complexes (93), identification of host cellular binding partners of poliovirus viral proteins (268), and identification of Venezuelan equine encephalitis virus temperature sensitive mutants (17).

1.8. Calicivirus protein-host interactions

As obligate intracellular organisms, viruses require the host cellular machinery for viral replication (179). Replication of (+) RNA viruses is a complex interplay between the virus and host. (+) RNA viruses use host cell organelles and membranes as a scaffold to establish replication complexes (170, 194), and host cellular proteins are co-opted to facilitate replication (280), while the function of many viral proteins is to specifically counteract the host defense response (3).

1.8.1. Host cellular proteins reported to interact with caliciviral proteins

While some of the key stages of the FCV life cycle have been determined, few host cellular proteins have been identified that participate in the viral life cycle of any calicivirus. VPg, linked to the 5'-end of the genome, is involved in translation and has been reported to interact with several elongation initiation factors such as eIF3, eIF4GI,

eIF4E, eIF2a, as well as the ribosomal protein S6 (48, 60, 61, 91). The human norovirus NS1-2 interacts with the SNARE regulator vesicle-associated membrane protein-associated protein A (VAP-A) (68), although its significance is not yet known. It was recently reported that the nucleolar shuttling phosphoprotein, nucleolin, interacts with both the human norovirus and the FCV NS6-7 viral protein (38). Furthermore, gene silencing of nucleolin in CRFK cells resulted in delayed cytopathic effect and reduced viral titers when infected with FCV.

1.8.2. Annexin A2

Annexin-A2 (ANXA2) is a member of the annexin family of proteins that are characterized as proteins that bind negatively charged phospholipids in a Ca^{2+}-dependent manner, and contain a conserved structural element which is referred to as an "annexin repeat" (88). ANXA2 is a multifunctional protein and it is involved in many cellular processes such as fibrinolysis, exocytosis, endocytosis, cell-cell adhesion, and cell motility (88, 224).

ANXA2 is reported to be involved in the life-cycle of other positive-sense single-stranded RNA viruses such as human immunodeficiency virus (HIV) and hepatitis C virus (HCV). In HIV, ANXA2 was first described as a binding partner of the Gag protein, and depletion of ANXA2 resulted in a reduction of infectivity of released virions (234). ANXA2 was subsequently determined to be part of the virion in a proteomics study that analyzed highly purified HIV virions from infected monocyte-derived macrophages (49). Consistent with these findings, another study determined that ANXA2 does not play a

role in virion production but does affect HIV infectivity in a cell-type dependent manner (222).

Similarly, ANXA2 was first identified to be involved in the HCV life cycle with a proteomics analysis of host cellular proteins that co-immunoprecipated with NS3A/NS4 protein (136). Furthermore, purification of the HCV replication complexes identified ANXA2 as an associated host factor, that when silenced, reduced viral titers but did not affect viral RNA replication (14). The proposed mechanism for the involvement of ANXA2 with the replication complex is that it recruits the nonstructural HCV proteins to lipid rafts in order to establish replication complexes (235).

1.9. Aim of the study

Vesiviruses encode a precursor of the capsid protein that is proteolytically cleaved by the virus-encoded proteinase to release two proteins: the leader of the capsid protein (LC) and the mature capsid protein (VP1). It is not clear why the LC protein is unique to vesiviruses, or what role the LC plays in the virus life cycle.

The aim of this study was to determine the evolutionary significance of the LC protein in the *Caliciviridae* and to determine its role in calicivirus replication. I hypothesized that the LC modulates the host cell environment in order to promote viral RNA replication. Molecular tools were devised to perform functional studies to study the significance of the LC in viral replication. The specific aims of this research are:

I. To identify if the LC can tolerate an insertion for protein purification and *in vivo* imaging.

II. To determine functional domains and essential residues of the LC required for FCV replication.

III. To identify host cellular proteins that interacts with the LC.

CHAPTER 2: MATERIALS AND METHODS

2.1. Viruses and Cells

Feline calicivirus strain vR6, derived from the infectious cDNA clone of the Urbana strain designated pR6 (252), will be referred to as wild-type (wt) virus.

Crandell-Rees feline kidney (CRFK) cells were grown in Dulbecco's modified Eagle's medium (designated as maintenance medium, Lonza Inc., Allendale, NJ) containing penicillin (250 U/ml, Mediatec), streptomycin (250 μg/ml, Mediatec) and L-Glutamine (2 mM, Mediatec) supplemented with 10% heat-inactivated fetal bovine serum (Invitrogen Corporation, Carlsbad, CA).

2.2. Construction of intermediate clones for transposon mutagenesis

Intermediate vectors were generated by cloning DNA fragments derived by PCR from pR6 as a template into Invitrogen's Topo TA vector (Fig. 2.2). The amplified and cloned FCV sequences (Table 1) included unique restriction sites, which were used for directional cloning back into the pR6 backbone following transposon mutagenesis.

Oligo	Sequence 5’-3’	Polarity
UrbanaFL5174F	GGCATGACCGCCCTACACTGT	+
UrbanaFL7391R	GCGTTGTTGTCCAAGCGCAGCC	-
UrbanaFL2537F	GTGCTTACTGCCCCTGACAAG	+
UrbanaFL5429R	GGGAGCAATTCAGGATAACAGC	-
pSportF	CTGGGGCCTCGGTGCACATGC	+
UrbanaFL3208R	GCCCCGATCAACTGCCCTAAG	-

TABLE 1. PCR primers used in generation of intermediate clones for transposon mutagenesis

2.3. Construction of cDNA library of FCV clones containing a randomly inserted 15-bp sequence

The protocol developed for the transposon mutagenesis is outlined in Figure 2.2. A cDNA library of Topo subclones with random transprimer insertions was created with the GPS-LS linker scanning system according to the manufacturer's instructions (New England Biolabs, Beverly, MA). The GPS-LS insertion mutagenesis was performed in three major steps: first, a 1383 bp transprimer sequence, that was flanked by PmeI restriction sites and encodes the chloramphenicol resistance gene, was randomly inserted into a DNA target; second, all but 10 bp of the transprimer is removed by PmeI digestion; and finally, the ligation of the mutagenized DNA target resulted in a 15 bp insertion (10 bp from the transprimer which included the PmeI site, and a 5 bp duplication of target DNA created by the transposition reaction).

Upon production of the GPS reaction mixture of an unamplified library of transprimer insertions, 5 µl of the reaction were transformed into competent cells. Competent cells were grown for 1 hour at 37°C with 600 µl of Super Optimal broth with Catabolite repression (S.O.C.) medium (Invitrogen). Two hundred µl of the cell mix were added to 3 plates containing both chloramphenicol and kanamycin to select for transformants, and incubated overnight at 37°C. Ten ml of lysogeny broth (LB) were added to the plates and the colonies were scraped and collected. Plasmid DNA was purified from the resuspended colonies using a DNA Mini-Prep kit (Qiagen, Valencia, CA). The three samples of DNA plasmid were then proportionally combined into a pool that contained approximately 3 µg of DNA. One µg of pooled DNA was digested using the restriction enzyme that flanked the region of interest, and separated on a 1% agarose

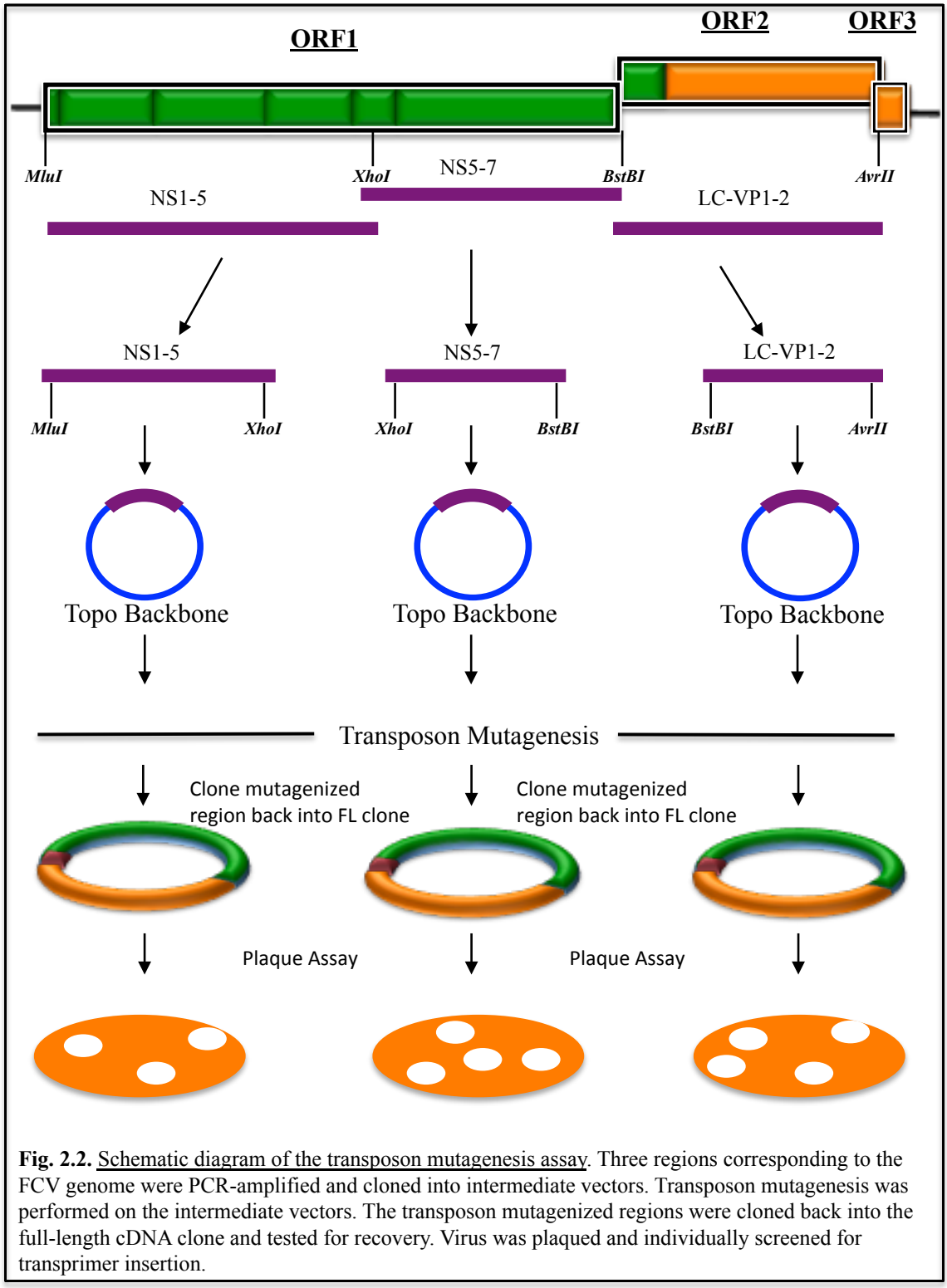

Fig. 2.2. Schematic diagram of the transposon mutagenesis assay. Three regions corresponding to the FCV genome were PCR-amplified and cloned into intermediate vectors. Transposon mutagenesis was performed on the intermediate vectors. The transposon mutagenized regions were cloned back into the full-length cDNA clone and tested for recovery. Virus was plaqued and individually screened for transprimer insertion.

gel. The scanned region of interest plus the transprimer insertion was identified based on its size, and gel purified. The region of interest plus the transprimer insertion was ligated back into the parental full-length cDNA backbone of the pR6 plasmid, and transformed into competent cells. Identical to the previous pooling step, competent cells were grown for 1 hour at 37°C with 600 µl of S.O.C. medium. Two hundred µl of the cell mix were added to 3 plates containing both chloramphenicol and carbenicillin to select for transformants, and incubated overnight at 37°C. Ten ml of LB broth were added to the plates and the colonies were scraped and collected. Plasmid DNA was purified from the resuspended colonies as described above and three samples of DNA plasmid were then proportionally combined into a pool that contained approximately 3 µg of DNA. One µg of the pool was digested using the restriction enzyme PmeI. The digestion reaction was separated on a 1% agarose gel, and the parental backbone, minus the transprimer, was excised and gel purified. The pool of mutagenized parental backbone was religated, and transformed into competent cells. Identical to the previous pooling steps, competent cells were grown for 1 hour at 37°C with 600 µl of S.O.C. media (Invitrogen). The cell mixture (200 µl) was added to 3 plates containing carbenicillin to select for transformants, and incubated overnight at 37°C. Ten ml of LB broth were added to the plates and the colonies were scraped and collected. Plasmid DNA was purified from the resuspended colonies as above, and the three samples of DNA plasmid were then proportionally combined into a pool that contained approximately 5 µg of DNA. Two µg of the final pool of mutagenized full-length FCV, containing 15-nt insertions randomly distributed in the regions of interest were used to test for recovery of virus.

2.4. Recovery of virus

Virus was recovered from plasmid DNA by using the MVA/T7 expression system, described above (254). Confluent CRFK cell monolayers in 6-well plates (approximately 2 × 10^6 cells) were infected with MVA/T7 (a gift of Dr. Bernard Moss, NIAID, NIH) at an MOI of 10 and incubated for 1 h at 37°C. The supernatant was removed, and 2 ml of maintenance media were added to the cells. Transfections were carried out using Lipofectamine 2000 (Invitrogen) according to the manufacturer's instructions. Following incubation for 24-48 hours at 37°C, medium from the transfected cell monolayer was transferred to a fresh cell monolayer, which was monitored for the development of viral CPE. If CPE was observed, the supernatant was used to perform a plaque assay, and individual plaques were analyzed.

To confirm that recovered virus originated from the engineered constructs, reverse-transcriptase (RT)-PCR products derived from viral RNA were analyzed by direct sequencing. RNA was purified using the RNeasy mini kit (Qiagen). As a control for the presence of DNA from the original plasmid used to synthesize the RNA for transfection, PCR was performed on the isolated viral RNA in the absence of RT.

2.5. Construction of recombinant FCV infectious clones

To reconstruct the recovered transposon-modified virus, the RNA extracted from the plaque of a mutagenized virus that contained a 15- nt insertion in the LC (encoding a PmeI restriction site; Table 1) was used for RT-PCR amplification using the following primer pair that is complementary to the FCV genome: sense primer UrbanaFL5174F and antisense primer UrbanaFL7391R. This DNA fragment was treated with BstBI and AvrII

and subsequently cloned back into the infectious cDNA clone pR6 using the same restriction sites to reconstruct the mutagenized LC viral sequence. The reconstructed plasmid containing the 15-nt insertion in the LC protein was designated pR6-LC-15.

The multiple cloning site was then inserted into the pR6 clone using a QuikChange XL Site-Directed Mutagenesis kit (Stratagene's, La Jolla, CA) and PCR mutagenesis. The infectious clone with the multiple cloning site was designated pR6- LC (Fig. 3.3A).

The DsRed and GFP monomeric proteins were PCR-amplified using the pDsRed-Monomer-N1 and pAcGFP1-Monomer-N1 vectors as templates (Clontech), respectively, to include bordering KpnI and AflII sites that flanked a ‘linker’ amino acid (GGS) sequence (Table 2). The PCR amplified DsRed or GFP fragments were digested, purified, and ligated into the KpnI and AflII sites of the pR6-LC clone using a Rapid Ligation kit (Roche). The resulting plasmids were designated pR6-LC-GFP and pR6-LC-DsRed (Fig. 3.3B).

Oligo	Sequence 5'-3'	Polarity
DsRedKpnIF-GGS	GGATCCACCGGTCGCCACCATGGTACCGGCGGCAGCGACAACACCGAGGACGTCATCAAGG	+
DsRedAflIIR-GGS	CTAGAGTCGCGGCCGCTCTTAAGGCCGCCGCTCTGGGAGCCGGAGTGGCGGGCC	-
acGFPKpnIF-GGS	GGGCCCGGGATCCACCGGTCATGGTACCGGCGGCAGCGTGAGCAAGGGCGCCGAGC	+
acGFPAflIIR-GGS	GATCTAGAGTCGCGGCCGCTCACTTAAGGCCGCCGGACTTGTACAGCTCATCC	-

TABLE 2. PCR primers for amplifying and cloning fluorescent proteins into the LC of the full-length clone

2.6. Plaque assay

Viruses were titered on CRFK cells. CRFK cells were seeded onto 6- well plates, and upon confluency, the monolayers were infected with serial dilutions of virus prepared in Dulbecco's modified Eagle's medium. Plates were incubated for 60 min (37°C, 5% CO_2), with gentle agitation every 15 min. The inocula were removed, and monolayers were overlaid with 2 ml maintenance media containing 1% agarose gel (Invitrogen). Plates were then incubated for approximately 48 hr at 37°C, in humidified 5% CO_2. Cells were fixed with 10% formaldehyde and the agarose overlay was removed. The fixed cells were stained with 1% (w/v) crystal violet solution, washed, and viral plaques were counted.

2.7. Western blot analysis

Confluent monolayers of CRFK cells in 150 cm2 flasks were infected with vR6, vR6-LC-GFP, and vR6-LC-DsRed respectively, and following complete lysis (approximately 48 hours), the flasks were submitted to three freeze-thaw cycles. The insoluble material was pelleted by centrifugation at 2,655 × g for 10 min and the pellet was resuspended in 500 µl PBS. A 10 µl aliquot was mixed with an equal volume of 2X Tris-glycine SDS sample buffer (Invitrogen) containing 5% beta-mercaptoethanol. The sample was subjected to SDS-PAGE and Western blot analysis as described below.

For VP1 detection over time, CRFK cells were infected at an MOI of 1 with vR6, vR6-LC-GFP, and vR6-LC-DsRed. At the desired time point, approximately 300 µl of Tris-glycine SDS sample buffer was added directly to the monolayer to disrupt the cells, and the lysate was stored at -70°C until further use.

Samples were heated at 95°C for 5 min in 1X Tris-glycine SDS sample buffer containing 5% beta-mercaptoethanol. Western blot analysis was performed using 4-20% Tris-glycine SDS-PAGE gels (Lonza). Proteins were transferred by dry blotting to nitrocellulose membranes using Invitrogen's iBlot apparatus, and membranes were incubated with guinea pig anti-FCV virion hyperimmune serum, rabbit anti-LC hyperimmune serum, rabbit polyclonal anti-DsRed (Clontech), mouse monoclonal anti-GFP (Clontech) or mouse monoclonal annexin A2 (BD Biosciences, San Jose, California; catalog number 610069). The binding of the primary antibodies was detected with goat anti-guinea pig (Kirkegaard & Perry Laboratories, Gaithersburg, MD), anti-rabbit or anti-mouse secondary antibodies (Thermo Scientific, Waltham, MA) conjugated with horseradish-peroxidase, followed by development with the SuperSignal Chemiluminescent Substrate (Thermo Scientific).

Western blots were stripped using the Restore Plus Western Blot Stripping Buffer (Thermo Scientific), and incubated with monoclonal HRP-conjugated α-actin antibody. SeeBlue Plus2 Pre-Stained Standard (Invitrogen) was used to estimate molecular weights of the proteins detected by Western blot.

2.8. Subgenomic expression plasmids

To construct vectors expressing the FCV capsid precursor protein for trans-cleavage analysis, the entire FCV subgenomic RNA region present in pR6, pR6-LC-GFP, or pR6-LC-DsRed was cloned into the pCI expression vector (Promega, Madison, WI). The following primer pair was used to amplify the subgenomic region of each construct (including ORF2, ORF3, the 3"-NTR, poly-A tail, and a unique NotI restriction site

downstream of the poly-A tail), and to introduce a SalI restriction site (boldface) upstream of the subgenomic transcription initiation site: sense primer 5'-CGCCCTACACTGTGA**GTCGAC**TGTGTTCGAAGTTTG (pR6-SubGen-SalI F) and antisense primer that is downstream of the NotI restriction site 5'-CCCAGTCACGACGTTGTAAAAC (pR6-Dnstream PolyA R). The DNA fragments were treated with SalI and NotI, and cloned into pCI vectors (Promega) using the same restriction sites. The plasmids were designated pCI-vR6, pCI-vR6-LC-GFP, and pCI-vR6-DsRed (Fig. 3.2C). All plasmids were confirmed by sequence analysis.

2.9. Coupled in vitro transcription and translation reaction and immunoprecipitation assay

One to 5 μg of plasmid DNA were used as template in a coupled transcription and translation reaction (TNT T7 Coupled Reticulocyte Lysate System; Promega). For radiolabeling of synthesized protein, [^{35}S] methionine (N1,000 Ci/mmol) from Amersham/GE Healthcare (Waukesha, WI) was added at a concentration of 1.5 mCi/ml.

20 μl of the TNT reaction were incubated with 40 μl of either mock- infected lysate or vR6 infected lysate at 37°C for 3 hr. The resulting mixture was diluted with 60 μl of radioimmunoprecipitation assay (RIPA) buffer. The mixtures were incubated with rabbit post-immunization serum (5 μl) raised against the FCV LC protein expressed in E. coli, and the immune complexes were precipitated with protein A beads (Sigma Chemical Co., Saint Louis, MO). Following separation of the proteins in a 4-12% Tris-glycine SDS-PAGE gel, the gel was dried and exposed to Biomax MR film (Kodak, Rochester, NY) for autoradiography.

2.10. Multiple-cycle growth kinetics

CRFK monolayers were infected with vR6, vR6-LC-GFP, or vR6-LC- DsRed at a multiplicity of infection (MOI) of 0.01 and incubated at 37°C in 5% CO_2. Cell lysates were collected at various times post-infection (p.i.) and frozen at -70°C. Following three freeze-thaw cycles, the titer at each time-point was determined by plaque assay in CRFK cells as described above. Results depicted in Fig. 3.3.1 represent the mean value of each time point duplicate determined in two independent plaque titration assays, and the error bars represent one standard deviation. The graph was prepared using the software Prism from GraphPad (La Jolla, CA).

2.11. Extraction of viral RNA for Northern blot analysis

CRFK monolayers (2×10^6 cells) were mock infected or infected with vR6, vR6-LC-DsRed or vR6-LC-GFP at a multiplicity of infection of 1 and incubated at 37°C in 5% CO_2. At 8 h.p.i. 300 µl of Trizol (Invitrogen) reagent was added directly to the monolayer, and RNA was extracted following the instructions of the manufacturer. The viral RNA of individual plaques was purified using the RNeasy mini kit (Qiagen).

2.12. Preparation of RNA transcripts and biotinylated RNA probes

Using pR6 as a template, a forward primer that contained a T7 RNA polymerase promoter sequence and a reverse primer were used to generate a DNA fragment that was complementary to nt 5686 to 5987 of the ORF2 (Table 3). DNA fragments were agarose gel purified and extracted from the agarose (Qiagen). Approximately 1 µg of the DNA fragment was used as the template for in vitro transcription with the Ribomax Express T7

transcription kit (Promega). Transcribed RNA was purified with the RNeasy mini kit (Qiagen).

Purified RNA fragments were subsequently biotinylated with the reagents in the BrightStar psoralen-biotin nonisotopic labeling kit (Ambion, Carlsbad, CA). 0.5 μg of RNA was cross-linked to the psoralen-biotin reagent on ice with a 365-nm UV light for 45 min. Unincorporated label was removed by 1-butanol extraction. The biotinylated RNA probe was stored at -70°C.

Oligo	Sequence 5’-3’	Polarity
FCVcapn5686F/T7	AATTCGTCTCACTGGTAATACGACTCACTATAGGG CTGATGACGGATCCATAACTGCCCCAGAGC	+
FCVcapn5987R	CCAGACCCAGAGATAGAAAACCTTACCTCAACAG ATCC	-

TABLE 3. PCR primers used to generate a DNA template for RNA probe synthesis

2.13. Northern blotting

Northern blot analysis for the detection of FCV RNA was performed with the NorthernMax-Gly system (Ambion). The viral RNA was denatured with glyoxal loading dye for 30 min at 50°C, and separated in a 1% LE-agarose gel. The RNA was transferred to a Bright- Star-Plus membrane by capillary blotting. The membrane was treated with UV light to cross-link the RNA to the membrane, and incubated with Ultrahyb buffer at 68°C for 30 min. The membrane was then incubated overnight at 68°C with the sense biotinylated RNA transcript probe. Detection of bound biotinylated RNA probe was conducted following the instructions of the Bright Star BioDetect kit (Ambion).

2.14. Microscopy analysis

Plaques were visualized using a Leica DMI4000 B microscope, and images were captured using a QImaging Retiga-2000R camera (Surrey, BC Canada). Images were processed using iVision 4.0.14 software (BioVision, Exton, PA).

For live-cell imaging of a single infection, cells were infected with vR6-LC-PmeIDsRed at an MOI of 10. For the co-infection experiment, cells were infected with both vR6-LC-GFP and vR6-LC-DsRed at a MOI of 2 and 1, respectively. The infected cells were then transferred to a temperature-controlled chamber (37°C/ 5% CO_2). Time-lapse confocal imaging was obtained using a Leica SP2-AOBS Confocal Microscope. Time-course images were processed using Imaris software (Bitplane, Zurich, Switzerland).

2.15. LC sequence alignment

Eighty-eight LC sequences from viruses in the genus *Vesivirus* were available in the GenBank database for alignment in the program Clustal X 2.1 (137). To address the diversity in nucleotide sequence and gene length, the program GeneDoc was used to optimize the alignment (165).

2.16. Phylogenetic analysis

A Bayesian phylogenetic tree was inferred using the software program MrBayes 3.2 (231). The parameters employed include the general time-reversible (GTR) model with a gamma distribution of substitution rates. Convergence was achieved after 12 million generations. The first 25% of trees were excluded as burn-in and tree topologies were calculated from the consensus of remaining tree samples. The tree was displayed using FigTree software (72).

2.17. Predicted secondary structure of LC sequences

The secondary structure of LC protein sequences was predicted using the DomPred server (162).

2.18. Construction of FCV full-length (FL) clones with LC deletions and LC chimeras

To introduce a unique KpnI cleavage site into the 5' end of the FCV VP1 sequence (downstream of the LC and VP1 border), the FL clone pR6 (252) was modified with a QuikChange XL Site-Directed Mutagenesis kit (Stratagene. La Jolla, CA) using

the primer pairs 5'- CTGCCCCAGAGCAAGGtACcGTGGTTGGAGGAG (designated Urb-VP1-KpnI_F) plus 5'- CTCCTCCAACCACgGTaCCTTGCTCTGGGGCAG (designated Urb-VP1-KpnI_R). The sequence of the primers corresponded to nt 5705 to 5735 of the FCV genome and included two synonomous nucleotide changes (nucleotide changes are shown in lowercase) to introduce a unique KpnI site (underlined). Clones with the desired mutation were screened by sequence analysis, and the resulting plasmid, designated pR6*, was selected for the construction of FL FCV clones with LC truncations.

To construct FL clones with consecutive in-frame deletions extending from the 5' end and 3' end of the LC region, sense and antisense primers were used to amplify DNA fragments from the plasmid pR6*. Purified DNA fragments were digested with BstBI and KpnI and ligated into the BstBI-KpnI-linearized pR6* vector, replacing the LC coding sequence with LC truncated sequences. The cleavage of the ORF2 precursor is essential for recovery of infectious virus (257), so four amino acids at the C-terminus of the LC (FRLE) were left intact to maintain intact the cleavage site. Clones with the desired truncations were screened by sequence analysis, and the resulting plasmids were designated based on the amino acids deleted (Fig. 3.9).

Oligo	Sequence 5'-3'	Polarity
pR6-KpnI-cdelta10R	CCTCCAACCACGGTACCTTGCTCTGGGGCAGTTATGGATCCGTCATCAGCTTCCAATCTGAAAACTTCCC	-
pR6-KpnI-cdelta20R	CCTCCAACCACGGTACCTTGCTCTGGGGCAGTTATGGATCCGTCATCAGCTTCCAATCTGAAACCAGGGTGGG	-
pR6-KpnI-cdelta30R	CCTCCAACCACGGTACCTTGCTCTGGGGCAGTTATGGATCCGTCATCAGCTTCCAATCTGAACTCATTCCAGTGCATTGGAG	-
pR6-KpnI-cdelta40R	CCTCCAACCACGGTACCTTGCTCTGGGGCAGTTATGGATCCGTCATCAGCTTCCAATCTGAAGTCGATAGCC	-
pR6-KpnI-cdelta50R	CCTCCAACCACGGTACCTTGCTCTGGGGCAGTTATGGATCCGTCATCAGCTTCCAATCTGAAATCATCGCCCAGGATAGACTC	-
pR6-KpnI-cdelta60R	CCTCCAACCACGGTACCTTGCTCTGGGGCAGTTATGGATCCGTCATCAGCTTCCAATCTGAATTGAAGTGGGGACTGGTCG	-
pR6-KpnI-cdelta70R	CCTCCAACCACGGTACCTTGCTCTGGGGCAGTTATGGATCCGTCATCAGCTTCCAATCTGAAGGTTCCGAATTCAGGGAGC	-
pR6-BstBI-ndelta10F	CTGTGATGTGTTCGAAGTTTGAGCATGTATAATTGGGACCCCCACTTC	+
pR6-BstBI-ndelta20F	CTGTGATGTGTTCGAAGTTTGAGCATGATCAATCCTAACAAATTCTTG	+
pR6-BstBI-ndelta30F	CTGTGATGTGTTCGAAGTTTGAGCATGTTCTGTGATAATCCACTTATG	+
pR6-BstBI-ndelta40F	CTGTGATGTGTTCGAAGTTTGAGCATGCCTGAATTGCTCCCTGAATTC	+
pR6-BstBI-ndelta50F	CTGTGATGTGTTCGAAGTTTGAGCATGTGGGATTGCGACCAGTCCC	+
pR6-BstBI-ndelta60F	CTGTGATGTGTTCGAAGTTTGAGCATGTATCTTGAGTCTATCCTGGG	+
pR6-BstBI-ndelta70	CTGTGATGTGTTCGAAGTTTGAGCATGTGGTCTTCAACTTATGAGGC	+

TABLE 4. PCR primers used in generation of full-length clones with N-terminal and C-terminal deletions in the LC protein

To generate a recombinant FL clone that expressed the LC as a fusion protein with unique tags, PCR amplification was performed with the following primer pair using a pCI-NV-VP1 clone (Parra et al, manuscript in preparation) as a template to produce a DNA fragment containing a FLAG tag and 22 amino acids of the Norwalk VP1 sequence, buffered by an amino acid linker sequence (GGS), and bordered by PmeI and AflII. The DNA fragment was purified and digested with PmeI and AflII and ligated into the PmeI-AflII-linearized pR6-LC vector. Clones with the desired mutation were screened by sequence analysis, and the resulting plasmid was designated pR6-LC-NV10 (Fig. 3.13A).

To generate recombinant FL clones that contained an entire or partial heterologous LC, SMSV-5 Hom-1 or Mink calicivirus 9 LC sequences were PCR amplified and cloned into the pR6* vector using the unique restriction sites BstBI and KpnI (Fig. 3.14A). The PCR was performed using cDNA consensus clones of SMSV-5 Hom-1 and Mink calicivirus 9 as templates.

Oligo	Sequence 5'-3'	Polarity
FCV-Hom1-LCchimera1F	CACTGTGATGTGTTCGAAGTTTGAGCATGTGCTCAACCTGCGCTAACGTGCTTAAATATTATAATTGGGACCCCCACCTCAACTTGGTCATCAACCC	+
FCV-Hom1-LCchimera1R	GCTATAACTCCTCCAACCACGGTACCTTGCTCTGGGGCAGTTATGGATCCGTCATCAGCTTCCAATCTGAACAATGGAAGGGAAGGATCCCAAGATGC	-
FCV-Hom1-LCchimera2F	GATGTGTTCGAAGTTTGAGCATGTGCTCAACCTGCGCTAACGTGCTTAAATATTATAATTGGGACCCCCACCTCAACTTGGTCATCAACCC	+
FCV-Hom1-LCchimera2R	CCAACCACGGTACCTTGCTCTGGGGCAGTTATGGATCCGTCATCAGCTTCCAATCTGAACAATGGAAGGGAAGGATCCCAAGATG	-
FCV-Mink-LCchimera1F	GCTTAAATATTATAATTGGGACCCCCACTTCAAATTAGTGATCAATCCTAACAAATTCTTGTCCATAGGTTTCTGTGATGACCCCTTCCATTGC	+
FCV-Mink-LCchimera1R	CCGTCATCAGCTTCCAATCTGAACAATGGCAGGTTTGGATCCCATGCCTTTGCAACTTTCTCCAGACATCGTTGG	-
FCV-Mink-LCchimera2F	CTGTGATGTGTTCGAAGTTTGAGCATGTGCTCAACCTGCGCTAACGTGCTTAAATATTATAATTGGGAC	+
FCV-Mink-LCchimera2R	GCTATAACTCCTCCAACCACGGTACCTTGCTCTGGGGCAGTTATGGATCCGTCATCAGCTTCCAATCTG	-

TABLE 5. PCR primers used to amplify Mink and Hom-1 LC sequences to clone into the FCV full-length clone

2.19. Scanning-alanine mutagenesis of conserved residues in the FL clone

To introduce alanine substitutions into the LC sequence of the FL clone, the QuikChange XL Site-Directed Mutagenesis kit (Stratagene) was used with sense and antisense primers and pR6 as a template. The clones were screened by sequence analysis, and those that were positive for the substitution were selected as a template for PCR amplification of a region that encompassed the unique restrictions sites BstBI and SpeI (upstream and downstream of the LC coding sequence, respectively). The purified DNA fragments were then digested with BstBI and SpeI and ligated into the BstBI-SpeI-linearized pR6 vector. The reconstructed clones were screened by sequence analysis, and plasmids containing the desired substitutions were selected and designated pR6-LC-X#A, where X corresponds to the amino acid matching the Urbana strain and # corresponds to the amino acid number within the LC coding sequence. FL clones with the compensatory mutations were generated using the same strategy of primer mutagenesis with the QuikChange mutagenesis kit (Fig. 3.11A).

Oligo	Sequence 5'-3'	Polarity
Urb-LC-C33A_F	CTTGTCCATAGGTTTCGCTGATAATCCACTTATG	+
Urb-LC-C33A_R	CATAAGTGGATTATCAGCGAAACCTATGGACAAG	-
Urb-LC-D34A_F	GTCCATAGGTTTCTGTGCTAATCCACTTATGTGCTG	+
Urb-LC-D34A_R	CAGCACATAAGTGGATTAGCACAGAAACCTATGGAC	-
Urb-LC-P36A_F	GGTTTCTGTGATAATGCTCTTATGTGCTGTTATCCTG	+
Urb-LC-P36A_R	CAGGATAACAGCACATAAGAGCATTATCACAGAAACC	-
Urb-LC-C39A_F	GTGATAATCCACTTATGGCTTGTTATCCTGAATTGC	+
Urb-LC-C39A_R	GCAATTCAGGATAACAAGCCATAAGTGGATTATCAC	-
Urb-LC-C40A_F	GATAATCCACTTATGTGCGCTTATCCTGAATTGCTCC	+
Urb-LC-C40A_R	GGAGCAATTCAGGATAAGCGCACATAAGTGGATTATC	-
Urb-LC-P81A_F	CTTATGAGGCTATCGACGCTGTTGTCCCTCCAATGC	+
Urb-LC-P81A_R	GCATTGGAGGGACAACAGCGTCGATAGCCTCATAAG	-
Urb-LC-P84A_F	GCTATCGACCCTGTTGTCGCTCCAATGCACTGG	+
Urb-LC-P84A_R	CCAGTGCATTGGAGCGACAACAGGGTCGATAGC	-
Urb-LC-P85A_F	CGACCCTGTTGTCCCTGCTATGCACTGGAATGAGG	+
Urb-LC-P85A_R	CCTCATTCCAGTGCATAGCAGGGACAACAGGGTCG	-
Urb-LC40A-S29P-Y41C_F	CCTAACAAATTCTTGCCCATAGGTTTCTGTGATAATCCACTTATGTGCGCTTGTCCTGAATTGCTCCCTGAATTCGG	+
Urb-LC40A-S29P-Y41C_R	CCGAATTCAGGGAGCAATTCAGGACAAGCGCACATAAGTGGATTATCACAGAAACCTATGGGCAAGAATTTGTTAGG	-
Urb-LC40A-Y41C_F	GATAATCCACTTATGTGCGCTTGTCCTGAATTGCTCCCTG	+
Urb-LC40A-Y41C_R	CAGGGAGCAATTCAGGACAAGCGCACATAAGTGGATTATC	–
Urb-LC40A-S29P_F	CAATCCTAACAAATTCTTGCCCATAGGTTTCTGTGATAATCC	+
Urb-LC40A-S29P_R	GGATTATCACAGAAACCTATGGGCAAGAATTTGTTAGGATTG	-

TABLE 6. PCR primers used in generation of scanning-alanine mutagenesis of conserved LC residues in the full-length clone

2.20. pCI plasmid construction for transient expression experiments

To construct eukaryotic expression clones for transient expression experiments, the LC sequence was cloned into the pCI expression vector (Promega, Madison, WI). The LC was PCR-amplified using pR6 as a template with primers that introduced a SalI restriction site at the 5' end and a stop codon followed by a NotI restriction site at the 3' end. DNA fragments were purified and digested with SalI and NotI and ligated into a SalI-NotI-linearized pCI vector. The clones were screened by sequence analysis, and a plasmid containing the correct sequence was selected and designated pCI-LC (Fig. 3.10).

pCI-LC clones that contained the red fluorescent protein mKate2 fused to the LC was generated in two steps. First, the mKate2 coding sequence was PCR-amplified using the pmKate2-N plasmid as a template (Evrogen, Moscow, Russia) to include bordering KpnI and AflII restriction sites and a linker sequence (GGSGGS). The PCR amplified mKate2 was digested, purified and ligated into the KpnI and AflII sites of pR6-LC FL clone (1). The clones were screened by sequence analysis, and a plasmid containing the correct sequence was selected and designated pR6-LC-mK. The LC-mKate fusion protein was amplified using pR6-LC-mK as a template with primers that introduced a SalI restriction site at the 5' end and a stop codon followed by a NotI restriction site at the 3' end. DNA fragments were purified and digested with SalI and NotI and ligated into a SalI-NotI-linearized pCI vector. The clones were screened by sequence analysis, and a plasmid containing the correct sequence was selected and designated pCI-LC-mK.

To generate pCI-LC-mK clones with consecutive in-frame deletions extending from the terminal ends and from the transposon insertion site (TIS) of the LC, sense and antisense primers were used to amplify DNA fragments from the plasmid pR6. Purified DNA fragments of truncated LC sequences were digested and ligated into the linearized pCI-LC-mKate vector, replacing the LC coding sequence with LC truncated sequences. The clones were verified by sequence analysis, and a plasmid containing the correct sequence was selected and designated pCI-LC-mK-ΔA-B, where A-B represent the amino acids removed from the LC sequence.

Oligo	Sequence 5'-3'	Polarity
pCI UrbLCmKate Ctermdelta10R	CTGCTCGAAGCGGCCGCTCACCATGCCTTAGCAACTTCCCC	-
pCI UrbLCmKate Ctermdelta20R	CTGCTCGAAGCGGCCGCTCAATGCATGAGAACACCAGGGTGG	-
pCI UrbLCmKate Ctermdelta30R	CTGCTCGAAGCGGCCGCTCATATCTTTCCAGCCTCATTC	-
pCI UrbLCmKate Ctermdelta36R	CTGCTCGAAGCGGCCGCTCATCTGTGCCCCAGTTTGCTAG	-
pCI UrbLCmKate FRLEdelta10R	CTGCTCGAAGCGGCCGCTCATTCCAATCTGAAAACTTCCCCAATGAT GTGATG	-
pCI UrbLCmKate FRLEdelta20R	CTGCTCGAAGCGGCCGCTCATTCCAATCTGAAACCAGGGTGGGGCT GGAATATC	-
pCI UrbLCmKate FRLEdelta30R	GTCTGCTCGAAGCGGCCGCTCATTCCAATCTGAACTCATTCTTAAGG CTGCCGC	-
pCI UrbLCmKate Ntermdelta10F	GTACCTCTAGAGTCGACATGTATAATTGGGACCCCCACTTC	+
pCI UrbLCmKate Ntermdelta20F	GTACCTCTAGAGTCGACATGATCAATCCTAACAAATTCTTG	+
pCI UrbLCmKate Ntermdelta30F	GTACCTCTAGAGTCGACATGTTCTGTGATAATCCACTTATG	+
pCI UrbLCmKate Ntermdelta40F	GTACCTCTAGAGTCGACATGCCTGAATTGCTCCCTGAATTC	+
pCI UrbLCmKate Ntermdelta50F	GTACCTCTAGAGTCGACATGTGGGATTGCGACCAGTCCC	+
pCI UrbLCmKate Ntermdelta60F	GTACCTCTAGAGTCGACATGTATCTTGAGTCTATCCTGGG	+
pCI UrbLCmKate Ntermdelta70F	GTACCTCTAGAGTCGACATGTGGTCTTCAACTTATGAGGC	+
pCI UrbLCmKate Ntermdelta80F	GTACCTCTAGAGTCGACATGGTTGTCCCTCCAATGCACTG	+
pCI UrbLCmKate Ntermdelta87F	GTACCTCTAGAGTCGACATGGTGAGCGAGCTGATTAAGGAG	+
pCI UrbLCmKate outNdelta10R	GCCGGTACCGTTTAAACAAGCCTCATAAGTTGAAGACC	-
pCI UrbLCmKate outNdelta20R	GCCGGTACCGTTTAAACAGCCCAGGATAGACTCAAG	-
pCI UrbLCmKate outNdelta30R	GCCGGTACCGTTTAAACATGGGGACTGGTCGCAATCCC	-
pCI UrbLCmKate outNdelta40R	GCCGGTACCGTTTAAACAGAATTCAGGGAGCAATTCAGG	-
pCI UrbLCmKate outNdelta50R	GCCGGTACCGTTTAAACACATAAGTGGATTATCACAG	-
pCI UrbLCmKate outNdelta60R	GCCGGTACCGTTTAAACACAAGAATTTGTTAGGATTG	-
pCI UrbLCmKate outNdelta70R	GCCGGTACCGTTTAAACAGAAGTGGGGGTCCCAATTATAATATTTAAG	-
pCI UrbLCmKate outNdelta80R	GCCGGTACCGTTTAAACACACGTTAGCGCAGGTTGAGC	-
pCI UrbLCmKate outNdelta87R	GCCGGTACCGTTTAAACACATGTCGACTCTAGAGGTACC	-
pCI UrbLCmKate NsiIoutC10R	CCAATGATGTGATGCATGAGAACACCAGGCTTAAGGCTGCCGCCG	-
pCI UrbLCmKate outCdelta20R	CTGCTCGAAGCGGCCGCTCATTCCAATCTGAACAATGGCAGGTTTGG ATCCCATGCCTTAGCAACTTCCTTAAGGCTGCCGCCGCTG	-
pCI UrbLCmKate outCdelta30R	CTGCTCGAAGCGGCCGCTCATTCCAATCTGAACAATGGCTTAAGGCT GCCGCCGC	-
pCI UrbLCmKate outCdelta36R	CTGCTCGAAGCGGCCGCTCACTTAAGGCTGCCGCCGC	-

TABLE 7. PCR primers used in generation of pCI-LC-mKate clones with deletions in the sequence of LC protein

2.21. Nucleotide sequence analysis

All plasmids were sequenced to confirm the presence of the desired engineered insertions. Nucleotide sequencing analysis was performed on an ABI 3730 automated sequencer (Applied Biosystems, Carlsbad, CA) with the Big Dye Terminator reagents, version 3.1.

Oligo	Sequence 5’-3’	Polarity
UrbanaFL5174F	GGCATGACCGCCCTACACTGT	+
UrbanaFL7391R	GCGTTGTTGTCCAAGCGCAGCC	-
UrbanaFL7104F	CCACTACTTGCTCCCACCTG	+
UrbanaFL6600R	GCGTAATCACCAGCCGGCACC	-
UrbanaFL6036F	CCCCATCCAAAGTACCTCGATGC	+
UrbanaFL6113R	GTGCTGCGCAAGTCAGGGATGG	-
UrbanaFL6721R	CCCCACGCTCTTTGGAGTGATCC	-
UrbanaFL2537F	GTGCTTACTGCCCCTGACAAG	+
UrbanaFL5429R	GGGAGCAATTCAGGATAACAGC	-
UrbanaFL3503F	GCCACTGAGTGGAAACCCAAG	+
UrbanaFL4551R	GCGGCCGAATCAACTATTGGGG	-
UrbanaFL4410F	GCCCTAGTGTTGAGGCTCTGC	+
UrbanaFL3623R	GTGCAATCCAGTTACCCTGCC	-
pSportF	CTGGGGCCTCGGTGCACATGC	+
UrbanaFL3208R	GCCCCGATCAACTGCCCTAAG	-
UrbanaFL613F	GGCATGCTACTGCAAATCCTATG	+
UrbanaFL707R	CGATGAAAGCGCCAATCAATGG	-
UrbanaFL1469F	GGCCCTCCGGGGTGTGGAAAG	+
UrbanaFL1759R	GCACGCCTGGAGGAGGGCTTC	-
UrbanaFL2457F	CGGTGTTTGATTTGGCCTGGG	+
UrbanaFL2537R	CCTTGTCAGGGGCAGTAAGCAC	-

TABLE 8. Primers used for sequencing full-length FCV clones

The following primer pair, that flanks the site of insertion into the LC coding sequence, was used in a "diagnostic" PCR to examine the stability of the insert: sense primer 5'- CTTGAGTCTATCCTGGGCGATG (UrbFL5500F), and the antisense primer 5'- ATCAGCAGCGGTTGACATTTG (UrbFL5758R).

2.22. Transient expression assays

Transfections were performed with the Polyjet DNA *In Vitro* transfection reagent (Signagen) according to the instructions from the manufacturer. The viability of transfected cells was assessed with the Invitrogen Live/Dead Fixable Dead Cell Stain Kit.

2.23. Recombinant LC immunoprecipitation from infected cells

Confluent CRFK cells (~1 x 10^7) were infected with vR6-LC-NV10 at an MOI of 5. Four hours post-infection, infected cells, and mock infected cells as a negative control, were lysed with Lysis Buffer (150 mM NaCl, 1% Triton X-100, 50 mM Tris HCl pH 8.0). Samples were mixed and incubated on ice for 30 minutes. The cell lysates were clarified by centrifugation for 10 minutes at 10,000 x g at 4°C. Clarified lysates were incubated with 1 µg of biotinylated C10 antibody for 30 minutes at 4°C. 250 µg of prewashed magnetic Dynabeads MyOne Strepavidin T1 (Invitrogen) was then added to the samples and incubated at 4°C for 30 minutes. Recombinant LC was purified using a magnetic rack to isolate the magnetic beads, and the bead-protein complex was washed four times with lysis buffer. SDS-PAGE Sample Buffer (Invitrogen) was used to release the protein complex from the beads, which was then analyzed by SDS-PAGE.

Protein bands of interest were cut out of the SDS-PAGE gel and submitted for mass spectrometry analysis. Digested proteins were analyzed using a Mascot search through the NCBInr database.

CHAPTER 3: RESULTS

3.1. Four sites were identified in the FCV genome that can tolerate the insertion of 15-nucleotides

In our initial experiments to identify sites in the FCV genome that can tolerate insertions, a transposon mutagenesis approach was used to insert a 15-bp sequence (with a unique PmeI restriction enzyme site) at random locations throughout almost the entire FCV genome. The mutagenized FCV region was then cloned back into the infectious full-length cDNA clone, pR6, replacing wt sequences with the mutagenized sequences. In general, the titer of virus recovered from the library of mutagenized plasmids was 10 plaque forming units per ml (pfu/ml), approximately 2 $\log_{10}$ lower than the titer of virus recovered from a full-length clone encoding wild-type (wt) virus. There was a high incidence of recovered wt virus after transfection with the mutagenized pool (95%), which was likely due to instability of the recombinant viruses and reversion to wt.

From the initial screening of recovered viruses, 9 out of 193 analyzed plaques were identified by sequence analysis as recombinant viruses containing a 15-nt insertion (Fig. 3.1), although several plaques were identical recombinants. VPg tolerated the 15-nt insertion at the N-terminus (bordered by nucleotides 2924 and 2925) and the C-terminus (bordered by nucleotides 3106 and 3107), the LC protein tolerated the insertion at the C-terminus (the site of insertion is bordered by nucleotides 5577 and 5578), and VP2 tolerated the insertion at its N-terminus (bordered by nucleotides 7322 and 7323).

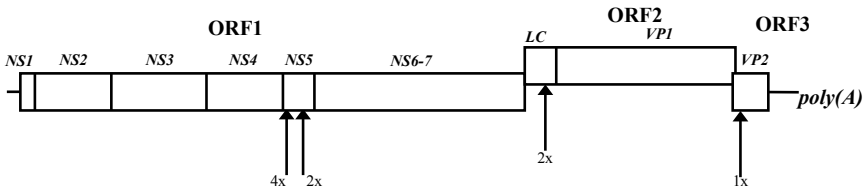

Fig. 3.1. Summary of sites that could tolerate a 15-nt insertion. The arrows indicate the sites within the FCV genome that could tolerate a 15-nt insertion. The number of viruses recovered with the same insertion site is indicated below each arrow.

3.2. The LC can tolerate small and large insertions of heterologous sequences

Reverse genetics was employed to insert small epitope tags into the sites identified that could tolerate the 15-nt insertion (HA, FLAG, and a tetra cysteine motif). Virus was recovered from recombinant cDNA clones expressing each of the three epitope tags fused to the LC region, and the presence of each sequence in the viral genome was confirmed by sequence analysis. Of the three epitope tags that were inserted into the VP2 coding sequence, virus was recovered only from the recombinant cDNA clone that contained the HA insertion.

The ability of the LC protein to tolerate the insertion of foreign sequences was of interest because the function of this protein, which is unique to the genus *Vesivirus*, has not yet been identified. To facilitate cloning of markers into the LC in order to study its function and to evaluate the characteristics of representative recombinant viruses, the pR6 infectious clone was engineered at the LC insertion site to create four new unique restriction sites (PmeI, KpnI, BspEI, AflII), bordered by nucleotides 5577 and 5578 of the FCV genome, (designated as pR6-LC; Fig. 3.2A). Viable viruses were recovered from the pR6-LC clone (data not shown).

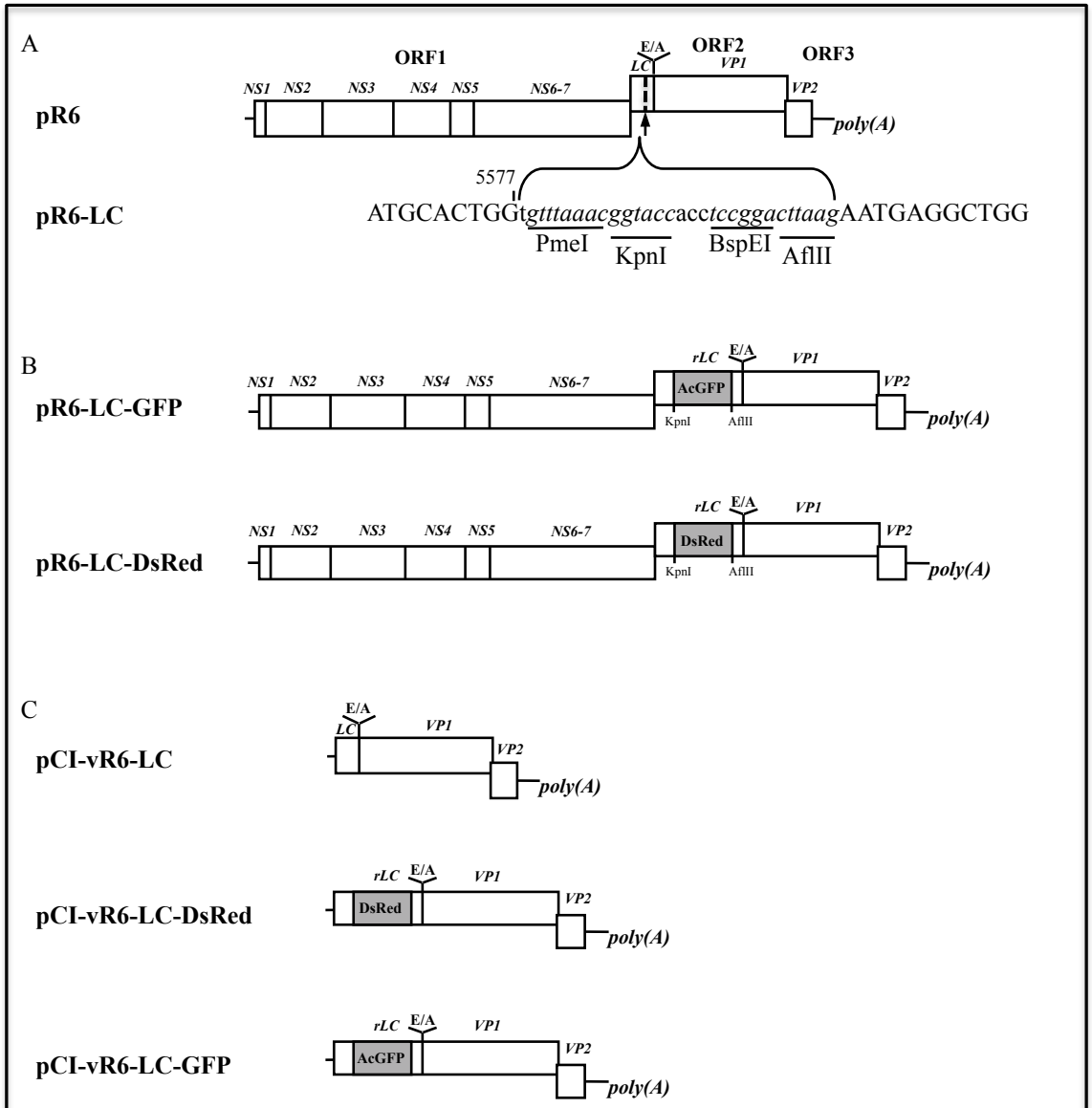

Fig. 3.2. Recombinant FCV constructs. (A) Schematic diagram showing the recombinant FCV that was engineered to have a multiple cloning site encoded within the LC. The location of the multiple cloning site in the LC is indicated by an arrow. E/A corresponds to the cleavage site of the ORF2 precursor. Nucleotide numbers correspond to the Urbana strain of FCV (Genbank accession no. L40021). (B) Recombinant FCV constructs. cDNA infectious clone constructs showing the site of insertion of GFP (pR6-LC-GFP) and DsRed (pR6-LC-DsRed). (C) pCI expression vectors containing the subgenomic region of pR6, pR6-LC-GFP or pR6-LC-DsRed. rLC, recombinant LC.

3.3. Recombinant FCV expressing GFP and DsRed fused to the LC are viable and show growth kinetics similar to wt FCV

In order to monitor a FCV infection in real-time, the coding sequence of the monomeric versions of GFP and DsRed were engineered into the pR6-LC clone using the unique KpnI and AflII sites (Fig. 3.2A), with the addition of a three amino acid "linker" sequence (GGS) flanking the fluorescent protein. The recombinant clones were designated pR6-LC-GFP and pR6-LC-DsRed, for the GFP and DsRed harboring constructs, respectively (Fig. 3.2B).

The recombinant clones yielded viable recombinant viruses that formed plaques in CRFK cell monolayers (Fig. 3.3, panels 1-4). There was no visible difference in the CPE caused by the recombinant viruses and vR6 (cell rounding; Fig. 3.3, panels 9-12). Microscopy revealed that plaques formed by vR6-LC-GFP and vR6-LC-DsRed were fluorescent at the expected wavelengths, and no fluorescence was observed in vR6-infected cells (Fig. 3.3, panels 5-8).

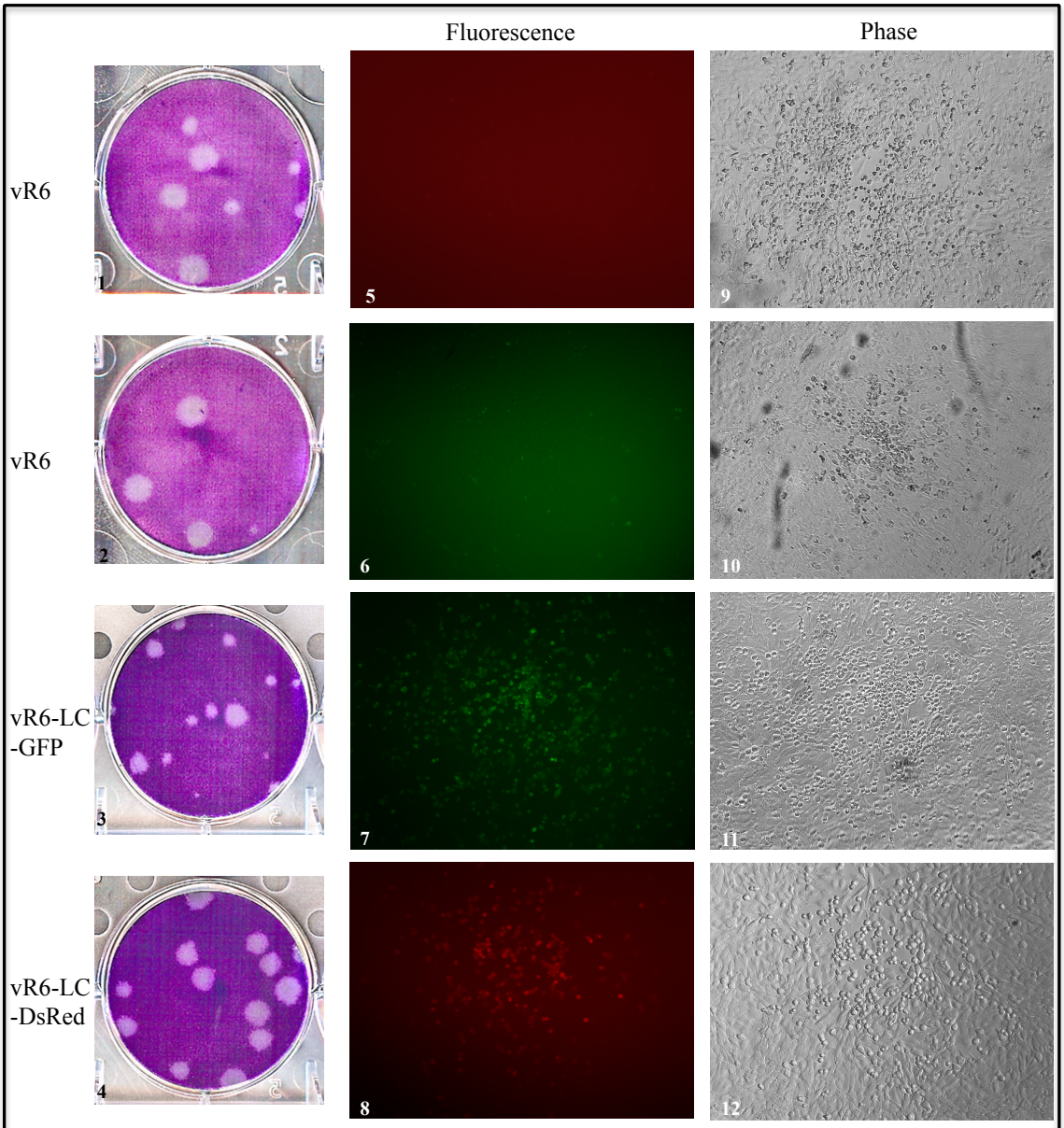

Fig. 3.3. Recombinant FCV expressing GFP and DsRed fused to the LC are viable. Virus serial dilutions were added to CRFK monolayers of a 6-well plate and incubated for 60 min, at which point an agarose overlay was added. Approximately 48 h later, fluorescent and phase images were captured of vR6 (panels 5–6, 9– 10), vR6-LC-GFP (panels 7, 11) and vR6-LC-DsRed (panels 8, 12) plaques using a Leica DMI4000 B microscope. Fluorescent images correspond to signals detected when using filters specific to GFP and DsRed (panels 5–8). The agarose overlay was removed, and the cells were stained with crystal violet and images were taken of plaques (panels 1–4).

The growth kinetics of the recombinant FCV viruses were compared with that of the wild-type parental virus, vR6, in a multi-step growth curve that was performed in duplicate (Fig. 3.3.1). Cell monolayers were infected with viruses at an MOI of 0.01 and samples were collected at 0, 6, 12, 18, 24, 30, and 48 hours p.i. The growth curves for all viruses were similar through the first 18 hours. At 24 hours p.i., vR6 reached a peak titer of approximately one $\log_{10}$ higher than the recombinant viruses. By 48 hours p.i., viral titers were similar for all three viruses. These data indicate that the recombinant viruses spread similarly to wild-type, however they have a maximum titer one $\log_{10}$ lower than wild-type.

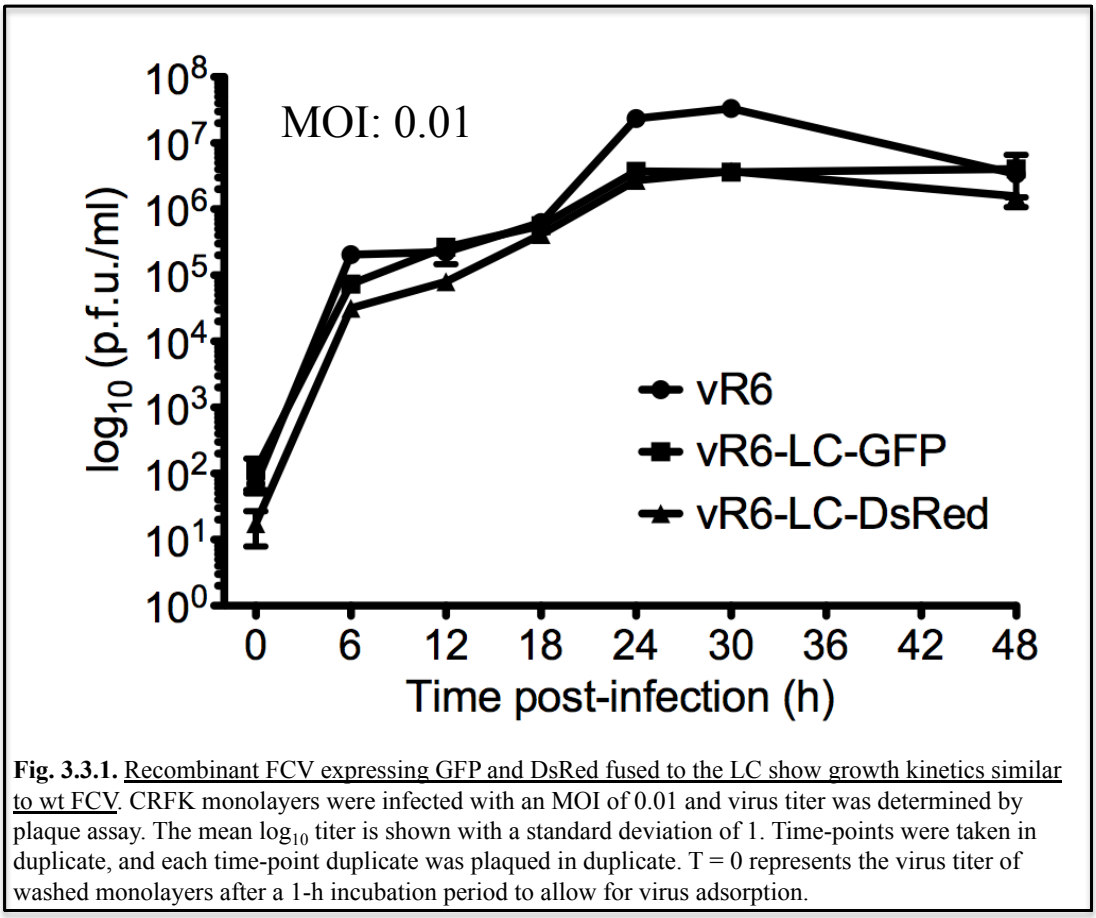

Fig. 3.3.1. Recombinant FCV expressing GFP and DsRed fused to the LC show growth kinetics similar to wt FCV. CRFK monolayers were infected with an MOI of 0.01 and virus titer was determined by plaque assay. The mean $\log_{10}$ titer is shown with a standard deviation of 1. Time-points were taken in duplicate, and each time-point duplicate was plaqued in duplicate. T = 0 represents the virus titer of washed monolayers after a 1-h incubation period to allow for virus adsorption.

3.4. The LC precursor of pR6-LC-GFP and pR6-LC-DsRed constructs are cleaved efficiently *in vitro* and *in vivo*

The recovery of viruses expressing relatively large fluorescent proteins fused to the LC prompted me to examine the cleavage efficiency between LC and VP1 in an *in vitro* cleavage assay. It was possible that the reduction in virus yield was due to a lower efficiency of the precursor cleavage event. The subgenomic regions of vR6, vR6- LC-GFP and vR6-LC-DsRed were each cloned into the pCI expression vector and the resulting plasmids, designated pCI-vR6, pCI-LC-GFP, pCI-LC-DsRed, contained the first AUG of ORF2 under the control of a T7 promoter. The radiolabeled translation products generated in a coupled *in vitro* transcription and translation reaction were resolved by SDS-PAGE, and the expected bands corresponding to proteins with predicted molecular masses of 73 (vR6), 101 (vR6-LC-GFP), and 100 (vR6-LC-DsRed) kDa were observed (Fig. 3.4A). Additional minor bands corresponding to proteins of lower molecular weight were likely the result of efficient internal translation at downstream AUGs of ORF2, as noted previously (257). To test for authentic cleavage of the recombinant precursor, radiolabeled TNT products derived from the pCI vectors were incubated at 37°C for 3 hr with a lysate (nonradiolabeled) prepared from either vR6-infected, or mock- infected, CRFK cells (Fig. 3.4B). The products of this incubation were immunoprecipitated using specific antibodies raised against the LC and the complexes were analyzed by SDS-PAGE and visualized with autoradiography. The expected cleavage event occurred only when the TNT samples were incubated with vR6-infected CRFK lysates, which are known to contain the active viral proteinase (lanes 4-6) (257). The cleaved LC protein in both the wt and recombinant form (indicated with an asterisk) were observed in addition

to the approximately 60 kDa mature capsid (indicated with an arrow) that co-precipitated, as observed previously (255).

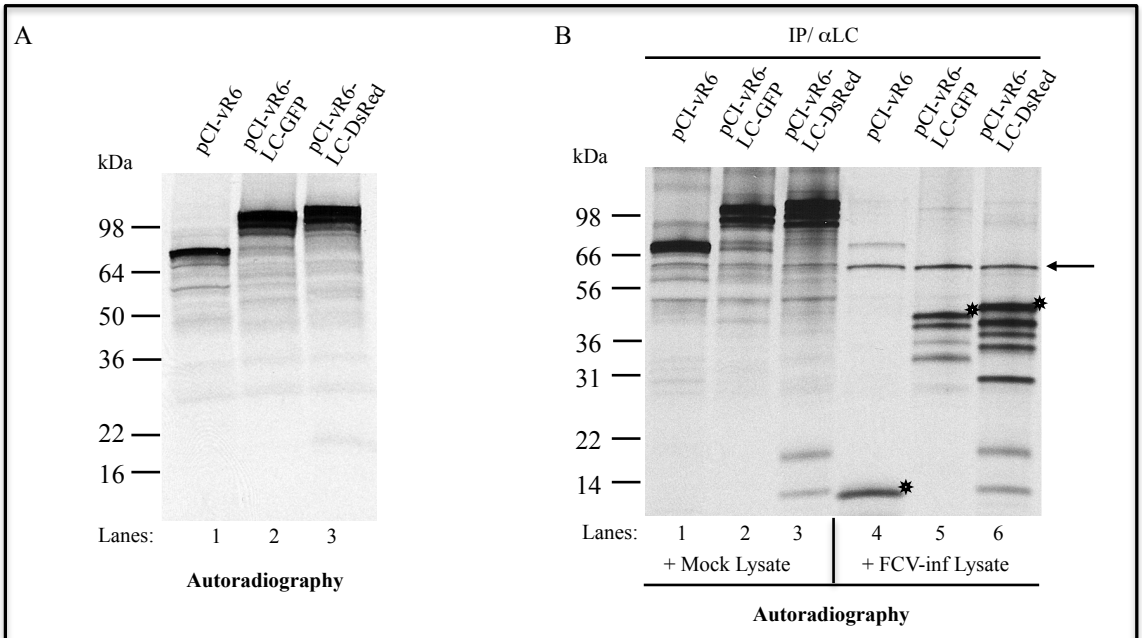

Fig. 3.4. Evidence for efficient cleavage of the LC precursor of pR6-LC-GFP and pR6-LC-DsRed constructs in vitro. (A) The subgenomic region of vR6, vR6-LC-GFP and vR6-LC- DsRed were cloned into the pCI expression vector. The cloned pCI expression vectors were used in a coupled in vitro transcription and translation reaction, and labeled with [^{35}S] methionine. The samples were subjected to SDS-PAGE in a 4–12% Tris-glycine gel. The proteins were stained with GelCode Blue Stain, dried and exposed to film. (B) Coupled transcription/translation samples were treated with either unlabeled mock (lanes 1–3) or vR6-infected (lanes 4–6) lysates for 3 h. The treated samples were immunoprecipitated using rabbit hyperimmune anti-LC sera, and subsequently subjected to SDS-PAGE in a 4-12% Tris-glycine gel. The proteins were stained with GelCode Blue Stain, dried and exposed to film. * = cleaved form of LC from ORF2.

Furthermore, anti-FCV virion serum was used to monitor VP1 processing over time in FCV-infected cells. The production of mature VP1 was similar for the three viruses (Fig. 3.4.1A), suggesting that processing of the capsid precursor by the viral proteinase (257) was unaffected. Taken together, these data show that the insertion of the fluorescent protein into the LC does not affect the observed efficiency of the capsid precursor cleavage both *in vitro* and in infected cells.

Western blot analyses of CRFK cells infected with vR6, vR6-LC-GFP, and vR6-LC-DsRed were performed to investigate whether the recombinant FCV variants expressed LC as an intact fusion protein (Fig. 3.4.1B). The anti-LC serum detected the

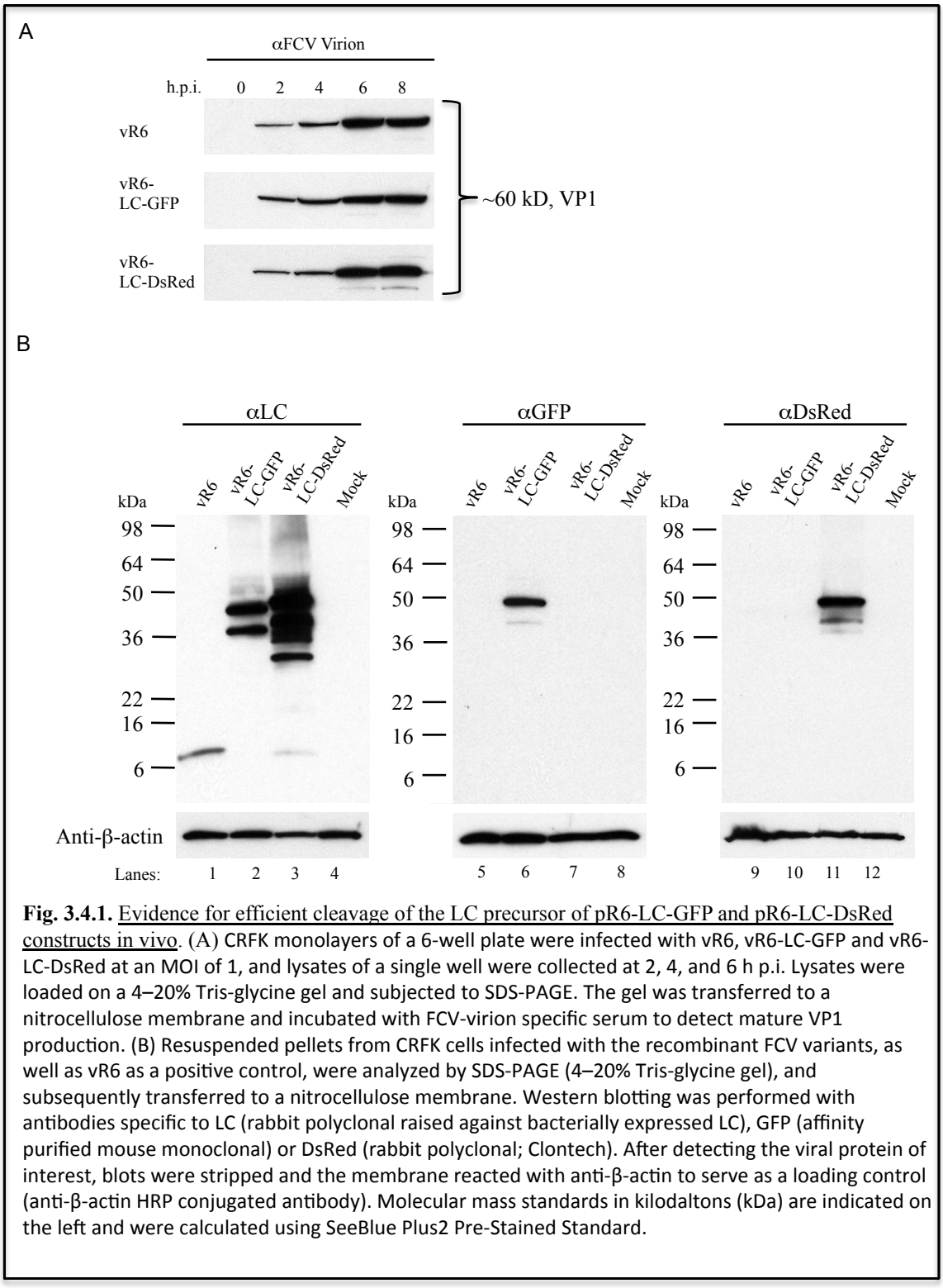

Fig. 3.4.1. Evidence for efficient cleavage of the LC precursor of pR6-LC-GFP and pR6-LC-DsRed constructs in vivo. (A) CRFK monolayers of a 6-well plate were infected with vR6, vR6-LC-GFP and vR6-LC-DsRed at an MOI of 1, and lysates of a single well were collected at 2, 4, and 6 h p.i. Lysates were loaded on a 4–20% Tris-glycine gel and subjected to SDS-PAGE. The gel was transferred to a nitrocellulose membrane and incubated with FCV-virion specific serum to detect mature VP1 production. (B) Resuspended pellets from CRFK cells infected with the recombinant FCV variants, as well as vR6 as a positive control, were analyzed by SDS-PAGE (4–20% Tris-glycine gel), and subsequently transferred to a nitrocellulose membrane. Western blotting was performed with antibodies specific to LC (rabbit polyclonal raised against bacterially expressed LC), GFP (affinity purified mouse monoclonal) or DsRed (rabbit polyclonal; Clontech). After detecting the viral protein of interest, blots were stripped and the membrane reacted with anti-β-actin to serve as a loading control (anti-β-actin HRP conjugated antibody). Molecular mass standards in kilodaltons (kDa) are indicated on the left and were calculated using SeeBlue Plus2 Pre-Stained Standard.

expected LC protein of 14 kDa in wt infected cells (lane 1), and larger LC fusion proteins in cells infected with vR6-LC-GFP (lane 2) and vR6-LC-DsRed (lane 3). A band of the expected molecular mass of approximately 42 kDa for the recombinant LC fusion protein was also detected using antibodies specific for GFP (lane 6) or DsRed (lane 11). It should be noted that when detecting recombinant LC proteins, bands corresponding to proteins of lower molecular masses were observed in some Western blots. Possible explanations include internal initiation of translation on the subgenomic RNA transcript, nonspecific degradation of the LC protein, or reversion of the population bearing recombinant LC to wt LC (see Fig. 3.7).

3.5. Northern blot analysis of genomic and subgenomic RNA from recombinant FCV-infected cells

Two abundant positive sense RNA species corresponding to an approximately 7.8 kb genomic and 2.5 kb subgenomic RNA are produced during an FCV infection. In order to determine whether expression of these RNA species were affected by the introduction of foreign RNA into the subgenomic region, a Northern blot analysis was performed to determine the characteristics of the replicating RNA of cells infected with vR6-LC-GFP and vR6-LC-DsRed (Fig. 3.5).

RNA was isolated 8 hours p.i. from CRFK cells infected with vR6, vR6-LC-GFP or vR6-LC-DsRed. A biotinylated probe specific for the FCV ORF2 detected RNA consistent with the expected size of the wt subgenomic (approximately 2.5 kb) and genomic (approximately 7.7kb) RNA for vR6 (Fig.3.5, lane 1), along with additional minor virus-specific RNA species noted in previous studies (42). In contrast, RNA

isolated from recombinant FCV infected cells yielded two larger abundant RNA species, with an expected shift in the size of subgenomic (approximately 3.2 kb) and genomic (approximately 8.4 kb) RNAs for the vR6-LC-GFP (Fig. 3.5, lane 2) and vR6-LC-DsRed viruses (Fig. 3.5, lane 3). A longer exposure of the vR6-LC-DsRed RNA Northern blot is included in lane 5 to show the presence of the genomic RNA. These data demonstrate that the fluorescent protein coding sequence is present and maintained in the genome throughout multiple replication cycles. It also demonstrates that the subgenomic RNA is transcribed at levels similar to wt, indicating that the subgenomic promoter was functional in the presence of a large proximal insertion.

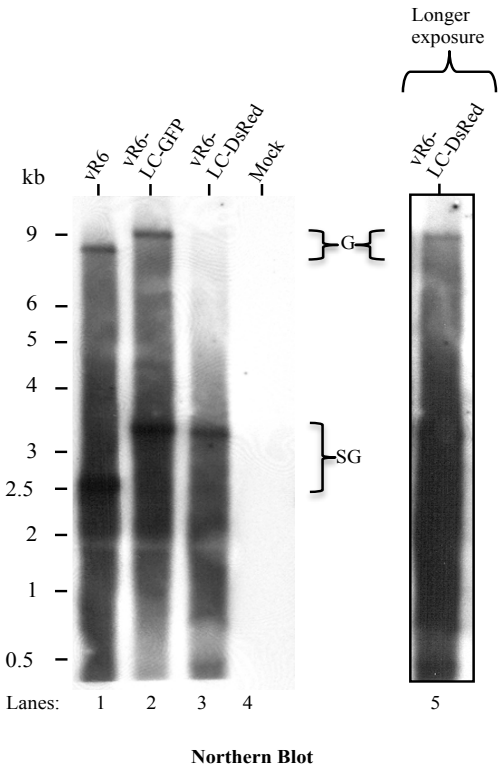

Fig. 3.5. Northern blot analysis of genomic and subgenomic RNA from recombinant FCV- infected cells. CRFK monolayers of a 6-well plate were infected with vR6, vR6-LC-GFP and vR6-LC-DsRed at an MOI of 1, and approximately 8 h later total RNA was extracted using Trizol reagent (Invitrogen). The RNA was analyzed on a 1% agarose gel that was dried and treated with a biotinylated RNA sense probe that was then exposed to film. G, genomic RNA; SG, subgenomic RNA.

3.6. Real-time visualization of LC production during a single and co-infection

The availability of two recombinant viruses expressing distinct reporter proteins prompted us to perform co-infection studies. Although evidence for recombination has been documented extensively in the caliciviruses, it has been difficult to elucidate the interactions of two viral genomes replicating in the same cell. Infection of a CRFK monolayer with the GFP and DsRed recombinant viruses yielded occasional cells expressing both red and green markers, with co-localization evidenced by a yellow signal in the merged images. One such single cell co-infected with both viruses was monitored over time, and the increase in expression of GFP and DsRed was consistent with the progression of CPE (Fig. 3.6). The most intense signal from recombinant LC in a co-infection was observed 8 hours p.i. (Fig. 3.6), although cells began to collapse and bleb approximately 5-6 hours p.i., a morphology consistent with reports of virus-induced apoptosis (182, 225, 256). Several other co-infected cells were monitored as well, but there was no clear pattern of one recombinant virus out-competing the other.

The image analysis of co-infection enabled by the visualization of LC trafficking suggests that different viruses within the same cell can both co-localize and maintain distinct replication sites.

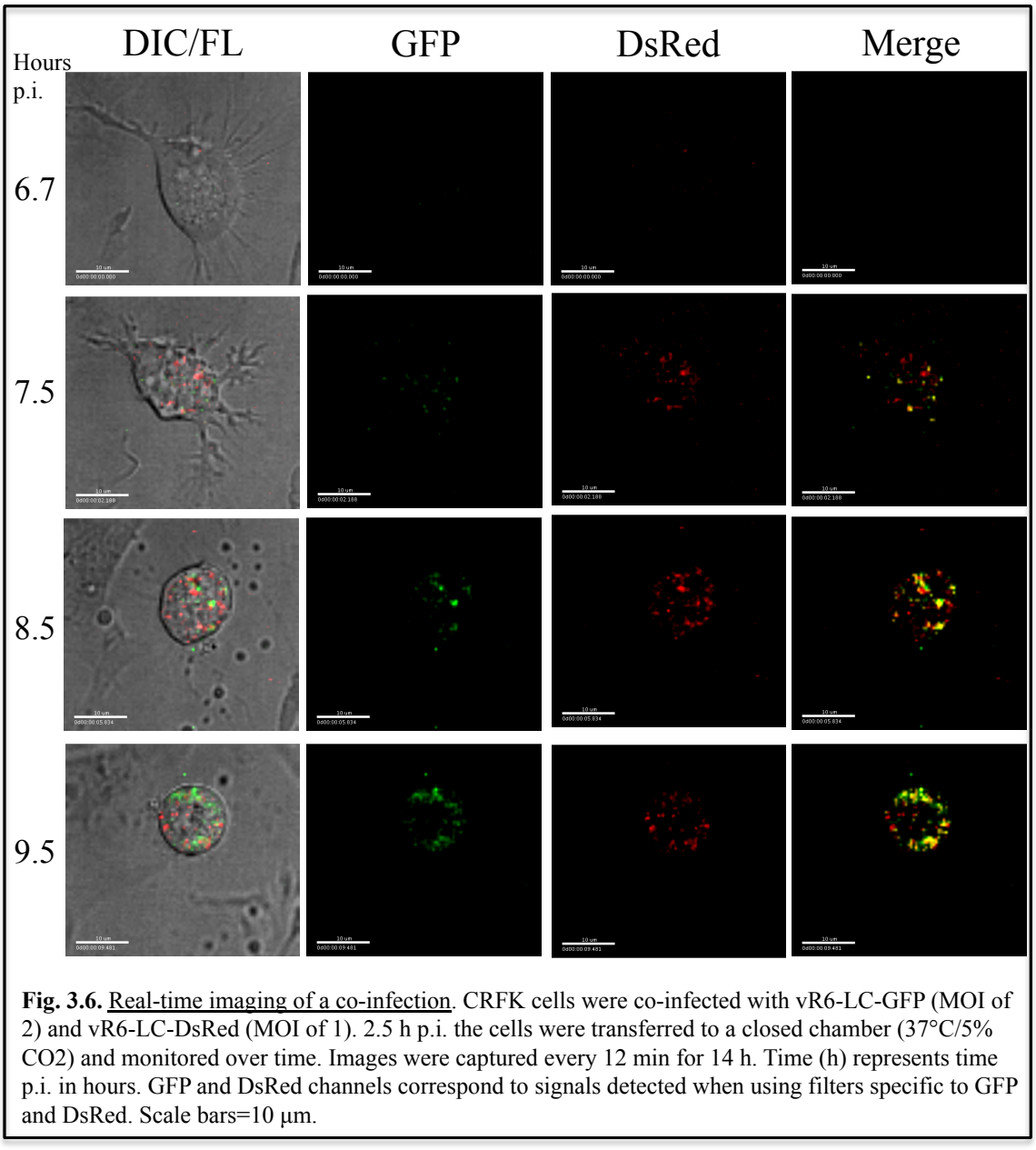

Fig. 3.6. Real-time imaging of a co-infection. CRFK cells were co-infected with vR6-LC-GFP (MOI of 2) and vR6-LC-DsRed (MOI of 1). 2.5 h p.i. the cells were transferred to a closed chamber (37°C/5% CO2) and monitored over time. Images were captured every 12 min for 14 h. Time (h) represents time p.i. in hours. GFP and DsRed channels correspond to signals detected when using filters specific to GFP and DsRed. Scale bars=10 µm.

3.7. Large insertions in the LC are not stably maintained in the FCV genome

A PCR assay was developed to track the stability of foreign inserts in the FCV genome, similar to studies that have been performed with recombinant polioviruses (177) (Fig. 3.7A). One clear indicator of changes in the inserted fluorescent protein gene was the appearance of non-fluorescent plaques in plaque-purified stocks. The RT-PCR diagnostics and sequencing analysis allowed us to track the sizes and types of deletions of revertant viruses.

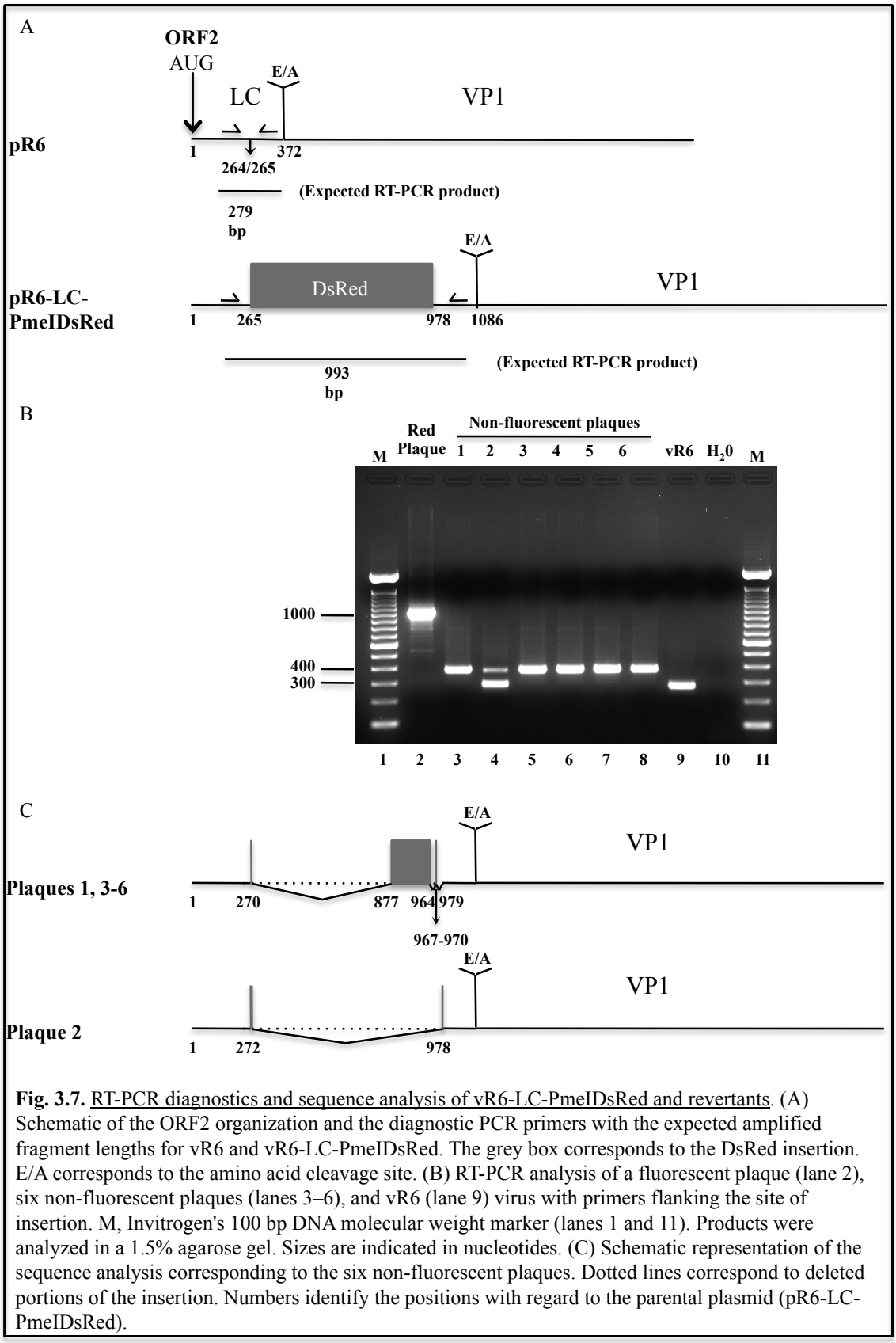

Fig. 3.7. RT-PCR diagnostics and sequence analysis of vR6-LC-PmeIDsRed and revertants. (A) Schematic of the ORF2 organization and the diagnostic PCR primers with the expected amplified fragment lengths for vR6 and vR6-LC-PmeIDsRed. The grey box corresponds to the DsRed insertion. E/A corresponds to the amino acid cleavage site. (B) RT-PCR analysis of a fluorescent plaque (lane 2), six non-fluorescent plaques (lanes 3–6), and vR6 (lane 9) virus with primers flanking the site of insertion. M, Invitrogen's 100 bp DNA molecular weight marker (lanes 1 and 11). Products were analyzed in a 1.5% agarose gel. Sizes are indicated in nucleotides. (C) Schematic representation of the sequence analysis corresponding to the six non-fluorescent plaques. Dotted lines correspond to deleted portions of the insertion. Numbers identify the positions with regard to the parental plasmid (pR6-LC-PmeIDsRed).

RT-PCR was performed on RNA purified from fluorescent and non- fluorescent plaques, and vR6 virus (Fig. 3.7B). The vR6 RNA yielded a band of approximately 300 bp (Fig. 3.7B, lane 9). The RNA from a fluorescent plaque produced a PCR amplicon of approximately 1000 bp, the expected size of the region if bearing an intact DsRed gene (lane 2). Five of the six nonfluorescent plaques from viruses obtained immediately after recovery from an infectious cDNA clone (lanes 3 and 4) or from pooled viruses amplified in a T-150 flask (lanes 5-8) yielded a similar sized band (approximately 400 bp, lanes 3, 5-8) that was intermediate when compared with the DsRed expressing virus and vR6. RNA from plaque 2 (lane 4) produced a major band matching that of vR6, and a minor band similar in size to that produced from the other non-fluorescent plaques, consistent with a mixed population of viruses undergoing deletions and reversion to near wild type.

PCR products from the non-fluorescent plaques were gel purified and sequenced. Plaques 1, and 3-6 contained six nucleotides from the 5'-end of the original DsRed insert, in addition to 101 nucleotides from the 3'-end of the insert separated by two small gaps (Fig. 3.7C). The major band of Plaque 2 was selected for sequencing, and this deletion variant contained 8 nucleotides of the 5'-end of the DsRed gene insertion, and a single nucleotide that likely corresponded to the last nucleotide of the 3'-end of the insertion (Fig. 3.7C).

An FCV variant that contained an HA epitope fused to the VP2 was also generated. The stability of the HA tag in ORF3 was analyzed by sequence analysis (data not shown). Following recovery, the VP2-HA virus was serially passaged three times, and sequence analysis of RT-PCR products obtained from the third passage virus showed

the presence of a modified HA epitope in the VP2 (Y—VPDYA, instead of the full YPYDVPDYA that had been introduced). No virus was recovered from a recombinant virus construct in which the FLAG epitope was introduced into the coding sequence of VP2, suggesting that the particular sequence of the insertion, in addition to length, may affect the stability and viability of recombinant viruses.

3.8. Phylogenetic analysis of vesivirus LC sequences

Vesivirus LC sequences are heterogeneous in size (14-18 kDa) and have marked sequence diversity across the genus (amino acid p-distance ranging from 66-82%) (Fig. 3.8). The amino acid identity can reach values as low as 15% (mink calicivirus versus FCV). However, within the four apparent genetic clusters (designated here as FCV-like, VESV-like, CaCV-like, and Mink calicivirus-like), there is high similarity at the amino acid level (amino acid p-distance ranging from 12-23%) (Fig. 3.8.1A and Fig. 3.8.1B). Despite the diversity, two conserved regions were identified and designated as conserved region I and II (CRI and CRII; Fig. 3.8B). CRI is a cysteine-rich region highlighted by three conserved cysteines, and CRII is a proline-rich region that contains three conserved prolines.

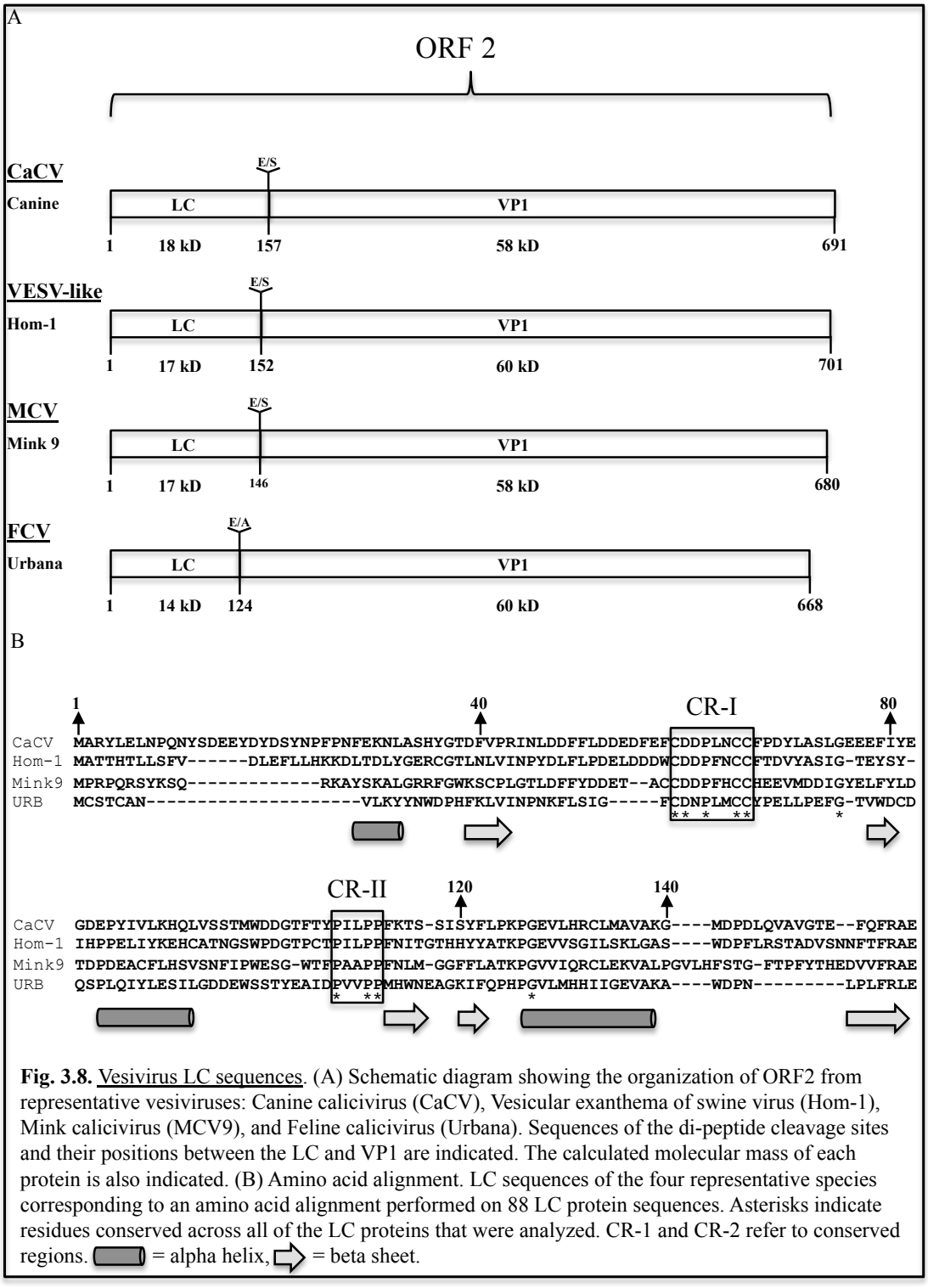

Fig. 3.8. Vesivirus LC sequences. (A) Schematic diagram showing the organization of ORF2 from representative vesiviruses: Canine calicivirus (CaCV), Vesicular exanthema of swine virus (Hom-1), Mink calicivirus (MCV9), and Feline calicivirus (Urbana). Sequences of the di-peptide cleavage sites and their positions between the LC and VP1 are indicated. The calculated molecular mass of each protein is also indicated. (B) Amino acid alignment. LC sequences of the four representative species corresponding to an amino acid alignment performed on 88 LC protein sequences. Asterisks indicate residues conserved across all of the LC proteins that were analyzed. CR-1 and CR-2 refer to conserved regions. = alpha helix, = beta sheet.

Linear sequence analysis using bioinformatic programs did not identify functional domains or motifs in representative sequences from the four different clusters. LC sequences do not share significant similarity with any protein that has been submitted to GenBank. One feature shared by representative sequences from all four clusters was the predicted secondary structure, which is highlighted in Fig. 3.8B.

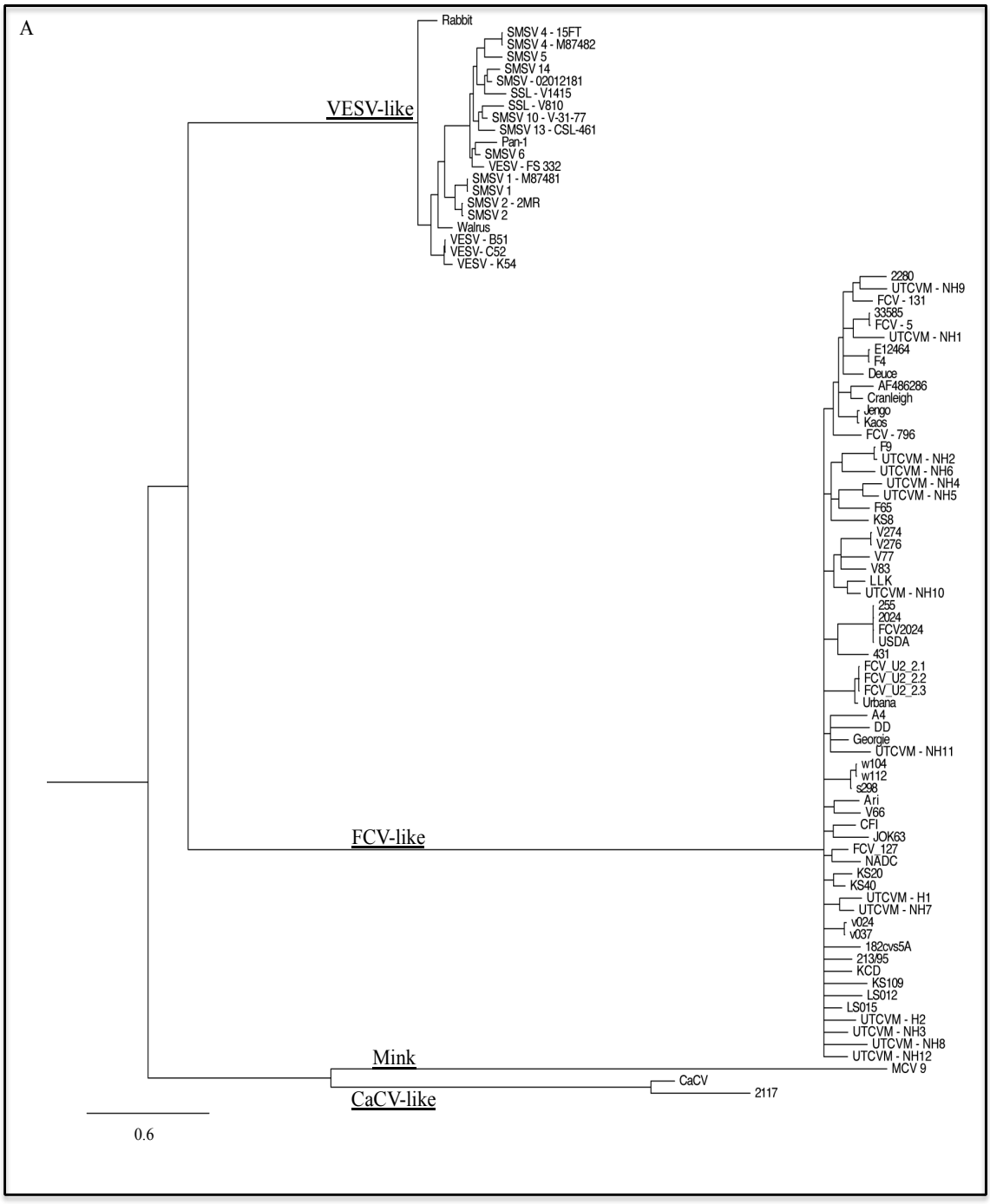
A
Rabbit
SMSV 4 - 15FT
SMSV 4 - M87482
SMSV 5
SMSV 14
SMSV - 02012181
SSL - V1415
SSL - V810
SMSV 10 - V-31-77
SMSV 13 - CSL-461
Pan-1
SMSV 6
VESV - FS 332
SMSV 1 - M87481
SMSV 1
SMSV 2 - 2MR
SMSV 2
Walrus
VESV - B51
VESV- C52
VESV - K54
VESV-like
2280
UTCVM - NH9
FCV - 131
33585
FCV - 5
UTCVM - NH1
E12464
F4
Deuce
AF486286
Cranleigh
Jengo
Kaos
FCV - 796
F9
UTCVM - NH2
UTCVM - NH6
UTCVM - NH4
UTCVM - NH5
F65
KS8
V274
V276
V77
V83
LLK
UTCVM - NH10
255
2024
FCV2024
USDA
431
FCV_U2_2.1
FCV_U2_2.2
FCV_U2_2.3
Urbana
A4
DD
Georgie
UTCVM - NH11
w104
w112
s298
Ari
V66
CFI
JOK63
FCV_127
NADC
KS20
KS40
UTCVM - H1
UTCVM - NH7
v024
v037
182cvs5A
213/95
KCD
KS109
LS012
LS015
UTCVM - H2
UTCVM - NH3
UTCVM - NH8
UTCVM - NH12
FCV-like
Mink
MCV 9
CaCV
2117
CaCV-like
0.6

B

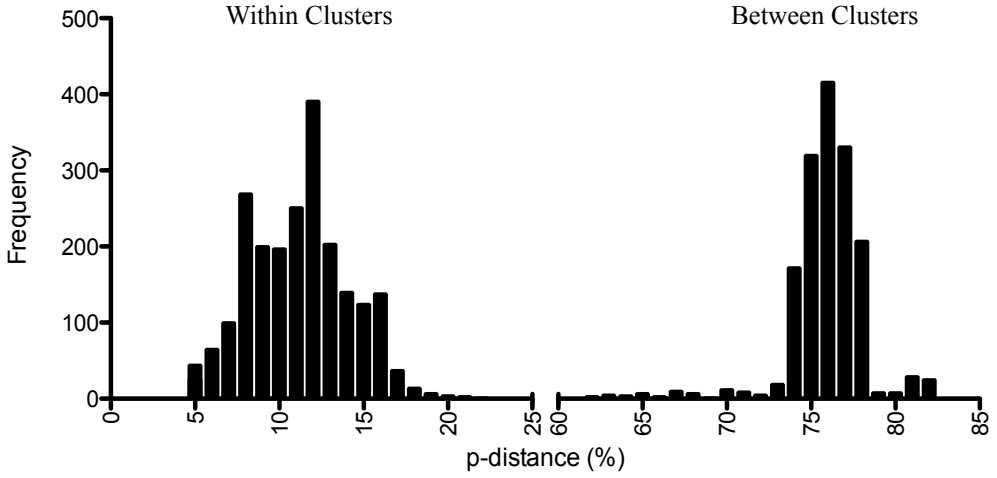

Fig. 3.8.1. Phylogenetic analysis of LC sequences. (A) Bayesian phylogenetic analysis of 88 LC nucleotide sequences. The parameters employed include the general time-reversible (GTR) model with a gamma distribution of substitution rates. Branches corresponding to the four different clusters are labeled: VESV-like, FCV-like, Mink and CaCV-like. The scale bar indicates expected nucleotide substitutions per site. (B) The proportion of amino acid variation (p-distance) within and between the four clusters.

A Bayesian phylogenetic analysis of eighty-eight LC nucleotide sequences depicts four main evolutionary lineages or clusters: FCV-like LC, a VESV-like, a CaCV-like and Mink calicivirus-like (Fig. 3.8.1A). Consistent with a previous report (195), isolate 2117, which was identified as a contaminating agent in fetal bovine serum, clusters closely with CaCV (Fig. 3.8.1A). A graphic representation comparing the amino acid p-distance values within clusters and among lineages clearly shows the high level of similarity within these clusters and the marked lack of similarity when comparing LC sequences from different lineages (Fig. 3.8.1B).

3.9. N- and C-terminal deletions of the LC and virus viability

To determine whether all or part of the LC is essential for recovery of infectious virus, a series of 14 FL clones was generated that contained sequential 10 aa deletions in the LC protein beginning from either the N- or C-terminus (Fig. 3.9). Cleavage of the capsid precursor is essential for the recovery of infectious virus (257), and the highly conserved C-terminal residues (FRLE) were present to maintain the cleavage site (E/A). The MVA-T7 based recovery system for FCV (258) was used to test the mutant FL clones for recovery of infectious virus.

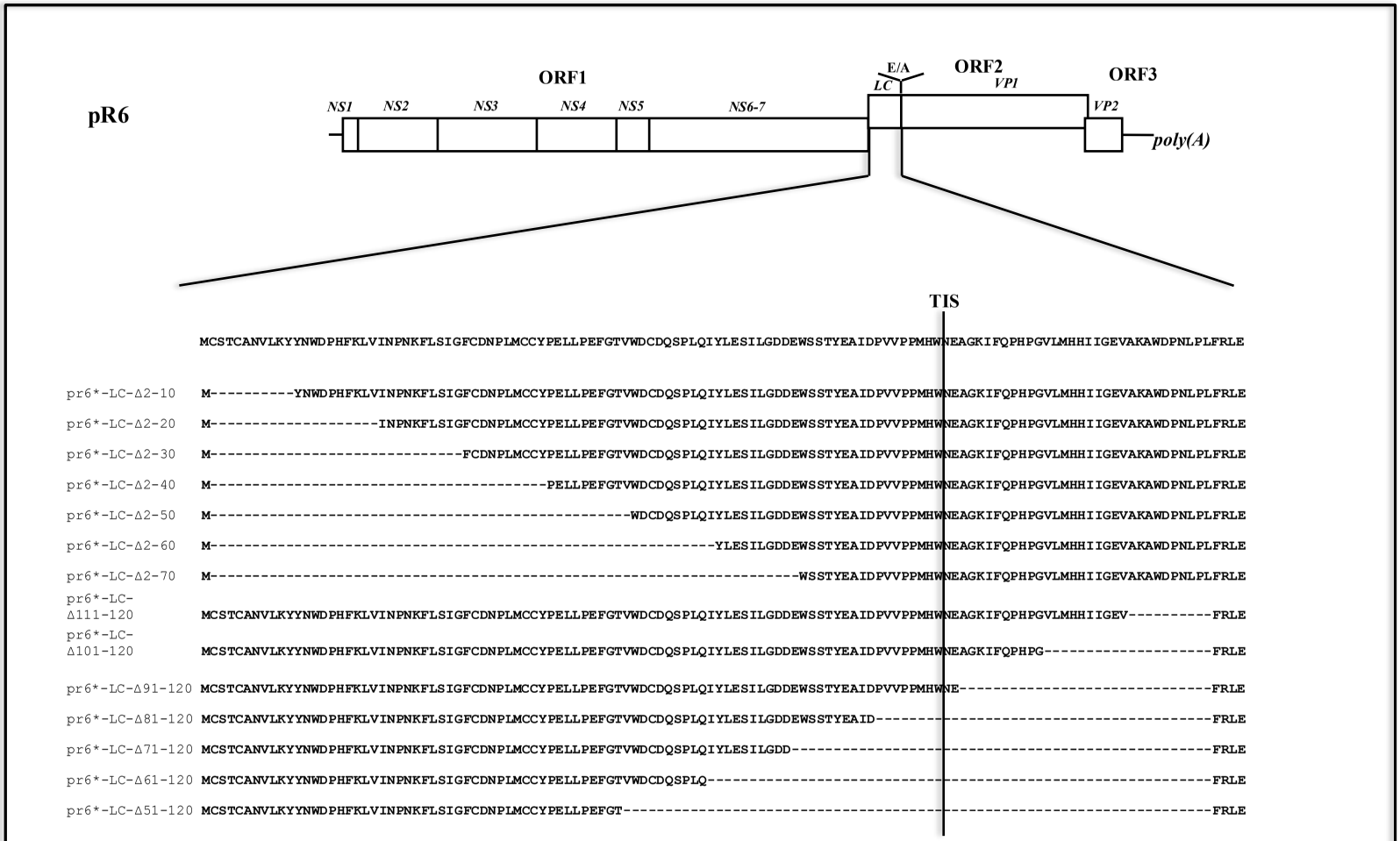

Fig. 3.9. Recombinant FCV FL clones with truncated LC sequences. Schematic diagram of plasmid constructions containing engineered deletions of the LC in the context of the FL genome. The transposon insertion site (TIS) is indicated with a line. The name of the FL clones refer to the LC amino acids that have been deleted.

Following FL plasmid transfection/MVA-T7 infection, cell culture supernatant was transferred to a fresh monolayer of CRFK cells (passage 1, P1) at 24-48 hours post-transfection (hpt) and the cells were monitored for FCV cytopathic effect (CPE), which appeared as cell-rounding of the CRFK cells and detachment of cells from the surface up to P3. Table 9 summarizes whether overt CPE could be observed at P3 for the constructs. In addition, RNA was extracted from the supernatant and reverse-transcription PCR (RT-PCR) was performed using FCV specific primers as a more sensitive detection method to detect low levels of viral replication. No clear CPE could be observed at P3 for any of the deletion constructs, although two (vR6*-LC-Δ111-120 and vR6*-LC-Δ91-120**)** were positive by RT-PCR. Sequence analysis of the amplicon generated from the RNA of vR6*-LC-Δ111-120 confirmed that the replicating virus lacked aa 111-120. RNA extracted from vR6*-LC-Δ91-120 yielded a weak RT-PCR amplicon that was not sufficient for sequence analysis.

	Passage 3	
Construct	CPE	PCR Positive
pR6*-LC-Δ2-10	-	-
pR6*-LC-Δ2-20	-	-
pR6*-LC-Δ2-30	-	-
pR6*-LC-Δ2-40	-	-
pR6*-LC-Δ2-50	-	-
pR6*-LC-Δ2-60	-	-
pR6*-LC-Δ2-70	-	-
pR6*-LC-Δ111-120	-	+
pR6*-LC-Δ101-120	-	-
pR6*-LC-Δ91-120	-	+
pR6*-LC-Δ81-120	-	-
pR6*-LC-Δ71-120	-	-
pR6*-LC-Δ61-120	-	-
pR6*-LC-Δ51-120	-	-
pR6-LC-C33A	-	+
pR6-LC-D34A	+	+
pR6-LC-P36A	+	+
pR6-LC-C39A	-	+
pR6-LC-C40A	-	+
pR6-LC-P81A	+	+
pR6-LC-P84A	+	+
pR6-LC-P85A	+	+
pR6-LC-81/4/5A	-	+

TABLE 9. Effects of LC deletions and alanine substitutions of conserved LC residues on virus recovery

The virus recovered from the vR6*-LC-Δ111-120 construct was investigated further. While complete CPE was observed in P1 and P2 during the initial recovery experiment, no CPE was detected by P3. However, evidence for continuing replication was supported by a positive immunofluorescence assay at P3 and P4 (Fig. 3.9.1A), and the detection of viral RNA by RT-PCR as noted above. The plaque phenotype of the mutant virus recovered from vR6*-LC-Δ111-120 was compared to that of the wild-type Urbana FCV strain (Fig. 3.9.1B). The plaques generated from vR6*-LC-Δ111-120 were approximately five times smaller when compared to the plaques produced by wild-type virus (P-value <0.0001; Fig. 3.9.1C).

One possible explanation for the growth attenuation of the vR6*-LC-Δ111-120 in cell culture was reduced efficiency in cleavage of the capsid precursor, which has previously been reported to severely affect virus growth and limit viral replication to one virus life-cycle (257). A Western blot analysis was performed using cell lysates from P2 of vR6*-LC-Δ111-120 to determine whether uncleaved precursor could be detected. Using hyperimmune sera specific to the Urbana virion, only the mature, cleaved, capsid protein was detected, indicating that cleavage efficiency was not affected (Fig. 3.9.1D). These data suggest that the while the N-terminal region of the LC is required for viral replication, the C-terminal region is not essential for viral replication but is important for virus spread.

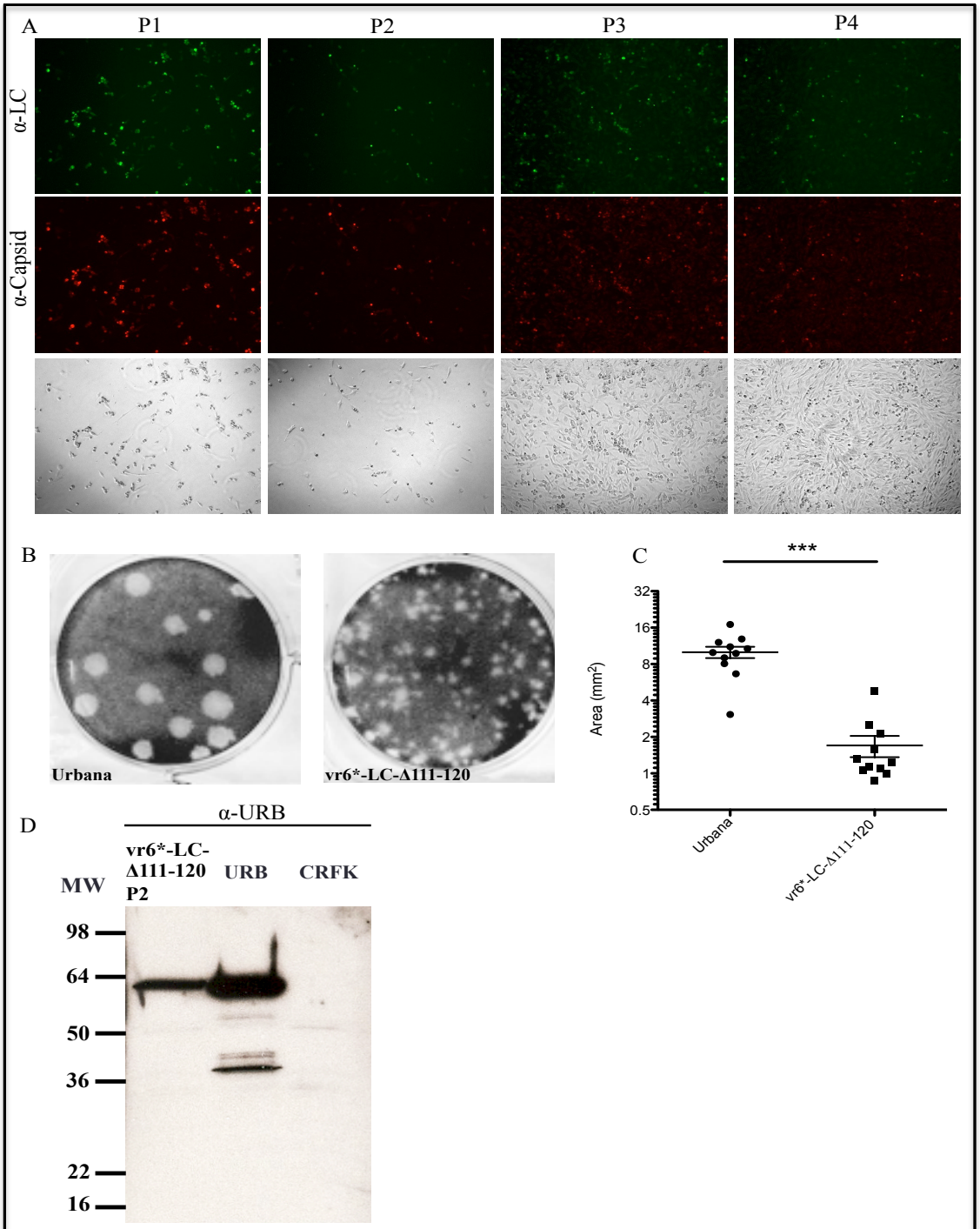

Fig. 3.9.1. Analysis of replication of vR6*-LC-Δ111-120. (A) Fluorescent microscopy analysis of LC and capsid expression in CRFK cells of a series of passages of vR6*-LC-Δ111-120. Bright field images are shown as well to demonstrate the difference between CPE observed between P1 and P2 with P3 and P4. CRFK cells were stained 48 hours post infection with hyperimmune sera raised against either FCV virions or recombinant LC. (B) Representative image of a plaque assay performed simultaneously comparing wild-type FCV (Urbana) and P1 of vR6*-LC-Δ111-120. (C) Plaque size was measured using the software program GraphClick, and the statistical significance in size was calculated using an unpaired t-test (P-value <0.0001). (D) Western blot analysis of a cell lysate from passage 2 of vR6*-LC-Δ111-120. A cell lysate of Urbana-infected cells (URB) was included as a positive control, and an un-infected cell lysate (CRFK) was included as a negative control.

3.10. Transient expression of the LC and LC-mKate in CRFK cells

The complete LC coding sequence of the Urbana strain was cloned into a pCI eukaryotic expression vector to examine the phenotype of cells that supported transient over-expression of the LC alone (Fig. 3.10A). In order to monitor LC expression in live cells, a recombinant LC protein was generated by cloning the red fluorescent protein mKate into the transposon insertion site (TIS; between amino acid 88 and 89 of the coding sequence of the LC), which was designated pCI-LC-mKate. mKate was used instead of DsRed or GFP because it is reported to be brighter and have a faster maturation rate (292).

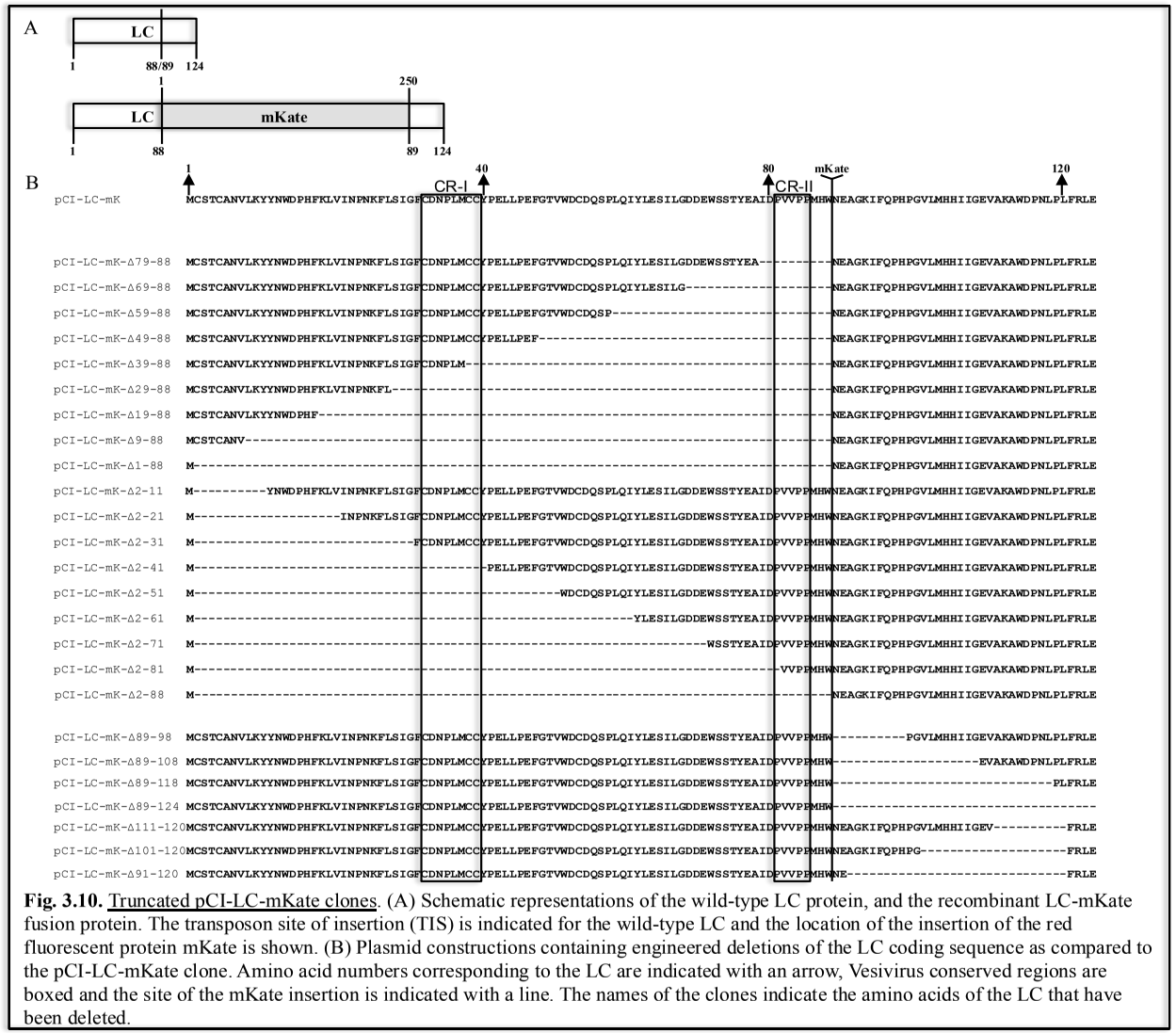

Fig. 3.10. Truncated pCI-LC-mKate clones. (A) Schematic representations of the wild-type LC protein, and the recombinant LC-mKate fusion protein. The transposon site of insertion (TIS) is indicated for the wild-type LC and the location of the insertion of the red fluorescent protein mKate is shown. (B) Plasmid constructions containing engineered deletions of the LC coding sequence as compared to the pCI-LC-mKate clone. Amino acid numbers corresponding to the LC are indicated with an arrow, Vesivirus conserved regions are boxed and the site of the mKate insertion is indicated with a line. The names of the clones indicate the amino acids of the LC that have been deleted.

Expression of wt-LC and LC-mKate in CRFK cells resulted in the appearance of rounded cells, similar to those observed during viral infection (Fig. 3.10.1A). To test whether the cell-rounding phenotype was associated with cell death, a commercially available reactive dye was used that emits a green signal when reacting with the free amines characteristic of dead cells. The majority of cells positive for LC-mKate expression were positive also for the reactive dye (Fig. 3.10.1B), indicating that the over-expression of the LC was toxic to CRFK cells and caused cell death.

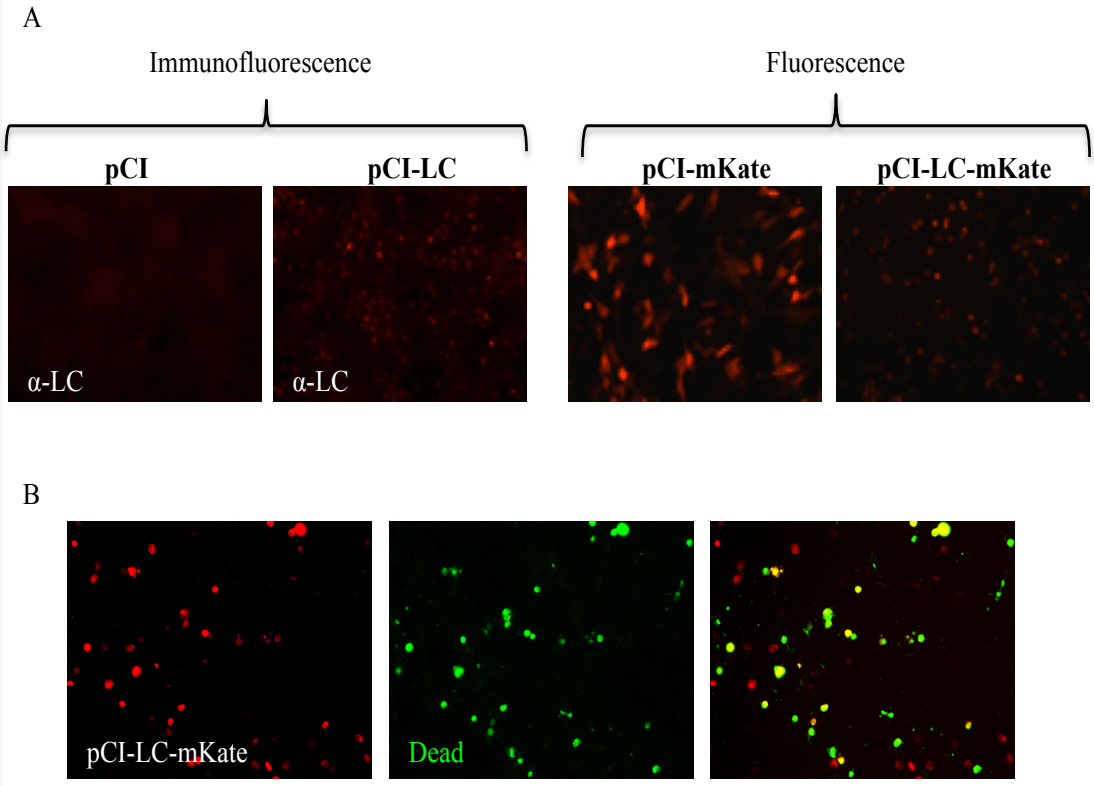

Fig. 3.10.1. Transient expression of LC and LC-mKate. (A) Immunofluorescent and fluorescent analysis of CRFK cells transfected with the indicated plasmids. The LC was detected using hyperimmune sera, and mKate and LC-mKate expression was visualized in live cells. (B) Representative image of CRFK cells transfected with pCI-LC-mKate that was treated with the Live/ Dead reagent that stains dead cells green.

To further investigate the cell-rounding phenotype, pCI-LC-mKate clones were generated that introduced sequential 10 aa deletions beginning at either at the N- or C-terminus or internally at the TIS (Fig. 3.10B). While some heterogeneity could be observed in the appearance of the cell-rounding phenotype, there was a clear association of cell-rounding with expression of the N-terminal region of the LC (aa 1-88; Fig. 3.10.2). Even when the entire C-terminal region of the LC (89-124) was deleted, cell-rounding was observed in constructs that contained the N-terminal region of the LC. In contrast, when only the C-terminal region was expressed, the flat, elongated morphology

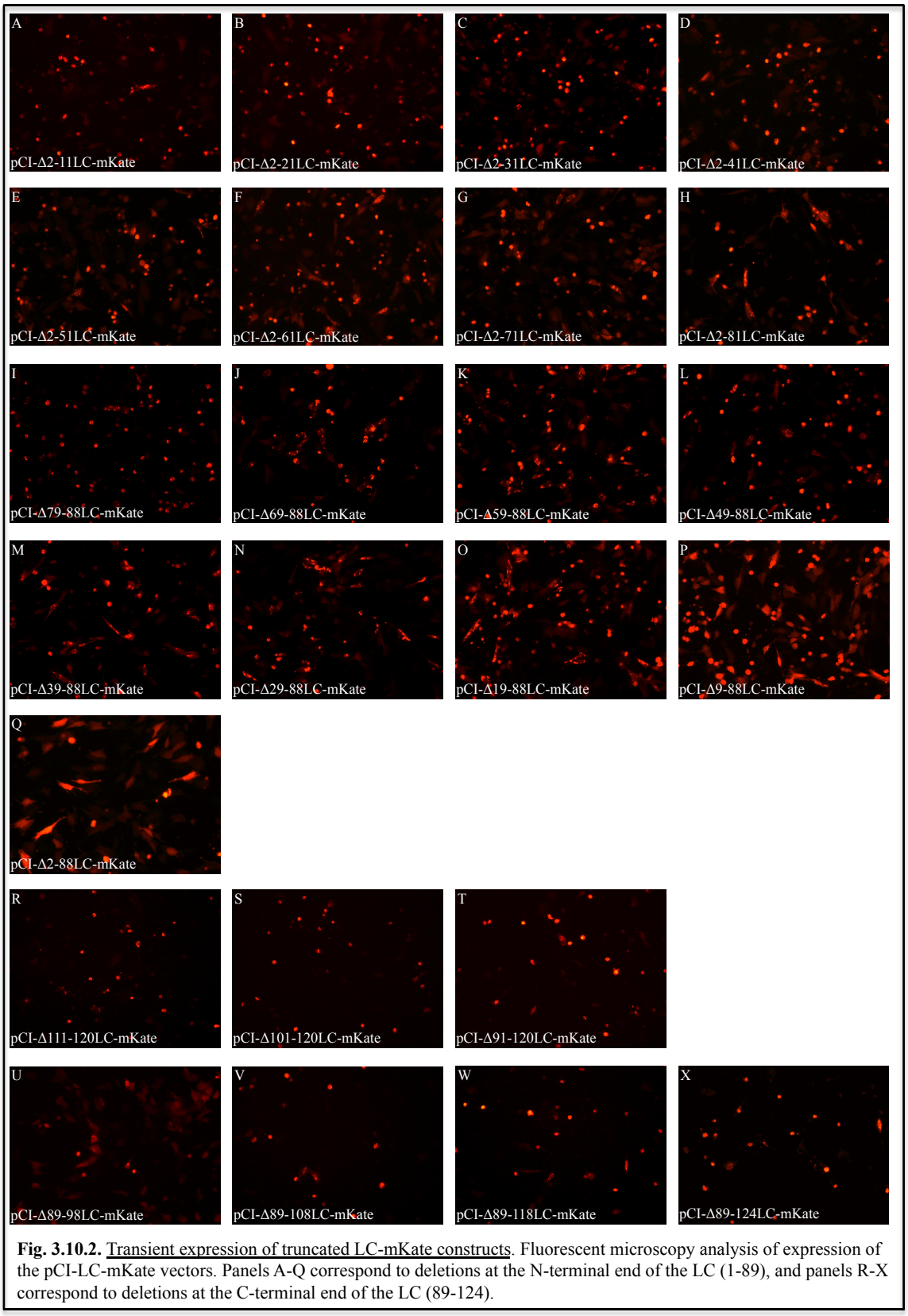

Fig. 3.10.2. Transient expression of truncated LC-mKate constructs. Fluorescent microscopy analysis of expression of the pCI-LC-mKate vectors. Panels A-Q correspond to deletions at the N-terminal end of the LC (1-89), and panels R-X correspond to deletions at the C-terminal end of the LC (89-124).

of the CRFK cells could be observed similar to that observed when mKate alone was expressed as a control (Fig. 3.10.1A).

3.11. Alanine-scanning mutagenesis of conserved residues in the LC

The phylogenetics analysis revealed that there were two conserved regions (CRs) found among all LC sequences (Fig. 3.8B), which was designated as CRI and CRII. To evaluate the significance of these conserved residues, scanning alanine mutagenesis was performed. Eight new FL constructs were generated in which a single conserved residue was substituted for an alanine (Fig. 3.11A) and transfected into MVA-T7-infected cells. Recovery of virus was monitored by CPE and RT-PCR for three passages as described above.

Substitution of any of the three prolines from the CRII with alanine had no effect on recovery of virus (Table 3), and CPE was similar to that of wt. The genetic stability of the recovered viruses was examined at P3, and no reversions were detected, indicating that these residues were not essential for recovery of infectious virus. Similarly, when D34 or P36 of CRI was substituted for alanine, virus was readily recovered and the substitutions were stable through P3.

Alanine substitutions introduced at positions C33, C39 or C40, of CR1 resulted in failure to recover lytic viruses by P3, although all three passages were positive by RT-PCR indicating low levels of replication (Table 3). Supernatants from the infected cells were continually passaged in an attempt to isolate the mutant virus or select for fast-growing lytic revertants. Viruses containing the C33A and C39A substitutions were negative by RT-PCR at P6, indicating that these mutations were deleterious for virus

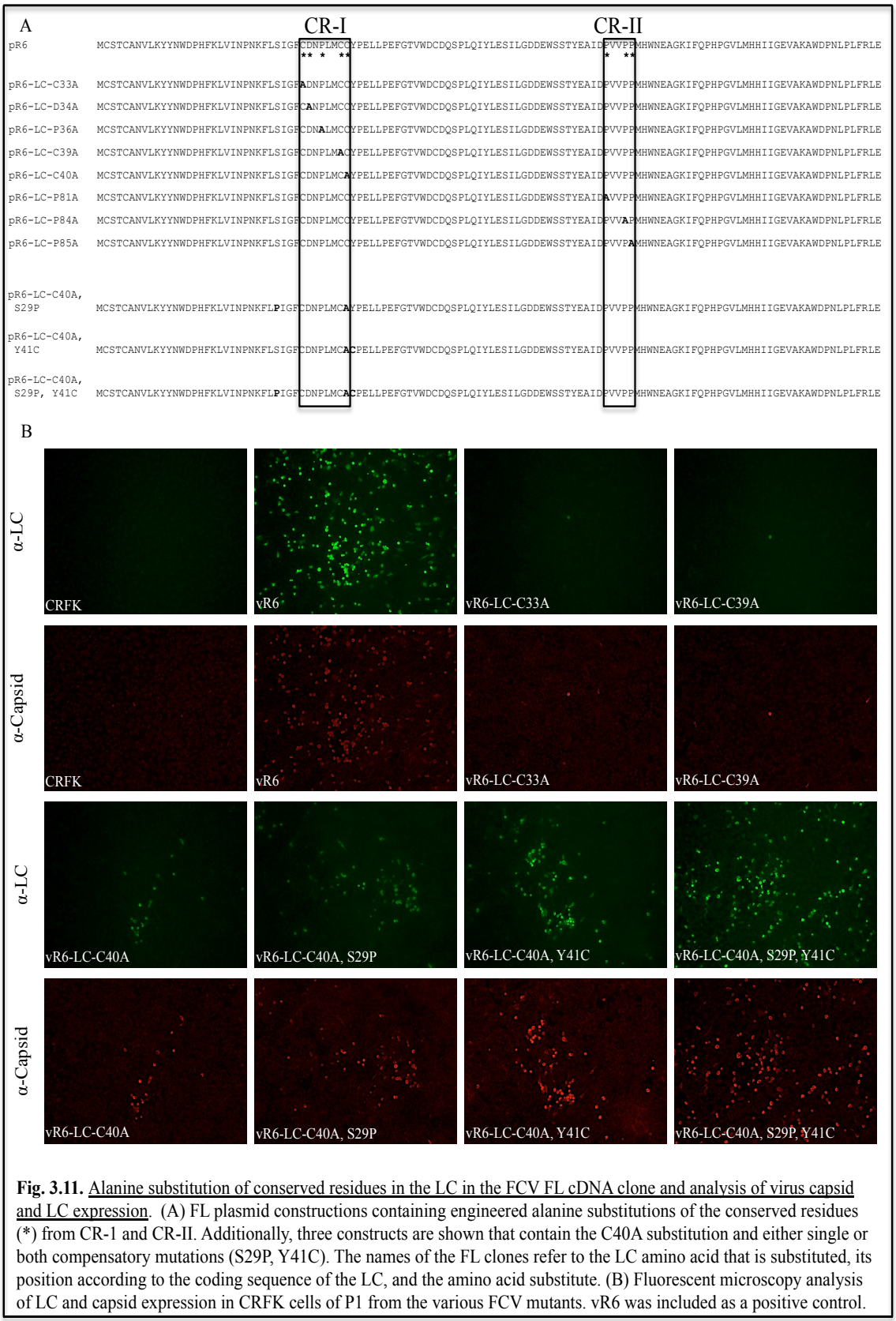

Fig. 3.11. Alanine substitution of conserved residues in the LC in the FCV FL cDNA clone and analysis of virus capsid and LC expression. (A) FL plasmid constructions containing engineered alanine substitutions of the conserved residues (*) from CR-1 and CR-II. Additionally, three constructs are shown that contain the C40A substitution and either single or both compensatory mutations (S29P, Y41C). The names of the FL clones refer to the LC amino acid that is substituted, its position according to the coding sequence of the LC, and the amino acid substitute. (B) Fluorescent microscopy analysis of LC and capsid expression in CRFK cells of P1 from the various FCV mutants. vR6 was included as a positive control.

growth. In contrast, the C40A virus remained RT-PCR positive through P9, at which point an overt CPE phenotype was restored. Sequence analysis of viral RNA from the C40A mutant at P9 revealed that the alanine substitution remained stable, but that two new non-synonymous mutations had been acquired in the LC coding sequence. A point mutation in position 5398 (codon 29 of the LC) resulted in the replacement of a UCC (Ser) codon with a CCC (Pro) codon, and another point mutation in position 5435 (codon 41 of the LC) resulted in the replacement of a UAU (Tyr) codon with a UGU (Cys) codon (Fig. 3.11.1).

Sequence analysis was performed on several passages of the revertant virus to examine if the substitutions arose simultaneously or separately. A mixed population could be observed at codon 41 of the LC as early as P3, and the point mutation resulting in the Y41C substitution was clearly dominant by P6 (Fig. 3.11.1). The substitution of codon 29 appeared after the Y41C substitution. It first appeared around P6, and was clearly fixed in the population by P9 (Fig. 3.11.1), when the fast-growing lytic phenotype was restored.

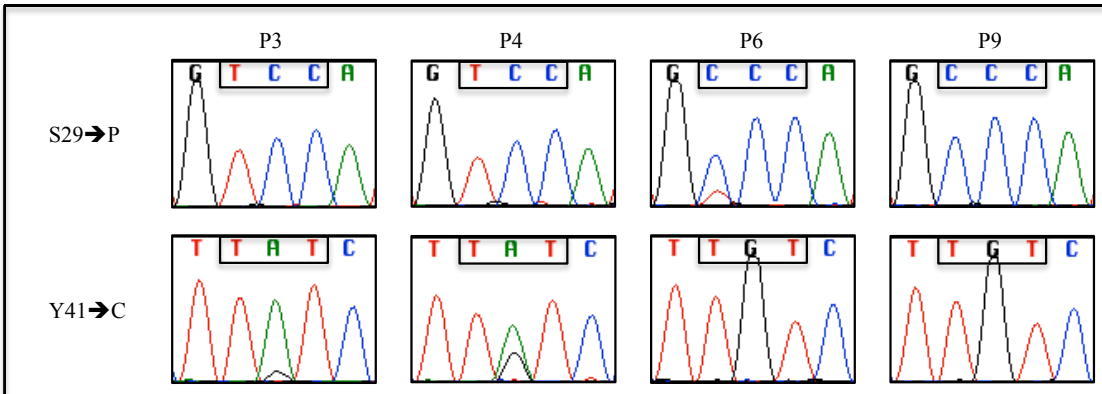

Fig. 3.11.1. Sequence analysis of vR6-LC-C40A from different passages. Chromatograms of LC codons (boxed nucleotides) at positions 29 and 41 corresponding to several different passages.

The sequential order of the acquired mutations suggested that both might be necessary to restore the fast-growing lytic phenotype. In order to examine whether one or both mutations were required to suppress the C40A mutation, three new FL clones were generated that introduced individual substitutions (S29P or Y41C FL) or both (S29P and Y41C FL) in the context of the C40A background (Fig. 3.11A). Lytic virus could not be recovered from either of the individual constructs in P1, although the presence of growing foci was more readily detected when either the S29P or Y41C substitution was present. However, when both substitutions were present together, fast-growing lytic virus was recovered at P1 (Fig. 3.11B).

3.12. Effects of alanine substitutions on cell-rounding phenotype

I next examined whether the conserved cysteines at positions 33, 39 and 40 of the LC were associated with the cell-rounding phenotype that was observed following transient expression of the LC and LC-mKate. Images were captured of LC-mKate transient expression in CRFK cells using modified pCI-LC-mKate clones in which the conserved cysteines of CRI were substituted with alanine. In contrast to the cell-rounding phenotype that was consistently observed with the wild-type sequence of the LC, expression of the three alanine mutants resulted in a heterogeneous phenotype in which the majority of cells positive for expression did not cause cell-rounding and produced a puncta-like localization (Fig. 3.12). These data were consistent with a correlation between the ability of the LC to induce a cell-rounding phenotype and virus spread, as viruses bearing these substitutions could not be recovered. I next investigated whether the compensatory mutations that allowed viruses with the C40A mutation to become lytic

were associated with cell rounding. A pCI-LC-mKate clone was generated that contained the C40A substitution, in addition to the two compensatory mutations (S29P and Y41C FL). Expression of this modified LC restored the cell-rounding phenotype, further supporting a correlation between the cell-rounding phenotype induced by the LC and the ability of FCV to spread efficiently.

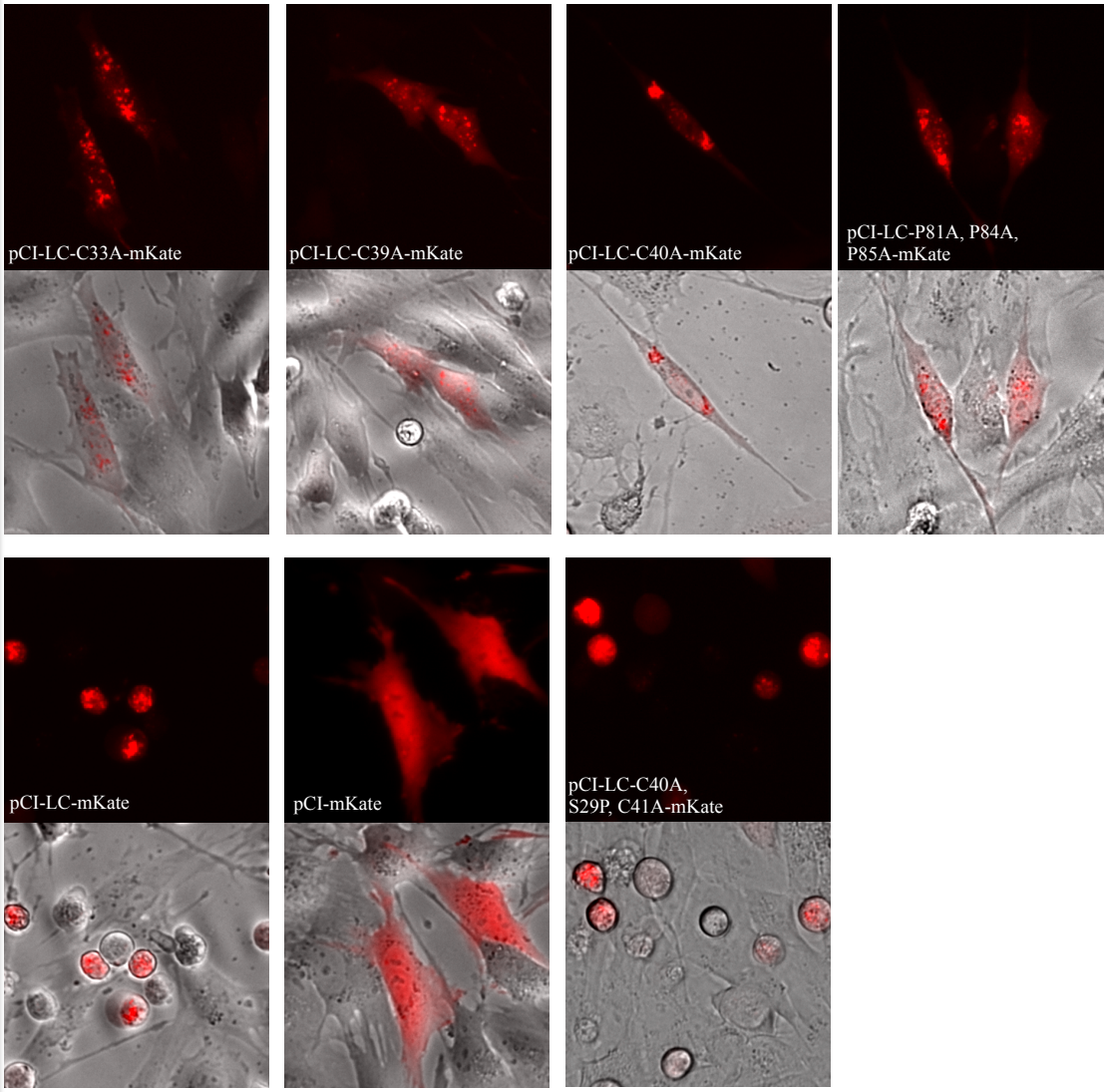

Fig. 3.12. Alanine substitution of conserved residues in the LC in the pCI-LC-mKate clone and analysis of cell morphology in transient expression experiments. Fluorescent microscopy analysis of CRFK cells transfected with LC-mKate, LC-mKate clones containing alanine substitutions of conserved cysteines in the CR-I, and a LC-mKate-C40A clone that contained the two compensatory mutations required to suppress the defect in virus spread caused by the C40A substitution.

3.13. Identification of host cellular partners of the LC

To identify cellular proteins that interact with the LC during an FCV infection, a FL clone was generated that introduced two unique epitopes (FLAG, and a 22 amino acid peptide corresponding a Norwalk virus VP1 epitope (Fig. 3.13A) fused to the LC to perform immunoprecipitation assays. Two tags were included in order to allow for tandem-affinity immunoprecipitation, should it be required. Infectious virus was readily recovered from the recombinant FL clone, and the stability of the insertions was confirmed after 3 passages.

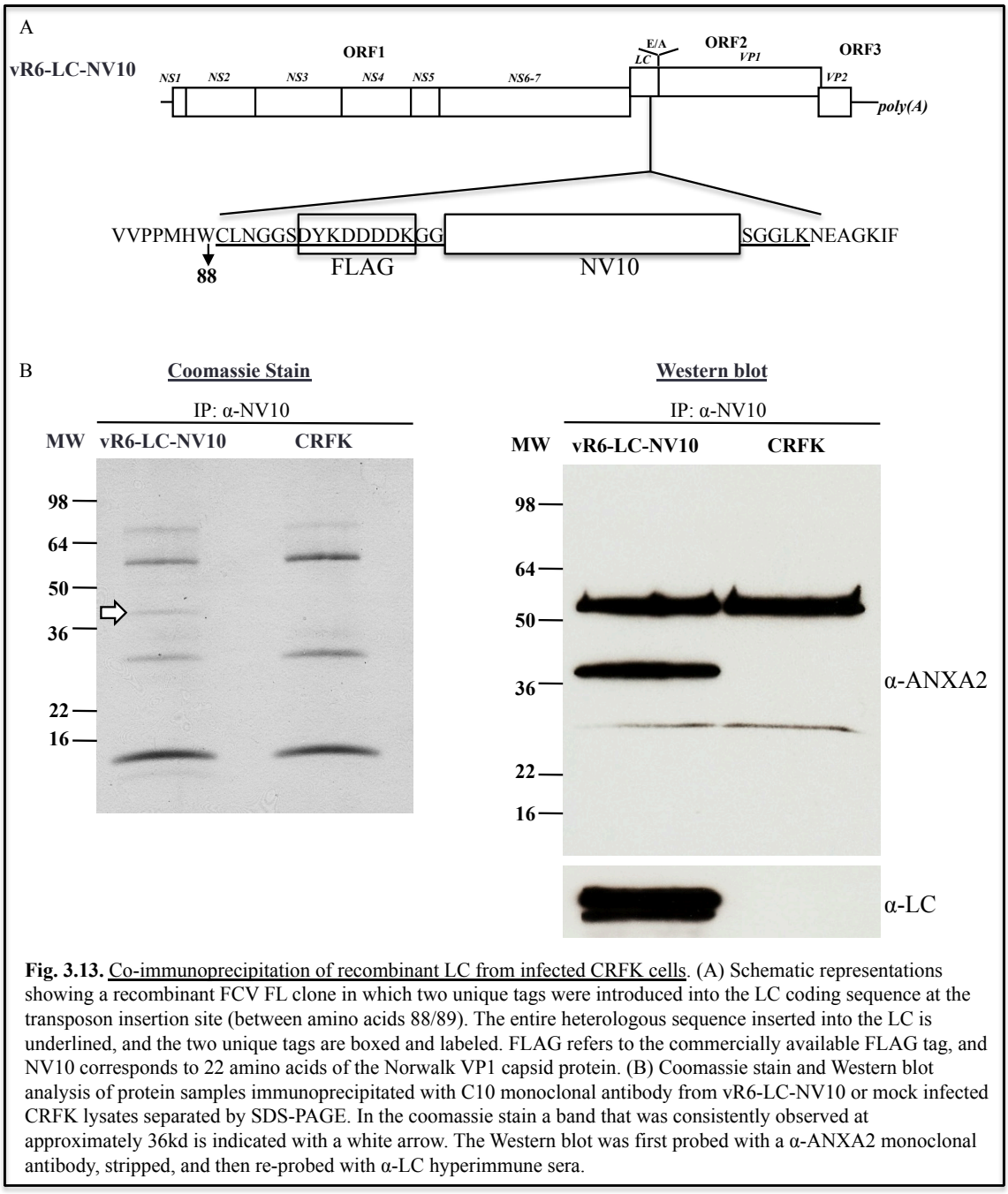

Fig. 3.13. Co-immunoprecipitation of recombinant LC from infected CRFK cells. (A) Schematic representations showing a recombinant FCV FL clone in which two unique tags were introduced into the LC coding sequence at the transposon insertion site (between amino acids 88/89). The entire heterologous sequence inserted into the LC is underlined, and the two unique tags are boxed and labeled. FLAG refers to the commercially available FLAG tag, and NV10 corresponds to 22 amino acids of the Norwalk VP1 capsid protein. (B) Coomassie stain and Western blot analysis of protein samples immunoprecipitated with C10 monoclonal antibody from vR6-LC-NV10 or mock infected CRFK lysates separated by SDS-PAGE. In the coomassie stain a band that was consistently observed at approximately 36kd is indicated with a white arrow. The Western blot was first probed with a α-ANXA2 monoclonal antibody, stripped, and then re-probed with α-LC hyperimmune sera.

Co-IP assays were performed using a biotinylated monoclonal antibody (C10), specific to a 22 aa peptide corresponding to the Norwalk VP1, in combination with strepavidin-conjugated beads to purify the recombinant LC. A 36-kd protein co-precipitating with the rLC was consistently observed when the pulled-down protein complex was analyzed by SDS-PAGE followed by coomassie staining (Fig. 3.13B). The protein band was submitted for mass spectrometry analysis and it was identified as annexin A2 (ANXA2), a host cellular protein associated with the cytoskeleton and cell motility (88, 224). Western blot analysis using a monoclonal antibody against ANXA2 confirmed the specificity of the interaction (Fig. 3.13B).

3.14. FCV LC chimeras

The phylogenetic analysis of the LC protein showed a marked diversity among vesiviruses in different genetic clusters. I explored whether the LC proteins representing the VESV-like or Mink calicivirus-like clusters could replace the LC protein of FCV. Four chimeric recombinant FL FCV clones were constructed in which either the entire LC sequence, or an internal portion, of the FCV LC was substituted with LC sequences from Mink calicivirus 9 or SMSV-5 Hom-1 (VESV-like) (Fig.3.14A). Recovery experiments did not yield lytic virus as judged by CPE, but evidence for a low level of virus replication was found when cells were observed by immunofluorescence. The SMSV LC (corresponding to the VESV-like cluster) appeared better tolerated than the MCV LC, in that larger foci of positive cells were observed (Fig. 3.14B). Viral RNA could be detected at P3 for both recombinant constructs that contained the entire or partial sequences corresponding to the SMSV LC but were negative for the recombinant

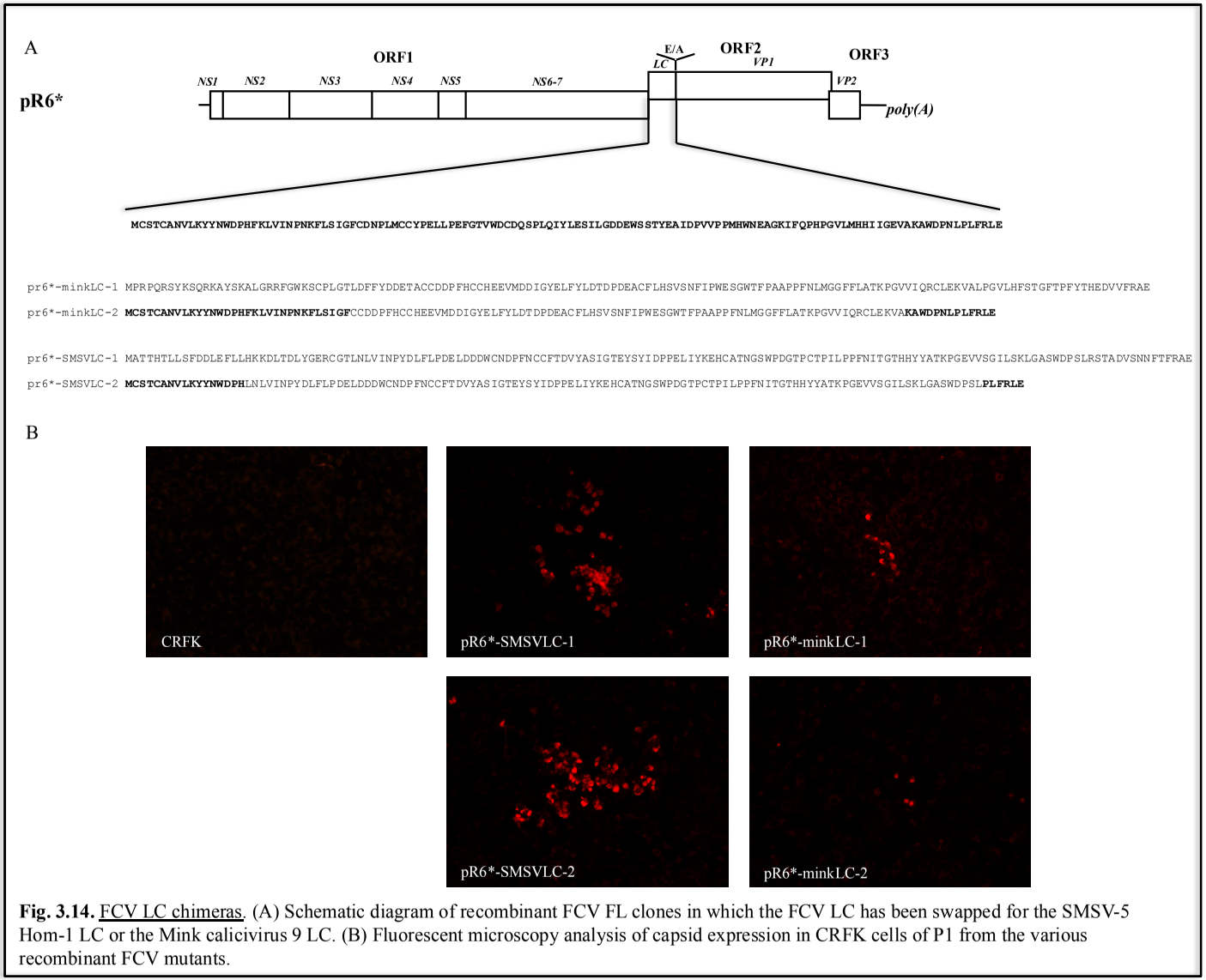

Fig. 3.14. FCV LC chimeras. (A) Schematic diagram of recombinant FCV FL clones in which the FCV LC has been swapped for the SMSV-5 Hom-1 LC or the Mink calicivirus 9 LC. (B) Fluorescent microscopy analysis of capsid expression in CRFK cells of P1 from the various recombinant FCV mutants.

viruses expressing Mink calicivirus LC protein. Sequence analysis of the FCV-SMSV-5-Hom-1-LC viruses revealed that there were no acquired mutations in the LC region at least through passage 3.

CHAPTER 4: DISCUSSION

4.1. Recombinant FCV strains

Until now, recombinant caliciviruses generated by reverse genetics have contained only highly-related domain swaps from other caliciviruses (190). The trans-encapsidation of a non-infectious FCV RNA that contains GFP fused to the VP1 sequence has been reported, although the low efficiency of the trans-encapsidation event did not allow for further characterization or analysis of the trans-encapsidated virion (271). The introduction of heterologous sequences into the genome of a single-stranded positive-sense RNA virus presents several challenges because the insertion may affect RNA secondary structure, proteolytic processing of a polyprotein, and RNA packaging. Some approaches that have been successfully applied to engineer recombinant single-stranded positive-sense viruses include: cloning the heterologous sequence in frame with a viral protein (29, 30, 36, 69), cloning an internal ribosomal entry site (IRES) adjacent to the heterologous sequence to create a dicistronic expression vector (5, 102, 153, 215), and cloning a heterologous sequence that contains an artificial viral cleavage site adjacent to a viral ORF (8, 31, 70, 103, 109, 163, 270). The Tn7 transposon mutagenesis system was employed to identify sites in FCV that can tolerate an insertion because it has been successfully applied to other single-stranded, positive sense RNA viruses (11, 173).

Random transposon mutagenesis was applied to FCV to determine whether the virus could tolerate a 15-nt insertion. Three viral proteins were found to tolerate the small 15-nt insertion: VPg (two different sites), VP2 and the LC. It was unexpected that the VP2 could tolerate an insertion because it has been shown that the N-terminus of VP2 contains domains that are essential for viral replication (252). Despite tolerating a

heterologous sequence fused to VP2 (an HA epitope), the insertion of the recombinant virus was rapidly modified by partial deletion of the foreign insertion. It is likely that there are other sites within the FCV genome that can tolerate an insertion, but our initial analysis resulted in the identification of only these four sites.

Two heterologous sequences were cloned into the site identified in the LC protein (AcGFP, DsRed), and recombinant viruses were recovered. Further study of these viruses showed that they produced the LC protein as an intact GFP or DsRed fusion protein. The published data concerning the vesivirus LC protein is limited, and little is known about its structure and function. The precursor cleavage event that releases the LC from the mature VP1 occurs shortly after the capsid precursor is translated (41, 43, 257) and is essential for a productive virus infection. Recent data suggests that the LC enhances the replication of the Norwalk norovirus RNA replicon (46), in association with an increase in low density lipoprotein receptor mRNA levels (45); however, the mechanism of enhancement is not clear. It has been proposed that the LC may function as a non-structural protein because it was not detected in purified FCV virions (272).

An unexpected observation from the study was that the fluorescently tagged LC protein was not clearly visualized by microscopy until 7.5 h.p.i. (Fig. 3.6). The LC protein is encoded as part of the capsid precursor protein in ORF2 of the subgenomic RNA, and abundantly produced and detected as early as 2 h.p.i. in Western blots (Fig. 3.5.1A). The lag in detection of fluorescence from the LC fusion proteins in the recombinant viruses may be due to the time required for the folding and maturation of the chromophore following expression of the fluorescent protein. It is possible also that

fusion of the fluorescent protein to the LC may affect the dynamics of the chromophore maturation, which could then lead to a lower signal readout.

4.2. Instability of large insertions fused to the LC

RNA viruses can rapidly adapt to selective pressures due to recombination events, in addition to the well-characterized poor fidelity of RNA-dependent RNA polymerases (66, 144). Serial passage of the viruses expressing fluorescent proteins fused to the LC resulted eventually in the reduction or loss of foreign protein expression, as the virus reverted back to wt or deleted sequences in the original insertion. Sequencing of these LC-modified viruses in individual plaques revealed that fragments of the foreign sequence often remained fused to the LC (Fig. 3.8), consistent with data reported for recombinant poliovirus revertants (177). The proposed mechanism by which recombinant polioviruses revert to wild-type is via nonhomologous RNA recombination during minus strand synthesis (177). It is possible that caliciviruses use the same mechanism for reversion, but further studies will be needed. Such studies may lead also to the design of recombinant viruses with greater stability. The length, primary nucleotide and amino acid sequences, and context of the insertion in the genome are likely important factors in stability. For example, variation was observed in the length of the insertions that were tolerated between LC and VP2 in the virus, with VP2 limited to small epitopes. And although a small HA epitope (9 amino acids) in VP2 was tolerated, albeit poorly, a six amino acid insertion that contained a tetra cysteine motif was lethal (unpublished data). Host cell factors may influence also the stability of recombinant viruses. The stability of a recombinant GFP-expressing hypovirus RNA genome was enhanced in its fungal host

cell (Cryphonectria parasitica) when the host cell dicer gene dcl-2 was disrupted (297). It is not known whether cellular factors affect the stability of foreign sequences in FCV.

There are several reports that caliciviruses undergo recombination in nature and emerging recombinants have been associated with at least two reported norovirus outbreaks (82, 279). The site of recombination has been predominantly located at, or near the ORF1/2 junction, within the polymerase or capsid sequence (34, 50, 57, 78, 82, 97, 116, 119, 183, 184, 212, 214, 229, 283). It has been shown that upon calicivirus infection, membrane rearrangement occurs (95, 152, 263), which is thought to allow the formation of replication complexes. Enzymatically-active replication complexes can be isolated from FCV-infected cells (95), but it is not known how the dynamics of replication complex formation are affected during a co-infection. It is possible that mixed replication complexes are formed during a co-infection, sequestering genomic RNA from different viruses inside the same replication complex, allowing recombination to occur.

4.3. Phylogenetic analysis and mutagenesis studies of the LC

The phylogenetic analysis of LC sequences determined that there are four different LC clusters: FCV-like, VESV-like, CaCV-like, and MCV-like. The LC sequences are strikingly divergent across clusters, but share a high amino acid identity within clusters. A noteworthy observation is that the predicted secondary structure of all LC sequences appears to be conserved. Attempts to successfully express soluble recombinant LC protein for structural analyses were unsuccessful, but based on the predicted secondary structure, it is possible that LC proteins will have similar tertiary structures.

The deletional mutagenesis analysis provided insight into functional domains of the LC and essential domains were mapped to the N-terminal region (1-88) of the LC. Virus could not be recovered from any of the N-terminal deletion constructs, although a possible effect on the RNA secondary structure signals involved in the translation of the subgenomic RNA cannot be excluded. The 5'-end of the FCV subgenomic RNA has been mapped to nt 5296/5297 (187) which is 17/18 nt upstream of the LC AUG, and RNA elements important for FCV subgenomic production can be inferred from work with other caliciviruses. For example, an RNA element upstream of the subgenomic RNA has been shown as essential for MNV replication and proposed as important for FCV (245). These data are consistent with a report that mapped the subgenomic promoter of another calicivirus, Rabbit hemorrhagic disease virus, to a 50-nt region upstream of the beginning of the subgenomic RNA (174). It is not known whether downstream signals are present in the subgenome region that drive translation of the calicivirus subgenomic RNA. In the alphaviruses, Frolov et al. have characterized an RNA secondary structure downstream of the initial AUG that is important for translation of the subgenomic RNA in Sindbis virus (79, 80). Preliminary analysis of the FCV LC sequences using the Vienna RNA Websuite (96), used to detect conserved secondary structures from aligned sequences using their RNAalifold server, identified a conserved stem-loop downstream of the LC AUG (nt 5327-5338). It is not known if the conserved stem-loop has a role in translation of the subgenomic RNA in FCV.

Surprisingly, two C-terminal LC truncation constructs were able to produce virus that replicated at low levels, suggesting that while the C-terminal region (89-124) was not essential for recovery of infectious virus, it was critical for recovery of fast-growing lytic

virus. The virus that contained the Δ111-120 was particularly interesting because this virus was able to grow relatively well for the first two passages, although it lost the appearance of CPE by passage 3. A plaque assay was performed with the Δ111-120 and wild-type virus in order to compare plaque phenotypes. The significantly smaller plaques of the Δ111-120 virus confirmed its severe attenuation, indicating that the Δ111-120 virus could not spread efficiently.

The diversity of LC sequences limited the number of conserved amino acid residues for scanning alanine mutagenesis. I focused on two conserved regions, CR-1 (cysteine-rich) and CR-II (proline-rich) to fine-map residues critical for recovery of infectious virus. It was possible that the conserved proline motif of CRII might be involved in important protein-protein interactions with cellular proteins that contain an SH3 domain (129, 223). However, substitution of individual prolines had no visible effect on recovery of virus through three passages, and the substitutions were stable. In contrast, certain cysteine residues in CR-1 proved important in the recovery of fast-growing lytic virus. Furthermore, serial passage of the virus containing the C40A substitution resulted in two compensatory mutations (S29P, Y41C) that restored the fast-growing lytic phenotype, suggesting a strong selective pressure to restore the function of the LC. The requirement for both mutations was confirmed by reverse genetics. Proline at position 29 is present in a few FCV strains from the 1970s and 80s (JOK63, F4, V83, 182cvs5A), as well as a more recent strain from 1998 (UTCVM_NH2) and a VS-FCV strain from 2002 (UTCVM_H2). There is no apparent commonality among FCV strains with a S29, and at this point it is difficult to interpret the significance of this substitution. The tyrosine to cysteine substitution at position 41 is surprising because the tyrosine at

position 41 is conserved in nearly all reported FCV LC sequences. The tyrosine lies within a predicted Janus kinase 2 tyrosine phosphorylation motif, YXX[L/I/V] (9), suggesting that it might be phosphorylated. The significance of the substitution to a cysteine may be to restore a disulfide bond to retain a higher order form of the protein, but structural and biochemical studies will be necessary to fully understand the role of the Y41C substitution.

4.4. Transient expression of the LC

Transient expression experiments of the wt LC and the LC-mKate fusion caused CRFK cells to round, a similar outcome observed during FCV infection. In order to map the domain that conferred the cell-rounding phenotype, I used the red fluorescence of the LC-mKate construct as a reporter, and generated pCI-LC-mKate clones that contained systematic deletions of the LC similar to those introduced into the FL clones. I had hypothesized that the domain conferring this cell-rounding phenotype would lie in the C-terminal region because the Δ111-120 LC deletion resulted in a severely attenuated virus that could not spread efficiently. Unexpectedly, the cell-rounding phenotype was solely conferred by the entire N-terminal region (1-88) and no morphologic changes were observed in the cells expressing mKate fused to the C-terminal region (89-124).

One limitation of transient expression experiments is that the behavior of a single viral protein out of the context of a viral infection and over-expressed, may not reveal meaningful insight into its normal function. In these studies I was able to correlate the cell-rounding phenotype observed in transient expression experiments with the recovery of fast-growing lytic virus. The C40A substitution in the LC resulted in a loss of the cell-

rounding phenotype in transfected cells and resulted in an attenuated virus in the context of the FL clone. More importantly, when the substitutions acquired during viral replication to compensate for the C40A mutation (S29P and Y41C) was introduced into the pCI-LC-mKate vector, the cell-rounding phenotype was restored in transfected cells.

4.5. A host cellular binding partner of the LC

The co-immunoprecipitation assay identified annexin-A2 (ANXA2) as a cellular protein interacting with the LC during an infection. Annexin-A2 is a member of the Annexin family of proteins that are characterized as proteins that bind negatively charged phospholipids in a Ca^{2+}-dependent manner, and contain several conserved structural domains (annexin repeats) (88). ANXA2 is a multifunctional protein and it is involved many cellular processes such as fibrinolysis, exocytosis, endocytosis, cell-cell adhesion, and cell motility (88, 224). ANXA2 has been linked to the life-cycle of other positive-sense single-stranded RNA viruses such as hepatitis C virus (14, 136, 235) and HIV (49, 222, 234). In the case of HCV, ANXA2 colocalizes with viral proteins in infected cells and has been proposed to be involved in maturation of virions. In HIV, it plays a cell type-dependent role in infectivity of macrophages.

It has been shown that the phosphorylation of Y23 of ANXA2 results in cell rounding and detachment of baby hamster kidney cells in a Rho/Rock dependent manner (224). An interesting observation from the *in silico* analysis of the FCV LC is that the predicted secondary structure of the entire protein matches the known secondary structure of phospholipase A2, a protein known to be regulated by ANXA2 (107, 108). It is

possible that the LC has phospholipase activity or that it adopts a structure similar to phospholipase A2 in order to interact with ANXA2.

CHAPTER 5: CONCLUSIONS AND FUTURE STUDIES

The LC protein is extremely divergent, varying in size (~14-18 kDa) and sequence (~66-82% p-distance at the amino acid level) among vesiviruses. At the sequence level, the LC shares no homology with any other reported protein, and does not contain any predicted functional motifs. Despite many efforts to express recombinant LC protein in several expression systems (bacteria, yeast and insect), I was not able to express sufficient soluble protein for structural analysis. The FCV LC can tolerate an insertion between amino acids 88/89, defining at least two domains: an N-terminal domain consisting of amino acids 1-88, and a C-terminal domain consisting of amino acids 89-124. Future studies will focus on expressing a single domain to determine if this improves solubility in order to perform structural analysis. Additionally, affinity tags such as glutathione-S-transferase, thioredoxin or a maltose-binding partner can be fused to the LC in order to increase expression, enhance solubility and improve protein folding. Of particular interest will be to solve the structure of the N-terminal region because this domain alone is sufficient to cause cell death in CRFK cells.

One aspect that should be analyzed with any soluble LC expression is to test for phospholipase A2 activity because the predicted secondary structure indicates that the LC may adopt a tertiary structure very similar to that of known phospholipase A2 proteins. There are several studies that have characterized the phospholipase A2 activity of the parvovirus VP1 unique region (65, 77, 154, 155, 294), which is the only viral protein reported to have this particular enzymatic activity. Furthermore, there are numerous reports that phospholipase A2 can induce apoptosis (13, 59, 138, 292, 293), which is consistent with our observation that the LC induces apoptosis when overexpressed.

The LC is expressed from the subgenomic RNA generated during viral replication, and this might suggest that the LC is involved in the latter stages of the virus life cycle as opposed to the initial steps of establishing replication complexes. Interestingly, it has been reported that the LC, when provided in *trans*, can enhance replication levels of the human norovirus replicon (46). The exact mechanism of replication enhancement is not clear, but this indicates that the LC modifies the host cell to create an environment more amenable to viral replication of human norovirus and the LC likely has a similar role with FCV.

One of the most interesting findings of my research was that while the C-terminal region could be partially deleted without abrogating replication, it greatly reduced the virus' ability to spread. The fact that this virus does not grow well makes it difficult to study. One question that needs to be addressed is what aspect of the virus life cycle is affected. An important experiment to perform will be to generate full-length RNA transcripts from the truncated LC plasmid *in vitro* and transfect the transcripts into CRFK cells. Virus release can be quantified by performing real-time PCR on RNA purified from clarified supernatant, and virus replication can be monitored by Western blot analysis of VP1 from lysates of the cells.

I determined that there is a correlation between the ability of the LC to cause cell death when expressed transiently and recovery of fast-growing fully lytic virus. What remains to be determined is if the same cysteine residues important for causing cell death and recovery of fully lytic virus are equally important in the observed enhancement of the replication of the human norovirus replicon. Likewise, it is not known if LC proteins

from different phylogenetic clusters also cause cell death when over-expressed transiently and if they can enhance the human norovirus replicon.

An intriguing finding was that the host cellular protein ANXA2 interacts with the LC during infection. ANXA2 has been reported to play a role in the life cycle of other positive-sense RNA viruses such as HCV and HIV, and it is possible that this is a common theme among positive-sense single-stranded RNA viruses. A sequence of the feline ANXA2 has yet not been published, but I was able to successfully amplify and clone the ANXA2 gene from CRFK cells. The availability of the feline ANXA2 will allow for silencing experiments to determine if the presence of ANXA2 is important for FCV to infect CRFK cells.

It has been reported that the phosphorylation of Y23 of ANXA2 leads to actin rearrangement and cell-rounding of baby hamster kidney cells (224). It should be determined if ANXA2 becomes phosphorylated upon FCV infection and LC transfection, and the phosphorylation state of the ANXA2 that immunoprecipitates with the recombinant LC from infected FCV must be established. In order to identify the significance of Y23, if any, the cloned feline ANXA2 can be mutagenized to block phosphorylation (Y23A) or mimic the phosphorylated state (Y23D). Similarly, the interaction of the LC with ANXA2 should be further characterized by performing immunoprecipitation assays with truncated forms of the LC to map the binding domain.

The exact mechanism by which the LC facilitates FCV replication, and replication of the human norovirus replicon, remains to be determined. Albeit, the findings and tools generated from these studies will allow for a more precise analysis of the function of this unique protein.

BIBLIOGRAPHY

1. **Abente, E. J., S. V. Sosnovtsev, K. Bok, and K. Y. Green.** 2010. Visualization of feline calicivirus replication in real-time with recombinant viruses engineered to express fluorescent reporter proteins. Virology **400:**18-31.
2. **Adler, J. L., and R. Zickl.** 1969. Winter vomiting disease. The Journal of infectious diseases **119:**668-673.
3. **Agol, V. I., and A. P. Gmyl.** 2010. Viral security proteins: counteracting host defences. Nature reviews. Microbiology **8:**867-878.
4. **Ahlquist, P.** 2006. Parallels among positive-strand RNA viruses, reverse-transcribing viruses and double-stranded RNA viruses. Nature reviews. Microbiology **4:**371-382.
5. **Alexander, L., H. H. Lu, and E. Wimmer.** 1994. Polioviruses containing picornavirus type 1 and/or type 2 internal ribosomal entry site elements: genetic hybrids and the expression of a foreign gene. Proceedings of the National Academy of Sciences of the United States of America **91:**1406-1410.
6. **Almeida, J. D., A. P. Waterson, J. Prydie, and E. W. Fletcher.** 1968. The structure of a feline picornavirus and its relevance to cubic viruses in general. Archiv fur die gesamte Virusforschung **25:**105-114.
7. **Ammann, C. G., R. J. Messer, K. Varvel, B. L. Debuysscher, R. A. Lacasse, A. K. Pinto, and K. J. Hasenkrug.** 2009. Effects of acute and chronic murine norovirus infections on immune responses and recovery from Friend retrovirus infection. Journal of virology **83:**13037-13041.
8. **Andino, R., D. Silvera, S. D. Suggett, P. L. Achacoso, C. J. Miller, D. Baltimore, and M. B. Feinberg.** 1994. Engineering poliovirus as a vaccine vector for the expression of diverse antigens. Science **265:**1448-1451.
9. **Argetsinger, L. S., J. L. Kouadio, H. Steen, A. Stensballe, O. N. Jensen, and C. Carter-Su.** 2004. Autophosphorylation of JAK2 on tyrosines 221 and 570 regulates its activity. Molecular and cellular biology **24:**4955-4967.
10. **Arness, M. K., B. H. Feighner, M. L. Canham, D. N. Taylor, S. S. Monroe, T. J. Cieslak, E. L. Hoedebecke, C. S. Polyak, J. C. Cuthie, R. L. Fankhauser, C. D. Humphrey, T. L. Barker, C. D. Jenkins, and D. R. Skillman.** 2000. Norwalk-like viral gastroenteritis outbreak in U.S. Army trainees. Emerging infectious diseases **6:**204-207.
11. **Atasheva, S., R. Gorchakov, R. English, I. Frolov, and E. Frolova.** 2007. Development of Sindbis viruses encoding nsP2/GFP chimeric proteins and their application for studying nsP2 functioning. Journal of virology **81:**5046-5057.
12. **Atmar, R. L., D. I. Bernstein, C. D. Harro, M. S. Al-Ibrahim, W. H. Chen, J. Ferreira, M. K. Estes, D. Y. Graham, A. R. Opekun, C. Richardson, and P. M. Mendelman.** 2011. Norovirus vaccine against experimental human Norwalk Virus illness. The New England journal of medicine **365:**2178-2187.
13. **Atsumi, G., M. Tajima, A. Hadano, Y. Nakatani, M. Murakami, and I. Kudo.** 1998. Fas-induced arachidonic acid release is mediated by Ca2+-independent phospholipase A2 but not cytosolic phospholipase A2, which undergoes

proteolytic inactivation. The Journal of biological chemistry **273:**13870-13877.

14. **Backes, P., D. Quinkert, S. Reiss, M. Binder, M. Zayas, U. Rescher, V. Gerke, R. Bartenschlager, and V. Lohmann.** 2010. Role of annexin A2 in the production of infectious hepatitis C virus particles. Journal of virology **84:**5775-5789.
15. **Bailey, D., W. J. Kaiser, M. Hollinshead, K. Moffat, Y. Chaudhry, T. Wileman, S. V. Sosnovtsev, and I. G. Goodfellow.** 2010. Feline calicivirus p32, p39 and p30 proteins localize to the endoplasmic reticulum to initiate replication complex formation. The Journal of general virology **91:**739-749.
16. **Barron, E. L., S. V. Sosnovtsev, K. Bok, V. Prikhodko, C. Sandoval-Jaime, C. R. Rhodes, K. Hasenkrug, A. B. Carmody, J. M. Ward, K. Perdue, and K. Y. Green.** 2011. Diversity of murine norovirus strains isolated from asymptomatic mice of different genetic backgrounds within a single U.S. research institute. PloS one **6:**e21435.
17. **Beitzel, B. F., R. R. Bakken, J. M. Smith, and C. S. Schmaljohn.** 2010. High-resolution functional mapping of the venezuelan equine encephalitis virus genome by insertional mutagenesis and massively parallel sequencing. PLoS pathogens **6:**e1001146.
18. **Belliot, G., S. V. Sosnovtsev, K. O. Chang, V. Babu, U. Uche, J. J. Arnold, C. E. Cameron, and K. Y. Green.** 2005. Norovirus proteinase-polymerase and polymerase are both active forms of RNA-dependent RNA polymerase. Journal of virology **79:**2393-2403.
19. **Belliot, G., S. V. Sosnovtsev, K. O. Chang, P. McPhie, and K. Y. Green.** 2008. Nucleotidylylation of the VPg protein of a human norovirus by its proteinase-polymerase precursor protein. Virology **374:**33-49.
20. **Belliot, G., S. V. Sosnovtsev, T. Mitra, C. Hammer, M. Garfield, and K. Y. Green.** 2003. In vitro proteolytic processing of the MD145 norovirus ORF1 nonstructural polyprotein yields stable precursors and products similar to those detected in calicivirus-infected cells. Journal of virology **77:**10957-10974.
21. **Bertolotti-Ciarlet, A., S. E. Crawford, A. M. Hutson, and M. K. Estes.** 2003. The 3' end of Norwalk virus mRNA contains determinants that regulate the expression and stability of the viral capsid protein VP1: a novel function for the VP2 protein. Journal of virology **77:**11603-11615.
22. **Bhella, D., D. Gatherer, Y. Chaudhry, R. Pink, and I. G. Goodfellow.** 2008. Structural insights into calicivirus attachment and uncoating. Journal of virology **82:**8051-8058.
23. **Bhella, D., and I. G. Goodfellow.** 2011. The cryo-electron microscopy structure of feline calicivirus bound to junctional adhesion molecule A at 9-angstrom resolution reveals receptor-induced flexibility and two distinct conformational changes in the capsid protein VP1. Journal of virology **85:**11381-11390.
24. **Biery, M. C., M. Lopata, and N. L. Craig.** 2000. A minimal system for Tn7 transposition: the transposon-encoded proteins TnsA and TnsB can execute

DNA breakage and joining reactions that generate circularized Tn7 species. Journal of molecular biology **297:**25-37.

25. **Binns, S. H., S. Dawson, A. J. Speakman, L. E. Cuevas, C. A. Hart, C. J. Gaskell, K. L. Morgan, and R. M. Gaskell.** 2000. A study of feline upper respiratory tract disease with reference to prevalence and risk factors for infection with feline calicivirus and feline herpesvirus. Journal of feline medicine and surgery **2:**123-133.
26. **Blakeney, S. J., A. Cahill, and P. A. Reilly.** 2003. Processing of Norwalk virus nonstructural proteins by a 3C-like cysteine proteinase. Virology **308:**216-224.
27. **Blanton, L. H., S. M. Adams, R. S. Beard, G. Wei, S. N. Bulens, M. A. Widdowson, R. I. Glass, and S. S. Monroe.** 2006. Molecular and epidemiologic trends of caliciviruses associated with outbreaks of acute gastroenteritis in the United States, 2000-2004. The Journal of infectious diseases **193:**413-421.
28. **Bok, K., G. I. Parra, T. Mitra, E. Abente, C. K. Shaver, D. Boon, R. Engle, C. Yu, A. Z. Kapikian, S. V. Sosnovtsev, R. H. Purcell, and K. Y. Green.** 2011. Chimpanzees as an animal model for human norovirus infection and vaccine development. Proceedings of the National Academy of Sciences of the United States of America **108:**325-330.
29. **Bonaldo, M. C., R. C. Garratt, P. S. Caufour, M. S. Freire, M. M. Rodrigues, R. S. Nussenzweig, and R. Galler.** 2002. Surface expression of an immunodominant malaria protein B cell epitope by yellow fever virus. Journal of molecular biology **315:**873-885.
30. **Bonaldo, M. C., R. C. Garratt, R. S. Marchevsky, E. S. Coutinho, A. V. Jabor, L. F. Almeida, A. M. Yamamura, A. S. Duarte, P. J. Oliveira, J. O. Lizeu, L. A. Camacho, M. S. Freire, and R. Galler.** 2005. Attenuation of recombinant yellow fever 17D viruses expressing foreign protein epitopes at the surface. Journal of virology **79:**8602-8613.
31. **Bonaldo, M. C., S. M. Mello, G. F. Trindade, A. A. Rangel, A. S. Duarte, P. J. Oliveira, M. S. Freire, C. F. Kubelka, and R. Galler.** 2007. Construction and characterization of recombinant flaviviruses bearing insertions between E and NS1 genes. Virol J **4:**115.
32. **Boniotti, B., C. Wirblich, M. Sibilia, G. Meyers, H. J. Thiel, and C. Rossi.** 1994. Identification and characterization of a 3C-like protease from rabbit hemorrhagic disease virus, a calicivirus. Journal of virology **68:**6487-6495.
33. **Bridger, J. C., G. A. Hall, and J. F. Brown.** 1984. Characterization of a calici-like virus (Newbury agent) found in association with astrovirus in bovine diarrhea. Infection and immunity **43:**133-138.
34. **Bull, R. A., M. M. Tanaka, and P. A. White.** 2007. Norovirus recombination. The Journal of general virology **88:**3347-3359.
35. **Bull, R. A., E. T. Tu, C. J. McIver, W. D. Rawlinson, and P. A. White.** 2006. Emergence of a new norovirus genotype II.4 variant associated with global outbreaks of gastroenteritis. Journal of clinical microbiology **44:**327-333.

36. **Burke, K. L., G. Dunn, M. Ferguson, P. D. Minor, and J. W. Almond.** 1988. Antigen chimaeras of poliovirus as potential new vaccines. Nature **332:**81-82.
37. **Burroughs, J. N., and F. Brown.** 1978. Presence of a covalently linked protein on calicivirus RNA. The Journal of general virology **41:**443-446.
38. **Cancio-Lonches, C., M. Yocupicio-Monroy, C. Sandoval-Jaime, I. Galvan-Mendoza, L. Urena, S. Vashist, I. Goodfellow, J. Salas-Benito, and A. L. Gutierrez-Escolano.** 2011. Nucleolin interacts with the feline calicivirus 3' untranslated region and the protease-polymerase NS6 and NS7 proteins, playing a role in virus replication. Journal of virology **85:**8056-8068.
39. **Cannon, J. L., L. C. Lindesmith, E. F. Donaldson, L. Saxe, R. S. Baric, and J. Vinje.** 2009. Herd immunity to GII.4 noroviruses is supported by outbreak patient sera. Journal of virology **83:**5363-5374.
40. **Carstens, E. B.** 2010. Ratification vote on taxonomic proposals to the International Committee on Taxonomy of Viruses (2009). Archives of virology **155:**133-146.
41. **Carter, M. J.** 1989. Feline calicivirus protein synthesis investigated by western blotting. Archives of virology **108:**69-79.
42. **Carter, M. J.** 1990. Transcription of feline calicivirus RNA. Archives of virology **114:**143-152.
43. **Carter, M. J., I. D. Milton, P. C. Turner, J. Meanger, M. Bennett, and R. M. Gaskell.** 1992. Identification and sequence determination of the capsid protein gene of feline calicivirus. Archives of virology **122:**223-235.
44. **Centers for Disease Control and Prevention.** 2011. Surveillance for foodborne disease outbreaks--United States, 2008.
45. **Chang, K. O.** 2009. Role of cholesterol pathways in norovirus replication. Journal of virology **83:**8587-8595.
46. **Chang, K. O., D. W. George, J. B. Patton, K. Y. Green, and S. V. Sosnovtsev.** 2008. Leader of the capsid protein in feline calicivirus promotes replication of Norwalk virus in cell culture. Journal of virology **82:**9306-9317.
47. **Chasey, D., and P. Duff.** 1990. European brown hare syndrome and associated virus particles in the UK. The Veterinary record **126:**623-624.
48. **Chaudhry, Y., A. Nayak, M. E. Bordeleau, J. Tanaka, J. Pelletier, G. J. Belsham, L. O. Roberts, and I. G. Goodfellow.** 2006. Caliciviruses differ in their functional requirements for eIF4F components. The Journal of biological chemistry **281:**25315-25325.
49. **Chertova, E., O. Chertov, L. V. Coren, J. D. Roser, C. M. Trubey, J. W. Bess, Jr., R. C. Sowder, 2nd, E. Barsov, B. L. Hood, R. J. Fisher, K. Nagashima, T. P. Conrads, T. D. Veenstra, J. D. Lifson, and D. E. Ott.** 2006. Proteomic and biochemical analysis of purified human immunodeficiency virus type 1 produced from infected monocyte-derived macrophages. Journal of virology **80:**9039-9052.
50. **Chhabra, P., R. K. Dhongade, V. R. Kalrao, A. R. Bavdekar, and S. D. Chitambar.** 2009. Epidemiological, clinical, and molecular features of norovirus infections in western India. Journal of medical virology **81:**922-932.

51. **Chiba, S., S. Nakata, K. Numata-Kinoshita, and S. Honma.** 2000. Sapporo virus: history and recent findings. The Journal of infectious diseases **181 Suppl 2:**S303-308.
52. **Chiba, S., Y. Sakuma, R. Kogasaka, M. Akihara, K. Horino, T. Nakao, and S. Fukui.** 1979. An outbreak of gastroenteritis associated with calicivirus in an infant home. J Med Virol **4:**249-254.
53. **Choe, S. S., D. A. Dodd, and K. Kirkegaard.** 2005. Inhibition of cellular protein secretion by picornaviral 3A proteins. Virology **337:**18-29.
54. **Coyne, K. P., S. Dawson, A. D. Radford, P. J. Cripps, C. J. Porter, C. M. McCracken, and R. M. Gaskell.** 2006. Long-term analysis of feline calicivirus prevalence and viral shedding patterns in naturally infected colonies of domestic cats. Veterinary microbiology **118:**12-25.
55. **Coyne, K. P., R. M. Gaskell, S. Dawson, C. J. Porter, and A. D. Radford.** 2007. Evolutionary mechanisms of persistence and diversification of a calicivirus within endemically infected natural host populations. Journal of virology **81:**1961-1971.
56. **Coyne, K. P., B. R. Jones, A. Kipar, J. Chantrey, C. J. Porter, P. J. Barber, S. Dawson, R. M. Gaskell, and A. D. Radford.** 2006. Lethal outbreak of disease associated with feline calicivirus infection in cats. The Veterinary record **158:**544-550.
57. **Coyne, K. P., F. C. Reed, C. J. Porter, S. Dawson, R. M. Gaskell, and A. D. Radford.** 2006. Recombination of Feline calicivirus within an endemically infected cat colony. The Journal of general virology **87:**921-926.
58. **Craig, N. L.** 1996. Transposon Tn7. Curr Top Microbiol Immunol **204:**27-48.
59. **Daniel, B., and M. A. DeCoster.** 2004. Quantification of sPLA2-induced early and late apoptosis changes in neuronal cell cultures using combined TUNEL and DAPI staining. Brain research. Brain research protocols **13:**144-150.
60. **Daughenbaugh, K. F., C. S. Fraser, J. W. Hershey, and M. E. Hardy.** 2003. The genome-linked protein VPg of the Norwalk virus binds eIF3, suggesting its role in translation initiation complex recruitment. Embo J **22:**2852-2859.
61. **Daughenbaugh, K. F., C. E. Wobus, and M. E. Hardy.** 2006. VPg of murine norovirus binds translation initiation factors in infected cells. Virol J **3:**33.
62. **Di Martino, B., F. Di Profio, V. Martella, C. Ceci, and F. Marsilio.** 2011. Evidence for recombination in neboviruses. Veterinary microbiology **153:**367-372.
63. **Dolin, R., N. R. Blacklow, H. DuPont, R. F. Buscho, R. G. Wyatt, J. A. Kasel, R. Hornick, and R. M. Chanock.** 1972. Biological properties of Norwalk agent of acute infectious nonbacterial gastroenteritis. Proc Soc Exp Biol Med **140:**578-583.
64. **Dolin, R., N. R. Blacklow, H. DuPont, S. Formal, R. F. Buscho, J. A. Kasel, R. P. Chames, R. Hornick, and R. M. Chanock.** 1971. Transmission of acute infectious nonbacterial gastroenteritis to volunteers by oral administration of stool filtrates. The Journal of infectious diseases **123:**307-312.
65. **Dorsch, S., G. Liebisch, B. Kaufmann, P. von Landenberg, J. H. Hoffmann, W. Drobnik, and S. Modrow.** 2002. The VP1 unique region of parvovirus

B19 and its constituent phospholipase A2-like activity. Journal of virology **76:**2014-2018.
66. **Duffy, S., L. A. Shackelton, and E. C. Holmes.** 2008. Rates of evolutionary change in viruses: patterns and determinants. Nat Rev Genet **9:**267-276.
67. **Dunham, D. M., X. Jiang, T. Berke, A. W. Smith, and D. O. Matson.** 1998. Genomic mapping of a calicivirus VPg. Archives of virology **143:**2421-2430.
68. **Ettayebi, K., and M. E. Hardy.** 2003. Norwalk virus nonstructural protein p48 forms a complex with the SNARE regulator VAP-A and prevents cell surface expression of vesicular stomatitis virus G protein. Journal of virology **77:**11790-11797.
69. **Evans, D. J., J. McKeating, J. M. Meredith, K. L. Burke, K. Katrak, A. John, M. Ferguson, P. D. Minor, R. A. Weiss, and J. W. Almond.** 1989. An engineered poliovirus chimaera elicits broadly reactive HIV-1 neutralizing antibodies. Nature **339:**385-388, 340.
70. **Fan, Z. C., J. C. Dennis, and R. C. Bird.** 2008. Bovine viral diarrhea virus is a suitable viral vector for stable expression of heterologous gene when inserted in between N(pro) and C genes. Virus research **138:**97-104.
71. **Fankhauser, R. L., S. S. Monroe, J. S. Noel, C. D. Humphrey, J. S. Bresee, U. D. Parashar, T. Ando, and R. I. Glass.** 2002. Epidemiologic and molecular trends of "Norwalk-like viruses" associated with outbreaks of gastroenteritis in the United States. The Journal of infectious diseases **186:**1-7.
72. **Fankhauser, R. L., J. S. Noel, S. S. Monroe, T. Ando, and R. I. Glass.** 1998. Molecular epidemiology of "Norwalk-like viruses" in outbreaks of gastroenteritis in the United States. The Journal of infectious diseases **178:**1571-1578.
73. **Farkas, T., K. Sestak, C. Wei, and X. Jiang.** 2008. Characterization of a rhesus monkey calicivirus representing a new genus of Caliciviridae. Journal of virology **82:**5408-5416.
74. **Fastier, L. B.** 1957. A new feline virus isolated in tissue culture. Am J Vet Res **18:**382-389.
75. **Fenner, F.** 2010. Deliberate introduction of the European rabbit, Oryctolagus cuniculus, into Australia. Rev Sci Tech **29:**103-111.
76. **Fernandez-Vega, V., S. V. Sosnovtsev, G. Belliot, A. D. King, T. Mitra, A. Gorbalenya, and K. Y. Green.** 2004. Norwalk virus N-terminal nonstructural protein is associated with disassembly of the Golgi complex in transfected cells. Journal of virology **78:**4827-4837.
77. **Filippone, C., N. Zhi, S. Wong, J. Lu, S. Kajigaya, G. Gallinella, L. Kakkola, M. Soderlund-Venermo, N. S. Young, and K. E. Brown.** 2008. VP1u phospholipase activity is critical for infectivity of full-length parvovirus B19 genomic clones. Virology **374:**444-452.
78. **Forrester, N. L., S. R. Moss, S. L. Turner, H. Schirrmeier, and E. A. Gould.** 2008. Recombination in rabbit haemorrhagic disease virus: possible impact on evolution and epidemiology. Virology **376:**390-396.
79. **Frolov, I., and S. Schlesinger.** 1996. Translation of Sindbis virus mRNA: analysis of sequences downstream of the initiating AUG codon that enhance translation. Journal of virology **70:**1182-1190.

80. **Frolov, I., and S. Schlesinger.** 1994. Translation of Sindbis virus mRNA: effects of sequences downstream of the initiating codon. Journal of virology **68:**8111-8117.
81. **Fuchs, A., and H. Weissenbock.** 1992. Comparative histopathological study of rabbit haemorrhagic disease (RHD) and European brown hare syndrome (EBHS). J Comp Pathol **107:**103-113.
82. **Fukuda, S., Y. Sasaki, S. Takao, and M. Seno.** 2008. Recombinant norovirus implicated in gastroenteritis outbreaks in Hiroshima Prefecture, Japan. Journal of medical virology **80:**921-928.
83. **Fukushi, S., S. Kojima, R. Takai, F. B. Hoshino, T. Oka, N. Takeda, K. Katayama, and T. Kageyama.** 2004. Poly(A)- and primer-independent RNA polymerase of Norovirus. Journal of virology **78:**3889-3896.
84. **Fullerton, S. W., M. Blaschke, B. Coutard, J. Gebhardt, A. Gorbalenya, B. Canard, P. A. Tucker, and J. Rohayem.** 2007. Structural and functional characterization of sapovirus RNA-dependent RNA polymerase. Journal of virology **81:**1858-1871.
85. **Gallimore, C. I., J. Green, D. Lewis, A. F. Richards, B. A. Lopman, A. D. Hale, R. Eglin, J. J. Gray, and D. W. Brown.** 2004. Diversity of noroviruses cocirculating in the north of England from 1998 to 2001. Journal of clinical microbiology **42:**1396-1401.
86. **Gaskell, C. J., R. M. Gaskell, P. E. Dennis, and M. J. Wooldridge.** 1982. Efficacy of an inactivated feline calicivirus (FCV) vaccine against challenge with United Kingdom field strains and its interaction with the FCV carrier state. Res Vet Sci **32:**23-26.
87. **Gavier-Widen, D., and T. Morner.** 1993. Descriptive epizootiological study of European brown hare syndrome in Sweden. J Wildl Dis **29:**15-20.
88. **Gerke, V., and S. E. Moss.** 2002. Annexins: from structure to function. Physiological reviews **82:**331-371.
89. **Glass, P. J., L. J. White, J. M. Ball, I. Leparc-Goffart, M. E. Hardy, and M. K. Estes.** 2000. Norwalk virus open reading frame 3 encodes a minor structural protein. Journal of virology **74:**6581-6591.
90. **Glass, P. J., C. Q. Zeng, and M. K. Estes.** 2003. Two nonoverlapping domains on the Norwalk virus open reading frame 3 (ORF3) protein are involved in the formation of the phosphorylated 35K protein and in ORF3-capsid protein interactions. Journal of virology **77:**3569-3577.
91. **Goodfellow, I., Y. Chaudhry, I. Gioldasi, A. Gerondopoulos, A. Natoni, L. Labrie, J. F. Laliberte, and L. Roberts.** 2005. Calicivirus translation initiation requires an interaction between VPg and eIF 4 E. EMBO Rep **6:**968-972.
92. **Gorbalenya, A. E., E. V. Koonin, and Y. I. Wolf.** 1990. A new superfamily of putative NTP-binding domains encoded by genomes of small DNA and RNA viruses. FEBS letters **262:**145-148.
93. **Gorchakov, R., N. Garmashova, E. Frolova, and I. Frolov.** 2008. Different types of nsP3-containing protein complexes in Sindbis virus-infected cells. Journal of virology **82:**10088-10101.

94. **Graham, D. Y., X. Jiang, T. Tanaka, A. R. Opekun, H. P. Madore, and M. K. Estes.** 1994. Norwalk virus infection of volunteers: new insights based on improved assays. The Journal of infectious diseases **170:**34-43.
95. **Green, K. Y., A. Mory, M. H. Fogg, A. Weisberg, G. Belliot, M. Wagner, T. Mitra, E. Ehrenfeld, C. E. Cameron, and S. V. Sosnovtsev.** 2002. Isolation of enzymatically active replication complexes from feline calicivirus-infected cells. Journal of virology **76:**8582-8595.
96. **Gruber, A. R., R. Lorenz, S. H. Bernhart, R. Neubock, and I. L. Hofacker.** 2008. The Vienna RNA websuite. Nucleic acids research **36:**W70-74.
97. **Guo, L., J. Song, X. Xu, L. Ren, J. Li, H. Zhou, M. Wang, J. Qu, J. Wang, and T. Hung.** 2009. Genetic analysis of norovirus in children affected with acute gastroenteritis in Beijing, 2004-2007. Journal of clinical virology : the official publication of the Pan American Society for Clinical Virology **44:**94-98.
98. **Hall, G. A., J. C. Bridger, B. E. Brooker, K. R. Parsons, and E. Ormerod.** 1984. Lesions of gnotobiotic calves experimentally infected with a calicivirus-like (Newbury) agent. Veterinary pathology **21:**208-215.
99. **Han, K. R., Y. Choi, B. S. Min, H. Jeong, D. Cheon, J. Kim, Y. Jee, S. Shin, and J. M. Yang.** 2010. Murine norovirus-1 3Dpol exhibits RNA-dependent RNA polymerase activity and nucleotidylylates on Tyr of the VPg. The Journal of general virology **91:**1713-1722.
100. **Hansman, G., X. Jiang, and K. Y. Green.** 2010. Caliciviruses: Molecular and Cellular Virology. Caister Academic Press, Norfolk, UK.
101. **Harbour, D. A., P. E. Howard, and R. M. Gaskell.** 1991. Isolation of feline calicivirus and feline herpesvirus from domestic cats 1980 to 1989. The Veterinary record **128:**77-80.
102. **Hefferon, K. L., H. Khalilian, H. Xu, and M. G. AbouHaidar.** 1997. Expression of the coat protein of potato virus X from a dicistronic mRNA in transgenic potato plants. The Journal of general virology **78 (Pt 11):**3051-3059.
103. **Henke, A., R. Zell, G. Ehrlich, and A. Stelzner.** 2001. Expression of immunoregulatory cytokines by recombinant coxsackievirus B3 variants confers protection against virus-caused myocarditis. Journal of virology **75:**8187-8194.
104. **Hensley, S. E., A. K. Pinto, H. D. Hickman, R. J. Kastenmayer, J. R. Bennink, H. W. Virgin, and J. W. Yewdell.** 2009. Murine norovirus infection has no significant effect on adaptive immunity to vaccinia virus or influenza A virus. Journal of virology **83:**7357-7360.
105. **Herbert, T. P., I. Brierley, and T. D. Brown.** 1996. Detection of the ORF3 polypeptide of feline calicivirus in infected cells and evidence for its expression from a single, functionally bicistronic, subgenomic mRNA. The Journal of general virology **77 (Pt 1):**123-127.
106. **Herbert, T. P., I. Brierley, and T. D. Brown.** 1997. Identification of a protein linked to the genomic and subgenomic mRNAs of feline calicivirus and its role in translation. The Journal of general virology **78 (Pt 5):**1033-1040.

107. **Hirata, F.** 1981. The regulation of lipomodulin, a phospholipase inhibitory protein, in rabbit neutrophils by phosphorylation. The Journal of biological chemistry **256:**7730-7733.
108. **Hirata, F., E. Schiffmann, K. Venkatasubramanian, D. Salomon, and J. Axelrod.** 1980. A phospholipase A2 inhibitory protein in rabbit neutrophils induced by glucocorticoids. Proc Natl Acad Sci U S A **77:**2533-2536.
109. **Hofling, K., S. Tracy, N. Chapman, K. S. Kim, and J. Smith Leser.** 2000. Expression of an antigenic adenovirus epitope in a group B coxsackievirus. Journal of virology **74:**4570-4578.
110. **Hosur, M. V., T. Schmidt, R. C. Tucker, J. E. Johnson, T. M. Gallagher, B. H. Selling, and R. R. Rueckert.** 1987. Structure of an insect virus at 3.0 A resolution. Proteins **2:**167-176.
111. **Hsu, C. C., L. K. Riley, and R. S. Livingston.** 2007. Molecular characterization of three novel murine noroviruses. Virus genes **34:**147-155.
112. **Hsu, C. C., L. K. Riley, H. M. Wills, and R. S. Livingston.** 2006. Persistent infection with and serologic cross-reactivity of three novel murine noroviruses. Comparative medicine **56:**247-251.
113. **Hughes, P. J., and G. Stanway.** 2000. The 2A proteins of three diverse picornaviruses are related to each other and to the H-rev107 family of proteins involved in the control of cell proliferation. The Journal of general virology **81:**201-207.
114. **Hurley, K. F., and J. E. Sykes.** 2003. Update on feline calicivirus: new trends. Vet Clin North Am Small Anim Pract **33:**759-772.
115. **Jiang, J., and J. F. Laliberte.** 2011. The genome-linked protein VPg of plant viruses-a protein with many partners. Current opinion in virology **1:**347-354.
116. **Jiang, X., C. Espul, W. M. Zhong, H. Cuello, and D. O. Matson.** 1999. Characterization of a novel human calicivirus that may be a naturally occurring recombinant. Archives of virology **144:**2377-2387.
117. **Jiang, X., M. Wang, D. Y. Graham, and M. K. Estes.** 1992. Expression, self-assembly, and antigenicity of the Norwalk virus capsid protein. Journal of virology **66:**6527-6532.
118. **Jiang, X., M. Wang, K. Wang, and M. K. Estes.** 1993. Sequence and genomic organization of Norwalk virus. Virology **195:**51-61.
119. **Jin, M., H. P. Xie, Z. J. Duan, N. Liu, Q. Zhang, B. S. Wu, H. Y. Li, W. X. Cheng, S. H. Yang, J. M. Yu, Z. Q. Xu, S. X. Cui, L. Zhu, M. Tan, X. Jiang, and Z. Y. Fang.** 2008. Emergence of the GII4/2006b variant and recombinant noroviruses in China. Journal of medical virology **80:**1997-2004.
120. **Johansen, K., K. Mannerqvist, A. Allard, Y. Andersson, L. G. Burman, L. Dillner, K. O. Hedlund, K. Jonsson, U. Kumlin, T. Leitner, M. Lysen, M. Thorhagen, A. Tiveljung-Lindell, C. Wahlstrom, B. Zweygberg-Wirgart, and A. Widell.** 2008. Norovirus strains belonging to the GII.4 genotype dominate as a cause of nosocomial outbreaks of viral gastroenteritis in Sweden 1997--2005. Arrival of new variants is associated with large nation-wide epidemics. Journal of clinical virology : the official publication of the Pan American Society for Clinical Virology **42:**129-134.

121. **Joubert, P., C. Pautigny, M. F. Madelaine, and D. Rasschaert.** 2000. Identification of a new cleavage site of the 3C-like protease of rabbit haemorrhagic disease virus. The Journal of general virology **81:**481-488.
122. **Kaiser, W. J., Y. Chaudhry, S. V. Sosnovtsev, and I. G. Goodfellow.** 2006. Analysis of protein-protein interactions in the feline calicivirus replication complex. The Journal of general virology **87:**363-368.
123. **Kapikian, A. Z.** 2000. The discovery of the 27-nm Norwalk virus: an historic perspective. The Journal of infectious diseases **181 Suppl 2:**S295-302.
124. **Kapikian, A. Z., R. G. Wyatt, R. Dolin, T. S. Thornhill, A. R. Kalica, and R. M. Chanock.** 1972. Visualization by immune electron microscopy of a 27-nm particle associated with acute infectious nonbacterial gastroenteritis. Journal of virology **10:**1075-1081.
125. **Kaplan, J. E., G. W. Gary, R. C. Baron, N. Singh, L. B. Schonberger, R. Feldman, and H. B. Greenberg.** 1982. Epidemiology of Norwalk gastroenteritis and the role of Norwalk virus in outbreaks of acute nonbacterial gastroenteritis. Annals of internal medicine **96:**756-761.
126. **Karakasiliotis, I., S. Vashist, D. Bailey, E. J. Abente, K. Y. Green, L. O. Roberts, S. V. Sosnovtsev, and I. G. Goodfellow.** 2010. Polypyrimidine tract binding protein functions as a negative regulator of feline calicivirus translation. PloS one **5:**e9562.
127. **Karst, S. M., C. E. Wobus, M. Lay, J. Davidson, and H. W. t. Virgin.** 2003. STAT1-dependent innate immunity to a Norwalk-like virus. Science **299:**1575-1578.
128. **Katpally, U., N. R. Voss, T. Cavazza, S. Taube, J. R. Rubin, V. L. Young, J. Stuckey, V. K. Ward, H. W. t. Virgin, C. E. Wobus, and T. J. Smith.** 2010. High-resolution cryo-electron microscopy structures of murine norovirus 1 and rabbit hemorrhagic disease virus reveal marked flexibility in the receptor binding domains. Journal of virology **84:**5836-5841.
129. **Kay, B. K., M. P. Williamson, and M. Sudol.** 2000. The importance of being proline: the interaction of proline-rich motifs in signaling proteins with their cognate domains. FASEB journal : official publication of the Federation of American Societies for Experimental Biology **14:**231-241.
130. **Koopmans, M. K., Green, K.Y., Ando, T., Clarke, I.N., Estes, M.K., Matson, D.O., Nakata, S., Neill, J.D., Smith, A.W., Studdert, M.J., and Thiel, H.J.** 2005. Eighth Report of the International Committee on Taxonomy of Viruses. Elsevier Inc., San Diego.
131. **Kovaliski, J.** 1998. Monitoring the spread of rabbit hemorrhagic disease virus as a new biological agent for control of wild European rabbits in Australia. J Wildl Dis **34:**421-428.
132. **Kreutz, L. C., and B. S. Seal.** 1995. The pathway of feline calicivirus entry. Virus research **35:**63-70.
133. **Kreutz, L. C., B. S. Seal, and W. L. Mengeling.** 1994. Early interaction of feline calicivirus with cells in culture. Archives of virology **136:**19-34.
134. **Kroneman, A., H. Vennema, J. Harris, G. Reuter, C. H. von Bonsdorff, K. O. Hedlund, K. Vainio, V. Jackson, P. Pothier, J. Koch, E. Schreier, B. E. Bottiger, and M. Koopmans.** 2006. Increase in norovirus activity reported

in Europe. Euro surveillance : bulletin europeen sur les maladies transmissibles = European communicable disease bulletin **11:**E061214 061211.

135. **Kroneman, A., L. Verhoef, J. Harris, H. Vennema, E. Duizer, Y. van Duynhoven, J. Gray, M. Iturriza, B. Bottiger, G. Falkenhorst, C. Johnsen, C. H. von Bonsdorff, L. Maunula, M. Kuusi, P. Pothier, A. Gallay, E. Schreier, M. Hohne, J. Koch, G. Szucs, G. Reuter, K. Krisztalovics, M. Lynch, P. McKeown, B. Foley, S. Coughlan, F. M. Ruggeri, I. Di Bartolo, K. Vainio, E. Isakbaeva, M. Poljsak-Prijatelj, A. H. Grom, J. Z. Mijovski, A. Bosch, J. Buesa, A. S. Fauquier, G. Hernandez-Pezzi, K. O. Hedlund, and M. Koopmans.** 2008. Analysis of integrated virological and epidemiological reports of norovirus outbreaks collected within the Foodborne Viruses in Europe network from 1 July 2001 to 30 June 2006. Journal of clinical microbiology **46:**2959-2965.
136. **Lai, C. K., K. S. Jeng, K. Machida, and M. M. Lai.** 2008. Association of hepatitis C virus replication complexes with microtubules and actin filaments is dependent on the interaction of NS3 and NS5A. Journal of virology **82:**8838-8848.
137. **Larkin, M. A., G. Blackshields, N. P. Brown, R. Chenna, P. A. McGettigan, H. McWilliam, F. Valentin, I. M. Wallace, A. Wilm, R. Lopez, J. D. Thompson, T. J. Gibson, and D. G. Higgins.** 2007. Clustal W and Clustal X version 2.0. Bioinformatics **23:**2947-2948.
138. **Lee, C., D. W. Park, J. Lee, T. I. Lee, Y. J. Kim, Y. S. Lee, and S. H. Baek.** 2006. Secretory phospholipase A2 induces apoptosis through TNF-alpha and cytochrome c-mediated caspase cascade in murine macrophage RAW 264.7 cells. European journal of pharmacology **536:**47-53.
139. **Lee, Y. F., A. Nomoto, B. M. Detjen, and E. Wimmer.** 1977. A protein covalently linked to poliovirus genome RNA. Proceedings of the National Academy of Sciences of the United States of America **74:**59-63.
140. **Lencioni, K. C., R. Drivdahl, A. Seamons, P. M. Treuting, T. Brabb, and L. Maggio-Price.** 2011. Lack of effect of murine norovirus infection on a mouse model of bacteria-induced colon cancer. Comparative medicine **61:**219-226.
141. **Lencioni, K. C., A. Seamons, P. M. Treuting, L. Maggio-Price, and T. Brabb.** 2008. Murine norovirus: an intercurrent variable in a mouse model of bacteria-induced inflammatory bowel disease. Comparative medicine **58:**522-533.
142. **Lenghaus, C., H. Westbury, B. J., Collins, N. Ratnamohan, and C. Morrissy.** 1994. Overview of the RHD Project in Australia. Bureau of Resource Science, Sydney, New South Wales, Australia.
143. **Li, Z., and P. D. Nagy.** 2011. Diverse roles of host RNA binding proteins in RNA virus replication. RNA biology **8:**305-315.
144. **Lin, S. S., H. W. Wu, S. F. Elena, K. C. Chen, Q. W. Niu, S. D. Yeh, C. C. Chen, and N. H. Chua.** 2009. Molecular evolution of a viral non-coding sequence under the selective pressure of amiRNA-mediated silencing. PLoS pathogens **5:**e1000312.

145. **Lindesmith, L. C., E. F. Donaldson, and R. S. Baric.** 2011. Norovirus GII.4 strain antigenic variation. Journal of virology **85:**231-242.
146. **Lindesmith, L. C., E. F. Donaldson, A. D. Lobue, J. L. Cannon, D. P. Zheng, J. Vinje, and R. S. Baric.** 2008. Mechanisms of GII.4 norovirus persistence in human populations. PLoS medicine **5:**e31.
147. **Liu, B., I. N. Clarke, and P. R. Lambden.** 1996. Polyprotein processing in Southampton virus: identification of 3C-like protease cleavage sites by in vitro mutagenesis. Journal of virology **70:**2605-2610.
148. **Liu, B. L., I. N. Clarke, E. O. Caul, and P. R. Lambden.** 1995. Human enteric caliciviruses have a unique genome structure and are distinct from the Norwalk-like viruses. Archives of virology **140:**1345-1356.
149. **Liu, B. L., G. J. Viljoen, I. N. Clarke, and P. R. Lambden.** 1999. Identification of further proteolytic cleavage sites in the Southampton calicivirus polyprotein by expression of the viral protease in E. coli. The Journal of general virology **80 (Pt 2):**291-296.
150. **Liu, S. J., Xue, H.P., Pu, B.Q., and Qian, N.H.** 1984. A new viral disease in rabbits. Journal of Veterinary Diagnostics Investigation **16:**253-255.
151. **Lopman, B. A., M. H. Reacher, I. B. Vipond, J. Sarangi, and D. W. Brown.** 2004. Clinical manifestation of norovirus gastroenteritis in health care settings. Clinical infectious diseases : an official publication of the Infectious Diseases Society of America **39:**318-324.
152. **Love, D. N., and M. Sabine.** 1975. Electron microscopic observation of feline kidney cells infected with a feline calicivirus. Archives of virology **48:**213-228.
153. **Lu, H. H., L. Alexander, and E. Wimmer.** 1995. Construction and genetic analysis of dicistronic polioviruses containing open reading frames for epitopes of human immunodeficiency virus type 1 gp120. Journal of virology **69:**4797-4806.
154. **Lu, J., N. Zhi, S. Wong, and K. E. Brown.** 2006. Activation of synoviocytes by the secreted phospholipase A2 motif in the VP1-unique region of parvovirus B19 minor capsid protein. The Journal of infectious diseases **193:**582-590.
155. **Lupescu, A., C. T. Bock, P. A. Lang, S. Aberle, H. Kaiser, R. Kandolf, and F. Lang.** 2006. Phospholipase A2 activity-dependent stimulation of Ca2+ entry by human parvovirus B19 capsid protein VP1. Journal of virology **80:**11370-11380.
156. **Luttermann, C., and G. Meyers.** 2007. A bipartite sequence motif induces translation reinitiation in feline calicivirus RNA. The Journal of biological chemistry **282:**7056-7065.
157. **Luttermann, C., and G. Meyers.** 2009. The importance of inter- and intramolecular base pairing for translation reinitiation on a eukaryotic bicistronic mRNA. Genes & development **23:**331-344.
158. **Machin, A., J. M. Martin Alonso, and F. Parra.** 2001. Identification of the amino acid residue involved in rabbit hemorrhagic disease virus VPg uridylylation. The Journal of biological chemistry **276:**27787-27792.

159. **Makino, A., M. Shimojima, T. Miyazawa, K. Kato, Y. Tohya, and H. Akashi.** 2006. Junctional adhesion molecule 1 is a functional receptor for feline calicivirus. Journal of virology **80:**4482-4490.
160. **Marin, M. S., R. Casais, J. M. Alonso, and F. Parra.** 2000. ATP binding and ATPase activities associated with recombinant rabbit hemorrhagic disease virus 2C-like polypeptide. Journal of virology **74:**10846-10851.
161. **Marionneau, S., N. Ruvoen, B. Le Moullac-Vaidye, M. Clement, A. Cailleau-Thomas, G. Ruiz-Palacois, P. Huang, X. Jiang, and J. Le Pendu.** 2002. Norwalk virus binds to histo-blood group antigens present on gastroduodenal epithelial cells of secretor individuals. Gastroenterology **122:**1967-1977.
162. **Marsden, R. L., L. J. McGuffin, and D. T. Jones.** 2002. Rapid protein domain assignment from amino acid sequence using predicted secondary structure. Protein science : a publication of the Protein Society **11:**2814-2824.
163. **Mattion, N. M., P. A. Reilly, S. J. DiMichele, J. C. Crowley, and C. Weeks-Levy.** 1994. Attenuated poliovirus strain as a live vector: expression of regions of rotavirus outer capsid protein VP7 by using recombinant Sabin 3 viruses. Journal of virology **68:**3925-3933.
164. **Maurin, T., D. Fenard, G. Lambeau, and A. Doglio.** 2007. An envelope-determined endocytic route of viral entry allows HIV-1 to escape from secreted phospholipase A2 entry blockade. Journal of molecular biology **367:**702-714.
165. **McCarthy, M., M. K. Estes, and K. C. Hyams.** 2000. Norwalk-like virus infection in military forces: epidemic potential, sporadic disease, and the future direction of prevention and control efforts. The Journal of infectious diseases **181 Suppl 2:**S387-391.
166. **McFadden, N., D. Bailey, G. Carrara, A. Benson, Y. Chaudhry, A. Shortland, J. Heeney, F. Yarovinsky, P. Simmonds, A. Macdonald, and I. Goodfellow.** 2011. Norovirus Regulation of the Innate Immune Response and Apoptosis Occurs via the Product of the Alternative Open Reading Frame 4. PLoS pathogens **7:**e1002413.
167. **Meyers, G.** 2007. Characterization of the sequence element directing translation reinitiation in RNA of the calicivirus rabbit hemorrhagic disease virus. Journal of virology **81:**9623-9632.
168. **Meyers, G.** 2003. Translation of the minor capsid protein of a calicivirus is initiated by a novel termination-dependent reinitiation mechanism. The Journal of biological chemistry **278:**34051-34060.
169. **Meyers, G., C. Wirblich, H. J. Thiel, and J. O. Thumfart.** 2000. Rabbit hemorrhagic disease virus: genome organization and polyprotein processing of a calicivirus studied after transient expression of cDNA constructs. Virology **276:**349-363.
170. **Miller, S., and J. Krijnse-Locker.** 2008. Modification of intracellular membrane structures for virus replication. Nature reviews. Microbiology **6:**363-374.
171. **Miller, W. A., and G. Koev.** 2000. Synthesis of subgenomic RNAs by positive-strand RNA viruses. Virology **273:**1-8.

172. **Mitra, T., S. V. Sosnovtsev, and K. Y. Green.** 2004. Mutagenesis of tyrosine 24 in the VPg protein is lethal for feline calicivirus. Journal of virology **78:**4931-4935.
173. **Moradpour, D., M. J. Evans, R. Gosert, Z. Yuan, H. E. Blum, S. P. Goff, B. D. Lindenbach, and C. M. Rice.** 2004. Insertion of green fluorescent protein into nonstructural protein 5A allows direct visualization of functional hepatitis C virus replication complexes. Journal of virology **78:**7400-7409.
174. **Morales, M., J. Barcena, M. A. Ramirez, J. A. Boga, F. Parra, and J. M. Torres.** 2004. Synthesis in vitro of rabbit hemorrhagic disease virus subgenomic RNA by internal initiation on (-)sense genomic RNA: mapping of a subgenomic promoter. The Journal of biological chemistry **279:**17013-17018.
175. **Morrow, C. D., M. Navab, C. Peterson, J. Hocko, and A. Dasgupta.** 1984. Antibody to poliovirus genome-linked protein (VPg) precipitates in vitro synthesized RNA attached to VPg-precursor polypeptide(s). Virus research **1:**89-100.
176. **Moss, S. R., S. L. Turner, R. C. Trout, P. J. White, P. J. Hudson, A. Desai, M. Armesto, N. L. Forrester, and E. A. Gould.** 2002. Molecular epidemiology of Rabbit haemorrhagic disease virus. The Journal of general virology **83:**2461-2467.
177. **Mueller, S., and E. Wimmer.** 1998. Expression of foreign proteins by poliovirus polyprotein fusion: analysis of genetic stability reveals rapid deletions and formation of cardioviruslike open reading frames. Journal of virology **72:**20-31.
178. **Mutze, G., B. Cooke, and P. Alexander.** 1998. The initial impact of rabbit hemorrhagic disease on European rabbit populations in South Australia. J Wildl Dis **34:**221-227.
179. **Nagy, P. D., and J. Pogany.** 2011. The dependence of viral RNA replication on co-opted host factors. Nature reviews. Microbiology **10:**137-149.
180. **Nakamura, K., Y. Someya, T. Kumasaka, G. Ueno, M. Yamamoto, T. Sato, N. Takeda, T. Miyamura, and N. Tanaka.** 2005. A norovirus protease structure provides insights into active and substrate binding site integrity. Journal of virology **79:**13685-13693.
181. **Nakata, S., K. Kogawa, K. Numata, S. Ukae, N. Adachi, D. O. Matson, M. K. Estes, and S. Chiba.** 1996. The epidemiology of human calicivirus/Sapporo/82/Japan. Archives of virology. Supplementum **12:**263-270.
182. **Natoni, A., G. E. Kass, M. J. Carter, and L. O. Roberts.** 2006. The mitochondrial pathway of apoptosis is triggered during feline calicivirus infection. The Journal of general virology **87:**357-361.
183. **Nayak, M. K., G. Balasubramanian, G. C. Sahoo, R. Bhattacharya, J. Vinje, N. Kobayashi, M. C. Sarkar, M. K. Bhattacharya, and T. Krishnan.** 2008. Detection of a novel intergenogroup recombinant Norovirus from Kolkata, India. Virology **377:**117-123.
184. **Nayak, M. K., D. Chatterjee, S. M. Nataraju, M. Pativada, U. Mitra, M. K. Chatterjee, T. K. Saha, U. Sarkar, and T. Krishnan.** 2009. A new variant of

Norovirus GII.4/2007 and inter-genotype recombinant strains of NVGII causing acute watery diarrhoea among children in Kolkata, India. Journal of clinical virology : the official publication of the Pan American Society for Clinical Virology.
185. **Neill, J. D.** 1990. Nucleotide sequence of a region of the feline calicivirus genome which encodes picornavirus-like RNA-dependent RNA polymerase, cysteine protease and 2C polypeptides. Virus research **17:**145-160.
186. **Neill, J. D.** 1992. Nucleotide sequence of the capsid protein gene of two serotypes of San Miguel sea lion virus: identification of conserved and non-conserved amino acid sequences among calicivirus capsid proteins. Virus research **24:**211-222.
187. **Neill, J. D.** 2002. The subgenomic RNA of feline calicivirus is packaged into viral particles during infection. Virus research **87:**89-93.
188. **Neill, J. D., and W. L. Mengeling.** 1988. Further characterization of the virus-specific RNAs in feline calicivirus infected cells. Virus research **11:**59-72.
189. **Neill, J. D., I. M. Reardon, and R. L. Heinrikson.** 1991. Nucleotide sequence and expression of the capsid protein gene of feline calicivirus. Journal of virology **65:**5440-5447.
190. **Neill, J. D., S. V. Sosnovtsev, and K. Y. Green.** 2000. Recovery and altered neutralization specificities of chimeric viruses containing capsid protein domain exchanges from antigenically distinct strains of feline calicivirus. Journal of virology **74:**1079-1084.
191. **Ng, K. K., M. M. Cherney, A. L. Vazquez, A. Machin, J. M. Alonso, F. Parra, and M. N. James.** 2002. Crystal structures of active and inactive conformations of a caliciviral RNA-dependent RNA polymerase. The Journal of biological chemistry **277:**1381-1387.
192. **Ng, K. K., N. Pendas-Franco, J. Rojo, J. A. Boga, A. Machin, J. M. Alonso, and F. Parra.** 2004. Crystal structure of norwalk virus polymerase reveals the carboxyl terminus in the active site cleft. The Journal of biological chemistry **279:**16638-16645.
193. **Noel, J. S., R. L. Fankhauser, T. Ando, S. S. Monroe, and R. I. Glass.** 1999. Identification of a distinct common strain of "Norwalk-like viruses" having a global distribution. The Journal of infectious diseases **179:**1334-1344.
194. **Novoa, R. R., G. Calderita, R. Arranz, J. Fontana, H. Granzow, and C. Risco.** 2005. Virus factories: associations of cell organelles for viral replication and morphogenesis. Biology of the cell / under the auspices of the European Cell Biology Organization **97:**147-172.
195. **Oehmig, A., M. Buttner, F. Weiland, W. Werz, K. Bergemann, and E. Pfaff.** 2003. Identification of a calicivirus isolate of unknown origin. The Journal of general virology **84:**2837-2845.
196. **Ohlinger, V. F., B. Haas, and H. J. Thiel.** 1993. Rabbit hemorrhagic disease (RHD): characterization of the causative calicivirus. Vet Res **24:**103-116.
197. **Oka, T., K. Katayama, S. Ogawa, G. S. Hansman, T. Kageyama, H. Ushijima, T. Miyamura, and N. Takeda.** 2005. Proteolytic processing of sapovirus ORF1 polyprotein. Journal of virology **79:**7283-7290.

198. **Oka, T., M. Yamamoto, K. Katayama, G. S. Hansman, S. Ogawa, T. Miyamura, and N. Takeda.** 2006. Identification of the cleavage sites of sapovirus open reading frame 1 polyprotein. The Journal of general virology **87:**3329-3338.
199. **Ossiboff, R. J., and J. S. Parker.** 2007. Identification of regions and residues in feline junctional adhesion molecule required for feline calicivirus binding and infection. Journal of virology **81:**13608-13621.
200. **Ossiboff, R. J., Y. Zhou, P. J. Lightfoot, B. V. Prasad, and J. S. Parker.** 2010. Conformational changes in the capsid of a calicivirus upon interaction with its functional receptor. Journal of virology **84:**5550-5564.
201. **Paik, J., Y. Fierce, R. Drivdahl, P. M. Treuting, A. Seamons, T. Brabb, and L. Maggio-Price.** 2010. Effects of murine norovirus infection on a mouse model of diet-induced obesity and insulin resistance. Comparative medicine **60:**189-195.
202. **Palmenberg, A. C.** 1990. Proteolytic processing of picornaviral polyprotein. Annual review of microbiology **44:**603-623.
203. **Patel, M. M., M. A. Widdowson, R. I. Glass, K. Akazawa, J. Vinje, and U. D. Parashar.** 2008. Systematic literature review of role of noroviruses in sporadic gastroenteritis. Emerging infectious diseases **14:**1224-1231.
204. **Pedersen, N. C., J. B. Elliott, A. Glasgow, A. Poland, and K. Keel.** 2000. An isolated epizootic of hemorrhagic-like fever in cats caused by a novel and highly virulent strain of feline calicivirus. Veterinary microbiology **73:**281-300.
205. **Pedersen, N. C., R. Sato, J. E. Foley, and A. M. Poland.** 2004. Common virus infections in cats, before and after being placed in shelters, with emphasis on feline enteric coronavirus. Journal of feline medicine and surgery **6:**83-88.
206. **Perdue, K. A., K. Y. Green, M. Copeland, E. Barron, M. Mandel, L. J. Faucette, E. M. Williams, S. V. Sosnovtsev, W. R. Elkins, and J. M. Ward.** 2007. Naturally occurring murine norovirus infection in a large research institution. Journal of the American Association for Laboratory Animal Science : JAALAS **46:**39-45.
207. **Pesavento, P. A., K. O. Chang, and J. S. Parker.** 2008. Molecular virology of feline calicivirus. Vet Clin North Am Small Anim Pract **38:**775-786, vii.
208. **Pesavento, P. A., N. J. MacLachlan, L. Dillard-Telm, C. K. Grant, and K. F. Hurley.** 2004. Pathologic, immunohistochemical, and electron microscopic findings in naturally occurring virulent systemic feline calicivirus infection in cats. Veterinary pathology **41:**257-263.
209. **Peters, J. E., and N. L. Craig.** 2001. Tn7: smarter than we thought. Nat Rev Mol Cell Biol **2:**806-814.
210. **Peterson, J. E., and M. J. Studdert.** 1970. Feline picornavirus. Structure of the virus and electron microscopic observations on infected cell cultures. Archiv fur die gesamte Virusforschung **32:**249-260.
211. **Pfister, T., and E. Wimmer.** 2001. Polypeptide p41 of a Norwalk-like virus is a nucleic acid-independent nucleoside triphosphatase. Journal of virology **75:**1611-1619.

212. **Phan, T. G., K. Kaneshi, Y. Ueda, S. Nakaya, S. Nishimura, A. Yamamoto, K. Sugita, S. Takanashi, S. Okitsu, and H. Ushijima.** 2007. Genetic heterogeneity, evolution, and recombination in noroviruses. Journal of medical virology **79:**1388-1400.
213. **Phan, T. G., T. Kuroiwa, K. Kaneshi, Y. Ueda, S. Nakaya, S. Nishimura, A. Yamamoto, K. Sugita, T. Nishimura, F. Yagyu, S. Okitsu, W. E. Muller, N. Maneekarn, and H. Ushijima.** 2006. Changing distribution of norovirus genotypes and genetic analysis of recombinant GIIb among infants and children with diarrhea in Japan. Journal of medical virology **78:**971-978.
214. **Phan, T. G., S. Nishimura, K. Sugita, T. Nishimura, S. Okitsu, and H. Ushijima.** 2007. Multiple recombinant noroviruses in Japan. Clin Lab **53:**567-570.
215. **Pierson, T. C., M. S. Diamond, A. A. Ahmed, L. E. Valentine, C. W. Davis, M. A. Samuel, S. L. Hanna, B. A. Puffer, and R. W. Doms.** 2005. An infectious West Nile virus that expresses a GFP reporter gene. Virology **334:**28-40.
216. **Prasad, B. V., M. E. Hardy, T. Dokland, J. Bella, M. G. Rossmann, and M. K. Estes.** 1999. X-ray crystallographic structure of the Norwalk virus capsid. Science **286:**287-290.
217. **Prasad, B. V., D. O. Matson, and A. W. Smith.** 1994. Three-dimensional structure of calicivirus. Journal of molecular biology **240:**256-264.
218. **Prasad, B. V., R. Rothnagel, X. Jiang, and M. K. Estes.** 1994. Three-dimensional structure of baculovirus-expressed Norwalk virus capsids. Journal of virology **68:**5117-5125.
219. **Radford, A. D., M. Bennett, F. McArdle, S. Dawson, P. C. Turner, M. A. Glenn, and R. M. Gaskell.** 1997. The use of sequence analysis of a feline calicivirus (FCV) hypervariable region in the epidemiological investigation of FCV related disease and vaccine failures. Vaccine **15:**1451-1458.
220. **Radford, A. D., K. P. Coyne, S. Dawson, C. J. Porter, and R. M. Gaskell.** 2007. Feline calicivirus. Vet Res **38:**319-335.
221. **Radford, A. D., L. M. Sommerville, S. Dawson, A. M. Kerins, R. Ryvar, and R. M. Gaskell.** 2001. Molecular analysis of isolates of feline calicivirus from a population of cats in a rescue shelter. The Veterinary record **149:**477-481.
222. **Rai, T., A. Mosoian, and M. D. Resh.** 2010. Annexin 2 is not required for human immunodeficiency virus type 1 particle production but plays a cell type-dependent role in regulating infectivity. Journal of virology **84:**9783-9792.
223. **Reebye, V., A. Frilling, A. Hajitou, J. P. Nicholls, N. A. Habib, and P. J. Mintz.** 2012. A perspective on non-catalytic Src homology (SH) adaptor signalling proteins. Cellular signalling **24:**388-392.
224. **Rescher, U., C. Ludwig, V. Konietzko, A. Kharitonenkov, and V. Gerke.** 2008. Tyrosine phosphorylation of annexin A2 regulates Rho-mediated actin rearrangement and cell adhesion. Journal of cell science **121:**2177-2185.
225. **Roberts, L. O., N. Al-Molawi, M. J. Carter, and G. E. Kass.** 2003. Apoptosis in cultured cells infected with feline calicivirus. Ann N Y Acad Sci **1010:**587-590.

226. **Rockx, B., M. De Wit, H. Vennema, J. Vinje, E. De Bruin, Y. Van Duynhoven, and M. Koopmans.** 2002. Natural history of human calicivirus infection: a prospective cohort study. Clinical infectious diseases : an official publication of the Infectious Diseases Society of America **35:**246-253.
227. **Rodak, L., Smid, B., Valicek, L., Vesely, T., Stepanek, J., Hampl, J., and Jurak, E. .** 1990. Enzyme-Linked-Immunosorbent-Assay of antibodies to rabbit hemorrhagic diseases virus and determination of its major structural proteins. Journal of General Virology **71:**1075-1080.
228. **Rohayem, J.** 2009. Norovirus seasonality and the potential impact of climate change. Clinical microbiology and infection : the official publication of the European Society of Clinical Microbiology and Infectious Diseases **15:**524-527.
229. **Rohayem, J., J. Munch, and A. Rethwilm.** 2005. Evidence of recombination in the norovirus capsid gene. Journal of virology **79:**4977-4990.
230. **Rohayem, J., I. Robel, K. Jager, U. Scheffler, and W. Rudolph.** 2006. Protein-primed and de novo initiation of RNA synthesis by norovirus 3Dpol. Journal of virology **80:**7060-7069.
231. **Ronquist, F., M. Teslenko, P. van der Mark, D. L. Ayres, A. Darling, S. Hohna, B. Larget, L. Liu, M. A. Suchard, and J. P. Huelsenbeck.** 2012. MrBayes 3.2: efficient Bayesian phylogenetic inference and model choice across a large model space. Systematic biology **61:**539-542.
232. **Ros Bascunana, C., N. Nowotny, and S. Belak.** 1997. Detection and differentiation of rabbit hemorrhagic disease and European brown hare syndrome viruses by amplification of VP60 genomic sequences from fresh and fixed tissue specimens. Journal of clinical microbiology **35:**2492-2495.
233. **Ruvoen-Clouet, N., J. P. Ganiere, G. Andre-Fontaine, D. Blanchard, and J. Le Pendu.** 2000. Binding of rabbit hemorrhagic disease virus to antigens of the ABH histo-blood group family. Journal of virology **74:**11950-11954.
234. **Ryzhova, E. V., R. M. Vos, A. V. Albright, A. V. Harrist, T. Harvey, and F. Gonzalez-Scarano.** 2006. Annexin 2: a novel human immunodeficiency virus type 1 Gag binding protein involved in replication in monocyte-derived macrophages. Journal of virology **80:**2694-2704.
235. **Saxena, V., C. K. Lai, T. C. Chao, K. S. Jeng, and M. M. Lai.** 2012. Annexin A2 is involved in the formation of hepatitis C virus replication complex on the lipid raft. Journal of virology **86:**4139-4150.
236. **Schaffer, F. L., H. L. Bachrach, F. Brown, J. H. Gillespie, J. N. Burroughs, S. H. Madin, C. R. Madeley, R. C. Povey, F. Scott, A. W. Smith, and M. J. Studdert.** 1980. Caliciviridae. Intervirology **14:**1-6.
237. **Schaffer, F. L., D. W. Ehresmann, M. K. Fretz, and M. I. Soergel.** 1980. A protein, VPg, covalently linked to 36S calicivirus RNA. The Journal of general virology **47:**215-220.
238. **Schorr-Evans, E. M., A. Poland, W. E. Johnson, and N. C. Pedersen.** 2003. An epizootic of highly virulent feline calicivirus disease in a hospital setting in New England. Journal of feline medicine and surgery **5:**217-226.
239. **Sharp, T. M., S. Guix, K. Katayama, S. E. Crawford, and M. K. Estes.** 2010. Inhibition of cellular protein secretion by norwalk virus nonstructural

protein p22 requires a mimic of an endoplasmic reticulum export signal. PloS one **5:**e13130.
240. **Sharp, T. W., K. C. Hyams, D. Watts, A. F. Trofa, G. J. Martin, A. Z. Kapikian, K. Y. Green, X. Jiang, M. K. Estes, M. Waack, and et al.** 1995. Epidemiology of Norwalk virus during an outbreak of acute gastroenteritis aboard a US aircraft carrier. Journal of medical virology **45:**61-67.
241. **Siebenga, J., A. Kroneman, H. Vennema, E. Duizer, and M. Koopmans.** 2008. Food-borne viruses in Europe network report: the norovirus GII.4 2006b (for US named Minerva-like, for Japan Kobe034-like, for UK V6) variant now dominant in early seasonal surveillance. Euro surveillance : bulletin europeen sur les maladies transmissibles = European communicable disease bulletin **13**.
242. **Siebenga, J. J., P. Lemey, S. L. Kosakovsky Pond, A. Rambaut, H. Vennema, and M. Koopmans.** 2010. Phylodynamic reconstruction reveals norovirus GII.4 epidemic expansions and their molecular determinants. PLoS pathogens **6:**e1000884.
243. **Siebenga, J. J., H. Vennema, E. Duizer, and M. P. Koopmans.** 2007. Gastroenteritis caused by norovirus GGII.4, The Netherlands, 1994-2005. Emerging infectious diseases **13:**144-146.
244. **Siebenga, J. J., H. Vennema, B. Renckens, E. de Bruin, B. van der Veer, R. J. Siezen, and M. Koopmans.** 2007. Epochal evolution of GGII.4 norovirus capsid proteins from 1995 to 2006. Journal of virology **81:**9932-9941.
245. **Simmonds, P., I. Karakasiliotis, D. Bailey, Y. Chaudhry, D. J. Evans, and I. G. Goodfellow.** 2008. Bioinformatic and functional analysis of RNA secondary structure elements among different genera of human and animal caliciviruses. Nucleic acids research **36:**2530-2546.
246. **Smiley, J. R., K. O. Chang, J. Hayes, J. Vinje, and L. J. Saif.** 2002. Characterization of an enteropathogenic bovine calicivirus representing a potentially new calicivirus genus. Journal of virology **76:**10089-10098.
247. **Smith, A. W., and T. G. Akers.** 1976. Vesicular exanthema of swine. J Am Vet Med Assoc **169:**700-703.
248. **Smith, A. W., T. G. Akers, S. H. Madin, and N. A. Vedros.** 1973. San Miguel sea lion virus isolation, preliminary characterization and relationship to vesicular exanthema of swine virus. Nature **244:**108-110.
249. **Smith, D. B., N. McFadden, R. J. Blundell, A. Meredith, and P. Simmonds.** 2012. Diversity of murine norovirus in wild-rodent populations: species-specific associations suggest an ancient divergence. The Journal of general virology **93:**259-266.
250. **Someya, Y., N. Takeda, and T. Wakita.** 2008. Saturation mutagenesis reveals that GLU54 of norovirus 3C-like protease is not essential for the proteolytic activity. Journal of biochemistry **144:**771-780.
251. **Sosnovtsev, S., and K. Y. Green.** 1995. RNA transcripts derived from a cloned full-length copy of the feline calicivirus genome do not require VpG for infectivity. Virology **210:**383-390.

252. **Sosnovtsev, S. V., G. Belliot, K. O. Chang, O. Onwudiwe, and K. Y. Green.** 2005. Feline calicivirus VP2 is essential for the production of infectious virions. Journal of virology **79:**4012-4024.
253. **Sosnovtsev, S. V., G. Belliot, K. O. Chang, V. G. Prikhodko, L. B. Thackray, C. E. Wobus, S. M. Karst, H. W. Virgin, and K. Y. Green.** 2006. Cleavage map and proteolytic processing of the murine norovirus nonstructural polyprotein in infected cells. Journal of virology **80:**7816-7831.
254. **Sosnovtsev, S. V., M. Garfield, and K. Y. Green.** 2002. Processing map and essential cleavage sites of the nonstructural polyprotein encoded by ORF1 of the feline calicivirus genome. Journal of virology **76:**7060-7072.
255. **Sosnovtsev, S. V., and K. Y. Green.** 2000. Identification and genomic mapping of the ORF3 and VPg proteins in feline calicivirus virions. Virology **277:**193-203.
256. **Sosnovtsev, S. V., E. A. Prikhod'ko, G. Belliot, J. I. Cohen, and K. Y. Green.** 2003. Feline calicivirus replication induces apoptosis in cultured cells. Virus research **94:**1-10.
257. **Sosnovtsev, S. V., S. A. Sosnovtseva, and K. Y. Green.** 1998. Cleavage of the feline calicivirus capsid precursor is mediated by a virus-encoded proteinase. Journal of virology **72:**3051-3059.
258. **Sosnovtsev, S. V., Sosnovtseva, S. and K. Y. Green.** 1996. Recovery of feline calicivirus from plasmid DNA containing a full-length copy of the genome. European Society for Veterinary Virology and Central Veterinary Laboratory, Reading, United Kingdom.
259. **Sosnovtseva, S. A., S. V. Sosnovtsev, and K. Y. Green.** 1999. Mapping of the feline calicivirus proteinase responsible for autocatalytic processing of the nonstructural polyprotein and identification of a stable proteinase-polymerase precursor protein. Journal of virology **73:**6626-6633.
260. **Stellwagen, A. E., and N. L. Craig.** 1997. Avoiding self: two Tn7-encoded proteins mediate target immunity in Tn7 transposition. Embo J **16:**6823-6834.
261. **Stellwagen, A. E., and N. L. Craig.** 1997. Gain-of-function mutations in TnsC, an ATP-dependent transposition protein that activates the bacterial transposon Tn7. Genetics **145:**573-585.
262. **Stuart, A. D., and T. D. Brown.** 2006. Entry of feline calicivirus is dependent on clathrin-mediated endocytosis and acidification in endosomes. Journal of virology **80:**7500-7509.
263. **Studdert, M. J., and J. D. O'Shea.** 1975. Ultrastructural studies of the development of feline calicivirus in a feline embryo cell line. Archives of virology **48:**317-325.
264. **Tan, M., P. Huang, J. Meller, W. Zhong, T. Farkas, and X. Jiang.** 2003. Mutations within the P2 domain of norovirus capsid affect binding to human histo-blood group antigens: evidence for a binding pocket. Journal of virology **77:**12562-12571.
265. **Taube, S., J. W. Perry, K. Yetming, S. P. Patel, H. Auble, L. Shu, H. F. Nawar, C. H. Lee, T. D. Connell, J. A. Shayman, and C. E. Wobus.** 2009. Ganglioside-linked terminal sialic acid moieties on murine macrophages function as

attachment receptors for murine noroviruses. Journal of virology **83:**4092-4101.
266. **Teterina, N. L., C. Lauber, K. S. Jensen, E. A. Levenson, A. E. Gorbalenya, and E. Ehrenfeld.** 2011. Identification of tolerated insertion sites in poliovirus non-structural proteins. Virology **409:**1-11.
267. **Teterina, N. L., E. A. Levenson, and E. Ehrenfeld.** 2010. Viable polioviruses that encode 2A proteins with fluorescent protein tags. Journal of virology **84:**1477-1488.
268. **Teterina, N. L., Y. Pinto, J. D. Weaver, K. S. Jensen, and E. Ehrenfeld.** 2011. Analysis of poliovirus protein 3A interactions with viral and cellular proteins in infected cells. Journal of virology **85:**4284-4296.
269. **Thackray, L. B., C. E. Wobus, K. A. Chachu, B. Liu, E. R. Alegre, K. S. Henderson, S. T. Kelley, and H. W. t. Virgin.** 2007. Murine noroviruses comprising a single genogroup exhibit biological diversity despite limited sequence divergence. Journal of virology **81:**10460-10473.
270. **Thomas, J. M., W. B. Klimstra, K. D. Ryman, and H. W. Heidner.** 2003. Sindbis virus vectors designed to express a foreign protein as a cleavable component of the viral structural polyprotein. Journal of virology **77:**5598-5606.
271. **Thumfart, J. O., and G. Meyers.** 2002. Feline calicivirus: recovery of wild-type and recombinant viruses after transfection of cRNA or cDNA constructs. Journal of virology **76:**6398-6407.
272. **Tohya, Y., H. Shinchi, Y. Matsuura, K. Maeda, S. Ishiguro, M. Mochizuki, and T. Sugimura.** 1999. Analysis of the N-terminal polypeptide of the capsid precursor protein and the ORF3 product of feline calicivirus. J Vet Med Sci **61:**1043-1047.
273. **Tu, E. T., R. A. Bull, G. E. Greening, J. Hewitt, M. J. Lyon, J. A. Marshall, C. J. McIver, W. D. Rawlinson, and P. A. White.** 2008. Epidemics of gastroenteritis during 2006 were associated with the spread of norovirus GII.4 variants 2006a and 2006b. Clinical infectious diseases : an official publication of the Infectious Diseases Society of America **46:**413-420.
274. **Tu, E. T., T. Nguyen, P. Lee, R. A. Bull, J. Musto, G. Hansman, P. A. White, W. D. Rawlinson, and C. J. McIver.** 2007. Norovirus GII.4 strains and outbreaks, Australia. Emerging infectious diseases **13:**1128-1130.
275. **Vazquez, A. L., J. M. Alonso, and F. Parra.** 2000. Mutation analysis of the GDD sequence motif of a calicivirus RNA-dependent RNA polymerase. Journal of virology **74:**3888-3891.
276. **Vazquez, A. L., J. M. Martin Alonso, R. Casais, J. A. Boga, and F. Parra.** 1998. Expression of enzymatically active rabbit hemorrhagic disease virus RNA-dependent RNA polymerase in Escherichia coli. Journal of virology **72:**2999-3004.
277. **Vega, E., L. Barclay, N. Gregoricus, K. Williams, D. Lee, and J. Vinje.** 2011. Novel surveillance network for norovirus gastroenteritis outbreaks, United States. Emerging infectious diseases **17:**1389-1395.
278. **Verhoef, L., E. Depoortere, I. Boxman, E. Duizer, Y. van Duynhoven, J. Harris, C. Johnsen, A. Kroneman, S. Le Guyader, W. Lim, L. Maunula, H.**

Meldal, R. Ratcliff, G. Reuter, E. Schreier, J. Siebenga, K. Vainio, C. Varela, H. Vennema, and M. Koopmans. 2008. Emergence of new norovirus variants on spring cruise ships and prediction of winter epidemics. Emerging infectious diseases **14:**238-243.

279. **Vidal, R., P. Roessler, V. Solari, J. Vollaire, X. Jiang, D. O. Matson, N. Mamani, V. Prado, and M. L. O'Ryan.** 2006. Novel recombinant norovirus causing outbreaks of gastroenteritis in Santiago, Chile. Journal of clinical microbiology **44:**2271-2275.
280. **Vidalain, P. O., and F. Tangy.** 2010. Virus-host protein interactions in RNA viruses. Microbes and infection / Institut Pasteur **12:**1134-1143.
281. **Vinje, J., S. A. Altena, and M. P. Koopmans.** 1997. The incidence and genetic variability of small round-structured viruses in outbreaks of gastroenteritis in The Netherlands. The Journal of infectious diseases **176:**1374-1378.
282. **Ward, J. M., C. E. Wobus, L. B. Thackray, C. R. Erexson, L. J. Faucette, G. Belliot, E. L. Barron, S. V. Sosnovtsev, and K. Y. Green.** 2006. Pathology of immunodeficient mice with naturally occurring murine norovirus infection. Toxicologic pathology **34:**708-715.
283. **Waters, A., S. Coughlan, and W. W. Hall.** 2007. Characterisation of a novel recombination event in the norovirus polymerase gene. Virology **363:**11-14.
284. **Wei, L., J. S. Huhn, A. Mory, H. B. Pathak, S. V. Sosnovtsev, K. Y. Green, and C. E. Cameron.** 2001. Proteinase-polymerase precursor as the active form of feline calicivirus RNA-dependent RNA polymerase. Journal of virology **75:**1211-1219.
285. **Widdowson, M. A., E. H. Cramer, L. Hadley, J. S. Bresee, R. S. Beard, S. N. Bulens, M. Charles, W. Chege, E. Isakbaeva, J. G. Wright, E. Mintz, D. Forney, J. Massey, R. I. Glass, and S. S. Monroe.** 2004. Outbreaks of acute gastroenteritis on cruise ships and on land: identification of a predominant circulating strain of norovirus--United States, 2002. The Journal of infectious diseases **190:**27-36.
286. **Wirblich, C., H. J. Thiel, and G. Meyers.** 1996. Genetic map of the calicivirus rabbit hemorrhagic disease virus as deduced from in vitro translation studies. Journal of virology **70:**7974-7983.
287. **Wobus, C. E., S. M. Karst, L. B. Thackray, K. O. Chang, S. V. Sosnovtsev, G. Belliot, A. Krug, J. M. Mackenzie, K. Y. Green, and H. W. Virgin.** 2004. Replication of Norovirus in cell culture reveals a tropism for dendritic cells and macrophages. PLoS Biol **2:**e432.
288. **Wolk, B., B. Buchele, D. Moradpour, and C. M. Rice.** 2008. A dynamic view of hepatitis C virus replication complexes. Journal of virology **82:**10519-10531.
289. **Woode, G. N., and J. C. Bridger.** 1978. Isolation of small viruses resembling astroviruses and caliciviruses from acute enteritis of calves. Journal of medical microbiology **11:**441-452.
290. **Wyatt, R. G., R. Dolin, N. R. Blacklow, H. L. DuPont, R. F. Buscho, T. S. Thornhill, A. Z. Kapikian, and R. M. Chanock.** 1974. Comparison of three agents of acute infectious nonbacterial gastroenteritis by cross-challenge in volunteers. The Journal of infectious diseases **129:**709-714.

291. **Xi, J. N., D. Y. Graham, K. N. Wang, and M. K. Estes.** 1990. Norwalk virus genome cloning and characterization. Science **250:**1580-1583.
292. **Yagami, T., K. Ueda, K. Asakura, S. Hata, T. Kuroda, T. Sakaeda, N. Takasu, K. Tanaka, T. Gemba, and Y. Hori.** 2002. Human group IIA secretory phospholipase A2 induces neuronal cell death via apoptosis. Molecular pharmacology **61:**114-126.
293. **Yagami, T., K. Ueda, K. Asakura, Y. Hayasaki-Kajiwara, H. Nakazato, T. Sakaeda, S. Hata, T. Kuroda, N. Takasu, and Y. Hori.** 2002. Group IB secretory phospholipase A2 induces neuronal cell death via apoptosis. Journal of neurochemistry **81:**449-461.
294. **Zadori, Z., J. Szelei, M. C. Lacoste, Y. Li, S. Gariepy, P. Raymond, M. Allaire, I. R. Nabi, and P. Tijssen.** 2001. A viral phospholipase A2 is required for parvovirus infectivity. Developmental cell **1:**291-302.
295. **Zamyatkin, D. F., F. Parra, A. Machin, P. Grochulski, and K. K. Ng.** 2009. Binding of 2'-amino-2'-deoxycytidine-5'-triphosphate to norovirus polymerase induces rearrangement of the active site. Journal of molecular biology **390:**10-16.
296. **Zeitler, C. E., M. K. Estes, and B. V. Venkataram Prasad.** 2006. X-ray crystallographic structure of the Norwalk virus protease at 1.5-A resolution. Journal of virology **80:**5050-5058.
297. **Zhang, X., and D. L. Nuss.** 2008. A host dicer is required for defective viral RNA production and recombinant virus vector RNA instability for a positive sense RNA virus. Proc Natl Acad Sci U S A **105:**16749-16754.
298. **Zheng, D. P., T. Ando, R. L. Fankhauser, R. S. Beard, R. I. Glass, and S. S. Monroe.** 2006. Norovirus classification and proposed strain nomenclature. Virology **346:**312-323.